UNIVERSITÀ DEGLI STUDI DI MILANO

DIPARTIMENTO DI SCIENZE BIOMEDICHE, CHIRURGICHE E ODONTOIATRICHE

XXIX Ciclo del Dottorato di Ricerca in Scienze Odontostomatologiche

Resin-based composites modulate oral biofilm formation

DOTTORANDA: **Gloria CAZZANIGA**

MATRICOLA: **R-10744**

COORDINATORE

Prof. Massimo **DEL FABBRO**

TUTORE

Prof. Eugenio **BRAMBILLA**

Anno 2016-2017

INDEX

Abstract

Sommario

1. INTRODUCTION

1.1 Resin-based composites: state of the art

1.2 Issues related to resin-based composites

1.3 Biofilms

1.3.1 Oral biofilms: composition and structure

1.3.2 Oral Biofilms and dental caries

1.3.3 Microbiological models to study oral biofilms

1.4 Strategies to control oral biofilm formation

1.4.1 Materials featuring a long-term release of antibacterial agents

1.4.2 Materials with contact-killing properties

1.4.3Materials featuring non-adhesive surfaces: optimizing materials formulation without the addition of antibacterial agents

1.4.4 Materials featuring biomimetic properties

1.4.5 Considerations on the different approaches

1.5 Aims of this PhD thesis

2. EXPERIMENTS

2.1 Optimization of RBCs microbiological properties without the addition of antibacterial compounds

2.1.1 Materials and methods

2.1.2 Results

2.1.3 Discussion and conclusions

2.2 Optimization of the microbiological properties of RBCs submitted to different surface finishing/polishing protocols

2.2.1 Materials and methods

2.2.2 Results

2.2.3 Discussion

2.3 Evaluation of RBCs featuring antibacterial properties

2.3.1 Materials and methods

2.3.2 Results

2.3.3 Discussion

2.4 Design of an experimental RBCs featuring bioactive and biomimetic properties

2.4.1 Materials and methods

2.4.2 Results

2.4.3 Discussion

3 General discussion and conclusions

4 References

Abstract

Resin-based composites (RBCs) are increasingly used because of their excellent aesthetic properties and improved mechanical features. Nevertheless, the main reason for failure of resin composite restorations is still secondary caries. Dental caries is a very common infectious disease driven by the metabolic activity of a dysbiotic biofilm able to colonize both natural and artificial surfaces.

In recent years, extensive research has been devoted to develop new restorative materials that could prevent the formation of recurrent carious lesions. Many approaches have been followed to reach this goal, particularly optimizing RBCs surfaces to obtain anti-adhesive properties, developing bioactive materials and synthesizing biomimetic materials. The aim of this PhD thesis was to explore the different approaches in order to discriminate the parameters influencing the microbiological behaviour of RBCs and therefore optimize their formulation to successfully control oral biofilms development. The three approaches were evaluated in the experimental part of the thesis.

Considering the first approach, the optimization of the microbiological properties of resin-based dental materials was evaluated from different points of view. Experimental RBCs with different compositions were studied, hypothesizing that surface features and nanotexture would have influenced biofilm formation. The anti-adhesive properties of the tested materials were evaluated as a possible way to control biofilm formation without the need of antibacterial agents. The results showed that both hydrophobicity of the resin matrix of RBCs and filler amount can influence oral biofilm formation. Furthermore, different commercially available RBCs were submitted to diverse finishing and polishing protocols in order to evaluate the influence of these procedures on the surface features and on the microbiological behaviour of each material. It was therefore showed that surface chemistry seemed to play an important role in influencing biofilm formation.

Regarding the second research field, the antimicrobial behaviour of experimental RBCs derived from a commercial formulation including different fractions of fluoride-releasing S-PRG filler particles was evaluated. The results of this study suggested an impact of fluoride-releasing S-PRG filler particles particularly on the early phases of biofilm formation. As the release of fluoride diminishes as a function of time, optimizing the fluoride-recharging abilities of the materials might help to control biofilm formation for longer periods. Moreover, the final polishing of the material may substantially influence the release of fluoride.

The third research approach evaluated the possibility that biomimetic materials may control oral biofilm formation, without the addition of specific antimicrobial agents. In this study functionalized dicalcium phosphate dihydrate nanoparticles (nDCPD) were incorporated into an experimental RBC. Results showed that the RBC with functionalized nDCPD nanoparticles showed a reduction in biofilm formation when compared to a RBC filled with non-functionalized nanoparticles.

All these approaches were effective in influencing oral biofilm formation on the tested materials. Recent studies regarding the human microbiome tend to consider biofilms as a part of the human body and show that many diseases, including dental caries, are due to an imbalance between host and biofilms. These diseases may be treated by modifying biofilms composition, without trying to eradicate biofilms.

Hence, the possibility to modulate oral biofilm formation on restorations through the optimization of materials surfaces without the addition of any antibacterial agent seems to be the most interesting approach.

Sommario

Grazie alle loro proprietà estetiche e meccaniche i materiali compositi sono largamente utilizzati in Odontoiatria Restaurativa. Tuttavia, lo sviluppo di carie secondaria rappresenta ancora la principale causa di rifacimento dei restauri in composito. La carie è una patologia infettiva legata all'attività metabolica di un biofilm disbiotico capace di colonizzare i tessuti orali naturali e artificiali. Per questo motivo, negli ultimi anni la ricerca è stata focalizzata sullo sviluppo di materiali da restauro capaci di modulare lo sviluppo di biofilm sulle loro superfici e quindi prevenire lo sviluppo di carie secondaria.

Differenti approcci sono stati proposti al fine di raggiungere questo obiettivo, in particolare l'ottimizzazione delle superfici per ottenere compositi con proprietà antiadesive, lo sviluppo di materiali bioattivi contenenti un principio antibatterico e la sintesi di materiali biomimetici.

Scopo di questa tesi è stato esplorare i differenti approcci al fine di discriminare i parametri capaci di influenzare il comportamento microbiologico dei materiali compositi e quindi ottimizzarne poi la formulazione per modulare efficacemente lo sviluppo di biofilm. I tre differenti approcci sono stati analizzati nella sezione sperimentale.

In relazione al primo approccio, l'ottimizzazione delle proprietà microbiologiche dei materiali compositi è stata valutata da differenti punti di vista. In primo luogo, sono stati testati compositi sperimentali con differenti composizioni ipotizzando che la formazione di biofilm su tali materiali potesse dipendere dalle loro caratteristiche di superficie e di nanotexture. Le proprietà antiadesive di tali compositi sono state valutate quale un possibile modo per garantire un controllo efficace della formazione di biofilm senza la necessità di incorporazione di molecole antimicrobiche. I risultati hanno dimostrato che sia l'idrofobicità della matrice resinosa che il tipo di filler possono influenzare la formazione del biofilm. Un secondo studio ha invece permesso di valutare l'influenza di diversi trattamenti di rifinitura e lucidatura sul comportamento microbiologico e sulle caratteristiche di superficie di materiali compositi disponibili in commercio. I risultati di questo studio hanno evidenziato l'importante ruolo che la composizione chimica di superficie gioca sullo sviluppo di biofilm.

Considerando il secondo approccio sperimentale è stato valutato il comportamento microbiologico di compositi sperimentali derivati da una formulazione commerciale e contenenti un filler antibatterico in grado di rilasciare fluoro in diverse proporzioni. I risultati hanno evidenziato un'influenza del rilascio di fluoro nelle prime fasi di sviluppo del biofilm batterico ed una progressiva riduzione del rilascio di fluoro in funzione del tempo. Per questo

motivo, l'ottimizzazione della formulazione del materiale in modo da favorirne le capacità di ricarica di principio antibatterico potrebbe aiutare il controllo del biofilm per un periodo prolungato. Inoltre, i risultati hanno mostrato come il trattamento di superficie sia in grado di influenzare il processo di rilascio di fluoro dal materiale composito.

Il terzo approccio ha valutato la possibilità di modulare lo sviluppo di biofilm orale sulle superfici di materiali biomimetici, cioè progettati per interagire positivamente con i tessuti duri del cavo orale, senza l'aggiunta di molecole ad azione antimicrobica.

In questo studio, nanoparticelle di fosfato bicalcico biidrato (nDCPD) funzionalizzate con monomeri di resina sono stati incorporati in un composito sperimentale. I risultati hanno dimostrato che il composito riempito con nDCPD funzionalizzate mostrava una ridotta formazione di biofilm rispetto a un composito con nDCPD non funzionalizzate.

Tutti gli approcci analizzati hanno dimostrato di avere un impatto significativo sulla formazione di biofilm sulle superfici dei compositi. Recenti studi sul microbioma umano hanno evidenziato come in realtà i biofilm siano parte importante del corpo umano e come molte malattie, tra cui anche la carie, siano dovute ad un squilibrio tra il biofilm e l'ospite.

Infatti, recenti studi riguardanti il microbioma umano mostrano che la carie dentaria così come molte altre malattie è causata da uno squilibrio tra i biofilm e l'ospite. Lo stato di salute potrebbe quindi essere ripristinato interagendo positivamente con i biofilms, modificandone la composizione senza però tentare di eliminarli.

Per tale motivo, la possibilità di modulare la formazione di biofilm batterico sui restauri in composito ottimizzandone la formulazione e le caratteristiche di superficie senza necessariamente aggiungere un principio antibatterico sembra essere l'approccio più promettente ed interessante.

1.INTRODUCTION

1.1 **Resin-based composites: state of the art**

The composition of resin-based composites (RBCs) has evolved significantly since the materials were first introduced to dentistry more than 50 years ago. Dental composites are aesthetically pleasing since they possess tooth like appearance, they have a broad range of application on both anterior and posterior teeth and they are relatively easy to handle (Demarco, Correa, Cenci, Moraes, & Opdam, 2012). They are used for a variety of applications in dentistry, including but not limited to restorative materials, cavity liners, pit and fissure sealants, cores and build-ups, inlays, onlays, crowns, provisional restorations, cements for single or multiple tooth prostheses and orthodontic devices, endodontic sealers, and root canal posts (Ferracane, 2011).

RBCs are usually composed of a polymeric matrix, usually a dimethacrylate, reinforcing fillers, typically made from radiopaque glass, a silane coupling agent for binding the filler to the matrix, and chemicals that promote or modulate the polymerization reaction. The predominant base monomer used in commercial dental composites is Bis-GMA **(Fig.1)**.

FIg.1: Bis-GMA molecule

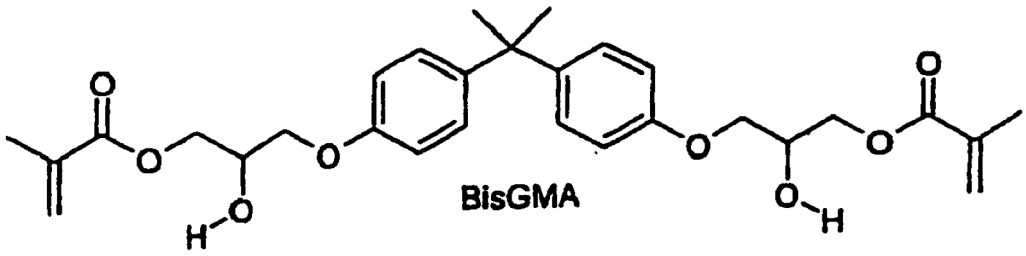

Nevertheless, the high viscosity of BisGMA limited the filler particle loading requiring the introduction of a lower molecular weight monomer such as TEGDMA, UDMA or other monomers to reduce the viscosity of the paste and allow for increased filler loading and appropriate handling characteristics (Bowen, 1963). While there have been attempts to develop different polymerization promoting systems, most RBCs are light-activated, either as the sole polymerization initiator or in a dual cure formulation containing a chemically cured component. The most common photoinitiator system is camphoroquinone (Stansbury, 2000).

Considering their consistency RBCs can be classified in Universal, Packable and Flowable. Universal RBCs are designated for both anterior and posterior restorations. These materials may present different consistencies, depending on the formulation and therefore may be placed with a syringe or an instrument (Cobb, MacGregor, Vargas, & Denehy, 2000). Packable RBCs have been required to provide handling properties like the condensability and ease of manipulation reported for amalgams. They have a high viscosity which is obtained through the modification of the filler size distribution or the addition of other types of particles (Choi, Ferracane, Hilton, & Charlton, 2000). Finally, Flowable materials have been developed and introduced to meet specific clinical requirements, such as pit and fissure sealants, repair of marginal defects, as liners in deep cavities and as stress absorbing layers. Flowable RBCs are characterised by a low viscosity usually obtained by reducing the filler amount of the mixture or through the addition of modifying agents such as surfactants. The latest are therefore able to increase the fluidity of the material while avoiding a large reduction in filler amount that would reduce the mechanical properties of the RBCs. This kind of RBCs could be arranged in cavities through fine bore syringes (Bayne, Thompson, Swift, Stamatiades, & Wilkerson, 1998).

The different types of composites could be also classified considering filler particles type and size (Lang, Jaarda, & Wang, 1992) **(Fig.2)**. The original RBCs contained macro-sized filler particles (Macrofill RBCs) with a mean size distribution of 10-100μm. They were composed by BisGMA/TEGDMA resin matrix additioned with inorganic filler particles such as quartz, borosilicate, ceramic or glass. These “Macrofill” materials were very strong, but difficult to polish and impossible to preserve surface smoothness. In order to solve the problem of long-term aesthetics, manufacturers developed the so called “Microfill RBCs”. These materials were made of finely dispersed radiolucent glass spheres with a mean size of 0.04-0.1μm. The filler level in these materials was low so they were more polishable than Macrofill RBCs but generally weak.

In order to further improve the properties or RBCs, the particle size of the conventional composites was reduced. The result was the development of composites with sub-micron particles of about 0.4-1.0 μm. These materials were called Micro-hybrids and they combined two important features: polishability and strength. Thanks to their good mechanical and aesthetic properties, they could be used both in anterior and posterior fillings so that to be considered universal composites.

The most recent innovation in this field has been the introduction of the "Nanofill" composites, developed to produce materials that are more easily and effectively polished and show improved mechanical and aesthetic properties (Mitra, Wu, & Holmes, 2003). Most manufacturers have modified the formulations of their Microhybrids to include more nanoparticles, and possibly pre-polymerized resin fillers, like those found in the Microfill RBCs. This group of material was called Nano-hybrids RBCs. Nevertheless, it is generally difficult to distinguish Nano-hybrid from Micro-hybrid RBCs since their properties are quite similar.

Nanofill and Nano-hybrid RBCs are therefore two different types of more commonly available Nanocomposites. Nanofills are made of filler particles with size of 1 to 100 nm while Nanohybrids included larger particles ranging from 0.4 to 5 μm. An alternative novel approach to the clinical application of 'Nanofill' has been the development of RBCs containing a combination of individually dispersed filler nano-particles and agglomerated nanosized particles, described as "nanoclusters". Nanoclusters has been synthesized to have controlled particle size distribution. Nanoclusters act as a bunch of grapes with an average size range of 0.6 μm. Moreover, they are also surface treated with silane to improve chemical bonding and adhesion with the organic resin matrix (M. H. Chen, 2010) (Khurshid et al., 2015).

Fig.2: Classification of dental RBCs based on filler particles type and size.

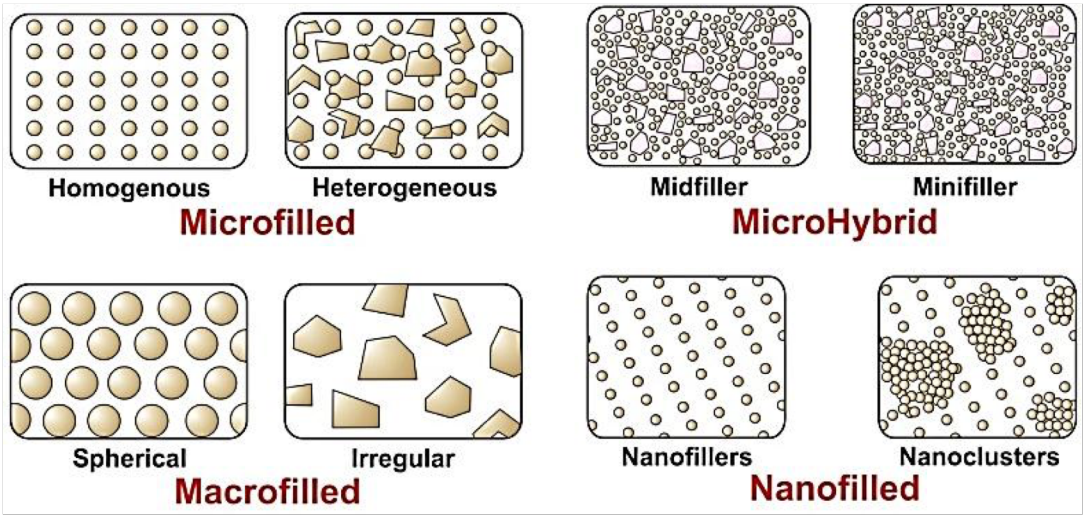

Current changes are focused on the polymeric matrix of the materials. Significant progress has been made in the development of new monomers with increased molecular weight, mainly to develop systems with reduced polymerization shrinkage or shrinkage stress and to make them self-adhesive to tooth structure.

An example was the epoxy-based silorane system (Weinmann, Thalacker, & Guggenberger, 2005) which provides lower shrinkage than typical dimethacrylate-based resins. This was due to the epoxide curing reaction that involves the opening of an oxirane ring.

Recently, a new RBC category called bulk fill composites has been introduced. The main characteristic of these materials is to be self-adapting and to offer the opportunity to be used in 4 mm-thick layers, without an increase in the polymerization shrinkage stress or a reduction of the degree of conversion (Al-Ahdal, Ilie, Silikas, & Watts, 2015).

Finally, the latest trend has been toward the development of flowable composites containing adhesive monomers. These formulations are based on traditional methacrylate systems incorporating acidic monomers like glycerolphosphate dimethacrylate (GPDM) which is typically found in dentin bonding agents. This material is therefore able to create adhesion through mechanical and possibly chemical interactions with tooth structure.

1.2 Issues related to resin-based composites

The incorporation of new monomers, new initiation systems and filler technologies have significantly improved the physical properties of RBCs, increasing their use as direct and indirect restorative materials. However, despite the continuing development these materials still present some limitations in their performances.

One of the limitation is due to the volumetric shrinkage that usually occurred during RBCs polymerization. The contraction in modern materials ranges from 1% to about 2,5% (Ilie, Jelen, Clementino-Luedemann, & Hickel, 2007) (Braga, Ballester, & Ferracane, 2005). Moreover, the polymerization process is characterized by the generation of internal stress as a rigid crosslinked structure is produced by conversion of carbon double bonds of the monomer to the physically shorter single bonds of the polymerized network (Sideridou, Tserki, & Papanastasiou, 2002) (Ferracane, 2005). Furthermore, during the polymerization process a gel point is reached. During this phase the increasing stiffness of the structure prevents further elastic deformations in response to shrinkage. This procedure generates traction forces on the adhesive system used to bond the restoration material to tooth structures. These forces, called polymerization stress, can produce cusp deformation and hard tissue micro fractures if bonding forces are higher than the contraction stress, conversely they can cause the material detachment and debonding (Fleming, Hall, Shortall, & Burke, 2005). This condition may compromise the marginal seal of the restorations placed within confined cavities and result in microleakage (Dauvillier, Aarnts, & Feilzer, 2000). The onset of marginal microgap may create microenvironment that can enhance biofilm formation and therefore the development of secondary caries (Palin, Fleming, Nathwani, Burke, & Randall, 2005). Secondary caries is a recurrence of the primary lesion in the tissues immediately adjacent to a restoration. Its onset is driven by the presence of a cariogenic biofilm colonizing the surfaces of a restoration (Deligeorgi, Mjor, & Wilson, 2001) (Mjor, 2005). Secondary caries is often cited as the most frequent reason for restoration replacement, accounting for approximately 50% of the reported replacements regardless of the restorative material (Demarco et al., 2012; Tyas, 2005) **(Fig.3a-3d)**. The latter studies reporting on over 18,229 restorations worldwide and spanning 20 years, provide data explaining the reasons for their replacement, ranking secondary caries as the predominant cause (Deligeorgi et al., 2001).

Fig. 3a: An example of the need for replacement of a RBC restoration due to secondary caries.

Fig. 3b: Clinical situation under isolation with dental dam.

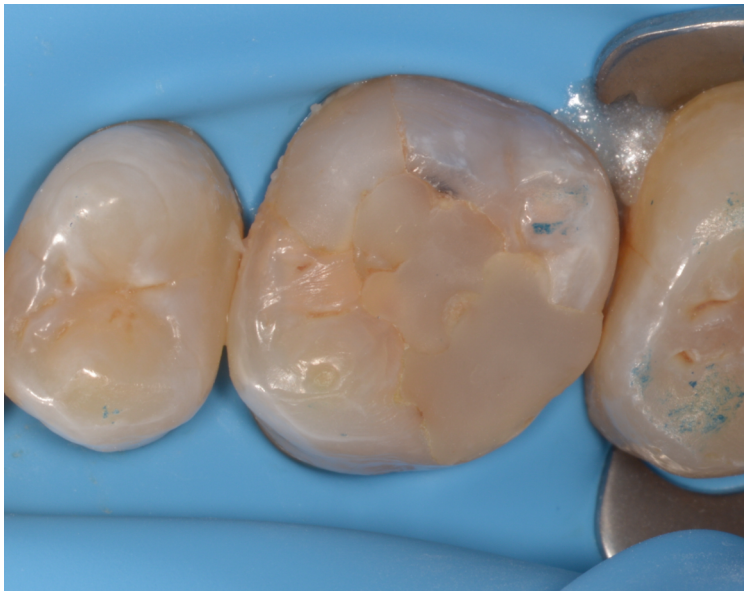

Fig. 3c: Clinical situation after the removing of the existing RBC, cleaning of the compromised tissues and preparation of the final cavity.

Fig. 3d: Clinical situation after overlay luting and before dental dam removal.

1.3 Biofilms

Biofilms are complex microbial communities in which cells can adhere to a surface and to each other. There is a high level of interest on the properties of biofilms and microbial communities across all sectors of industrial, environmental and medical microbiology.

1.3.1 Oral biofilms: composition and structure

The oral microbiome is comprised of hundreds of micro-organisms that colonize natural and artificial surfaces growing as a biofilm also known as dental plaque. Dental plaque consists of at least 800 bacterial species and this number is expected to rise into the thousands (Filoche, Wong, & Sissons, 2010) (Paster et al., 2001).
The survival of micro-organisms within the oral cavity depends on their ability to colonize oral surfaces and develop a biofilm. This process is influenced by the physico- chemical properties of the underlying surface. Oral biofilm formation follows an ordered sequence of events, resulting in a structurally- and functionally-organized, microbial community rich of different species (P. D. Marsh, 2004) **(Fig.4)**
In detail, it involves four stages:

*Pellicle coating formation***:** all surfaces exposed to the oral environment are steadily covered by a pellicle derived from the adsorption of organic and inorganic molecules to tooth, RBCs or prosthetic surfaces. These molecules are mainly derived from saliva and act as receptors for bacteria. This phase is very important since the pellicle mediates the interactions among oral surfaces, oral fluids and microorganisms (C. Hannig & Hannig, 2009). The formation of the salivary pellicle could mask the effect of these interactions. This aspect should be considered especially when evaluating the use of dental materials with their physico-chemical surface properties. Nevertheless, bacterial adhesion is more influenced by long-range forces transferred through the pellicle layer. The salivary pellicle is also important since it mediates demineralization and remineralization processes and contains antibacterial components such as IgA and Lysozyme (M. Hannig & Joiner, 2006).

Reversible adhesion: Brownian motion and salivary flow lead to an initial transport of single microbial cells or microbial aggregates near to the solid substrates. This phase involves the

formation of weak, long-range, reversible physico-chemical interactions between microbial surface structures and salivary pellicle coating.

Irreversible adhesion: this phase includes the formation of a firm and strong anchorage between bacteria and surface by specific interactions such as covalent, ionic or hydrogen bonding.

Co-adhesion and biofilm formation: in this last phase, secondary colonizers adhere to the receptors of firmly attached microorganisms leading to an increase in biofilm development.

The biofilm mode of growth is thus clearly distinguished from planktonic growth. This is why biofilms express properties not shown by the same organisms growing in planktonic form. For instance, biofilms are able to resist to antimicrobial agents concentrations 1000 times higher than that necessary to kill microorganisms in planktonic form (Jenkinson & Lamont, 2005).

Fig.4: SEM (scanning electron microscopy) micrograph of a biofilm grown on an enamel specimen. The scale bar for all images is 10 μm (×2,000 magnification).

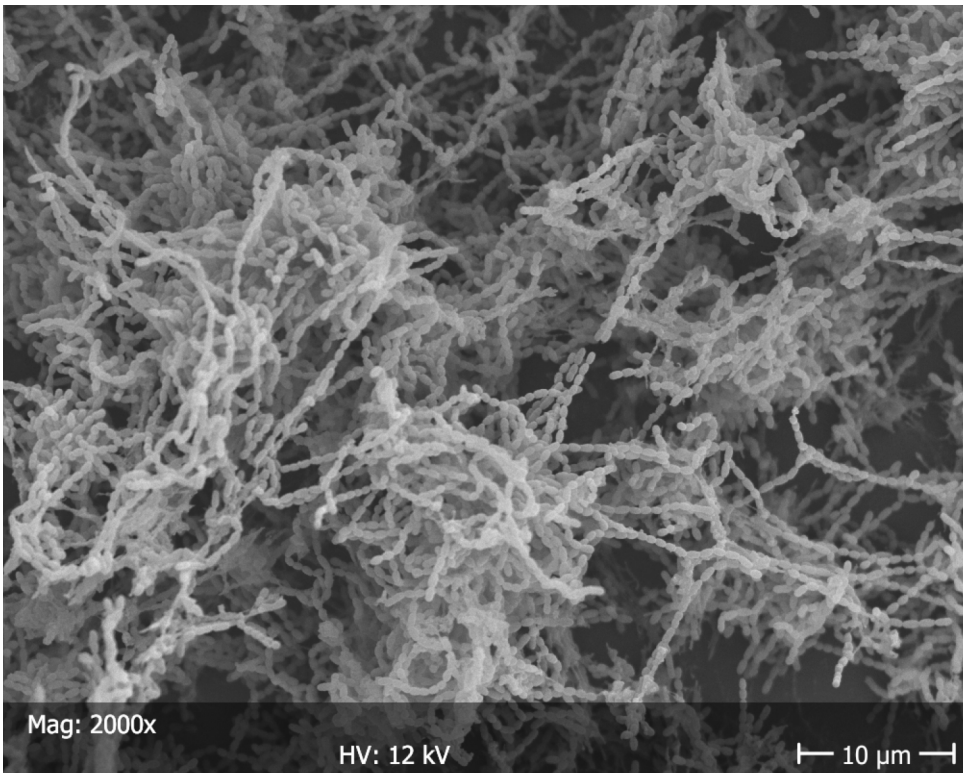

1.3.2 Oral Biofilms and dental caries

Biofilms in the oral cavity do not exist as independent entities but function as a co-ordinated, spatially organized and fully metabolically integrated microbial community with properties that are greater than the sum of the component. In health conditions this complex ecosystem usually exists in commensal harmony with the host. Shifts in this equilibrium may lead to dysbiosis and promote the onset and progression of oral diseases such as dental caries, periodontal disease, and mycoses (Jenkinson, 2011) (P. D. Marsh, 2012). Therefore, the development of plaque-mediated disease should be considered a breakdown of the homeostatic mechanisms that normally maintain a beneficial relationship between the resident oral microflora and the host.

Dental caries is a very common infectious disease driven by the metabolic activity of a pathogenic biofilm (Selwitz, Ismail, & Pitts, 2007) while secondary caries is the recurrence of caries at the tooth–restoration interface [5]. In dental caries, indeed, there is a shift toward community dominance by acidogenic and acid-tolerating species including *Streptococcus mutans* (*S. mutans), Streptococcus sobrinus* (*S. sobrinus*), and lactobacilli, spp. although other species with relevant traits may be involved (P. D. Marsh, 2006). The presence of bacteria between the tooth and restoration is a major challenge and may promote the demineralization of the tooth interface thereby contributing to the onset of postoperative sensitivity, secondary caries, pulp inflammation, and necrosis (Svanberg, Mjör, & Ørstavik, 1990). Among the species colonizing the cariogenic biofilm, *S. mutans* is considered the key etiological agent of the disease and is one of the primary inhabitants present at the marginal interface (Forssten, Bjorklund, & Ouwehand, 2010). *In vivo* and *in vitro* studies have indeed shown that mutans streptococci are the main bacteria isolated in plaque samples from natural and artificial surfaces during the early stages of caries development (Kleinberg, 2002) (Sbordone & Bortolaia, 2003).

Initial bacterial adhesion on tooth surfaces preferably starts where surface irregularities such as cracks, grooves and abrasion defects are present.

The susceptibility of restorative materials to microorganism adhesion is considered of outmost importance for their longevity in the oral cavity. Among dental restorative materials, RBCs are particularly susceptible to the development of biofilms (He, Söderling, Österblad, Vallittu, & Lassila, 2011).

This aspect may be due to the presence of unreacted monomers leaching out and promoting the growth of cariogenic bacteria or to the surface roughness features that may simplify bacterial adhesion (Beyth, Bahir, Matalon, Domb, & Weiss, 2008). It may nevertheless be that both factors play a role in the growth of bacteria on resin composites (Cazzaniga, Ottobelli, Ionescu, Garcia-Godoy, & Brambilla, 2015). Furthermore, it has been suggested that *S. mutans* also has esterase activities at levels capable of degrading RBCs and adhesive system (Bourbia, 2013).

It has been demonstrated that biofilms formed on RBCs are different from those developed on natural, sound hard tissues: they mainly contain microorganisms able to survive a highly acidic environment, such as streptococci and lactobacilli (Auschill et al., 2002). The study of the relationships between resin-based dental materials and oral biofilm formation would be the key to better understand the problems related to caries development(Beyth et al., 2008).

The design of restorative materials featuring unfavourable conditions for microbial adhesion and biofilm formation is therefore a promising approach in contemporary dental materials science.

1.3.3 Microbiological models to study oral biofilms

It is well documented that bacteria in biofilms, including *S. mutans* , are considerably more resistant to treatment with antimicrobials than their planktonic counterparts(Tenover, 2006). This implies that the efficacy of caries-preventive compounds should be evaluated in biofilms and not in the traditional liquid cultures.

Biofilms can be studied according to different models: *in vivo*, *in situ* or *in vitro* (C. Hannig & Hannig, 2009).

Nevertheless, the complexity of the oral environment, and ethical problems associated with *in vivo* studies in humans have inevitably led to the development of laboratory models aimed at simulating the oral environment *in vitro*. These model systems are usually called ‘artificial mouth’ (AM). The basis of an artificial mouth model is to provide a continuous or intermittent supply of nutrients to bacterial plaque or biofilms growing within an environment, which mimics the *in vivo* oral niches and habitats. During such experimental procedures, real-time growth and development of dental plaque/biofilm can be observed with different microscopy tools or analysed using microbiological, biochemical and molecular methods. Broadly speaking, such models may be used to replicate environmental

controlled conditions within the laboratory and experiments can be repeated by applying a standardized protocol in order to examine the specific role of each parameter before performing an *in situ* testing.

The Drip-flow reactor (DFR) is one of the widely-used reactor to perform *in vitro* studies. The DFR is a plug-flow reactor since the nutrient concentration change along the length of the coupon. The flow of nutrient in the DFR can be laminar or turbulent depending on the density and viscosity of the liquid, the flow velocity and the geometry of the reactor. The main features of the DFR are the following (Adams et al., 2002):

- The biofilm is formed close to the air–liquid interface. This reactor is therefore ideal to model environment like the oral cavity,
- The gas in the head space may be varied to accommodate the growth of various anaerobic biofilms,
- The Biofilm developed into the DFR can be easily analyzed using various techniques, including MTT assay, viable plate counts, confocal microscopy(Xu, McFeters, & Stewart, 2000) **(Fig.5)**,
- The design of the DFR allows the evaluation of the efficacy of disinfectant or antimicrobial agents on biofilm formation (Stewart, Rayner, Roe, & Rees, 2001),
- The design of the DFR allows the evaluation of biofilm formation on different surfaces (RBCs, implant…).

The continuous culture system used in our laboratory is a modified version of commercially available Drip Flow Reactor (MDFR 110, BioSurface Technologies, Bozeman, MT, USA) **(Fig.6-7).** The modified design allows the use of customized PTFE specimen trays to maintain the specimen surfaces into the flowing medium. A multichannel computer-controlled peristaltic pump (RP-1, Rainin, Emeryville, CA, USA) is used to obtain a constant flow of nutrient medium through the flow chambers.

Fig. 5: 3D reconstruction from a confocal laser-scanning microscopy (CLSM) field showing initial biofilm formation on a RBCs specimen. Live/ Dead stain is applied (Syto9/propidium iodide). Live bacteria exhibited green fluorescence and bacteria with compromised membranes exhibited red fluorescence.

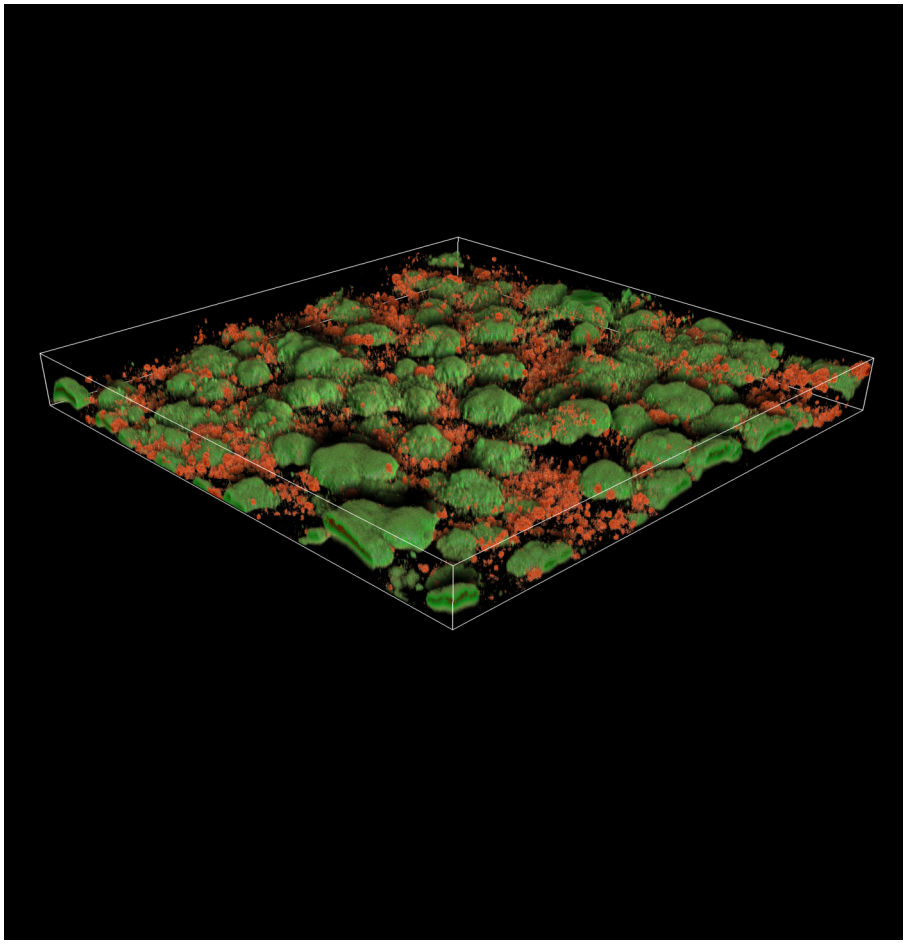

Fig.6: The MDFR operation diagram.

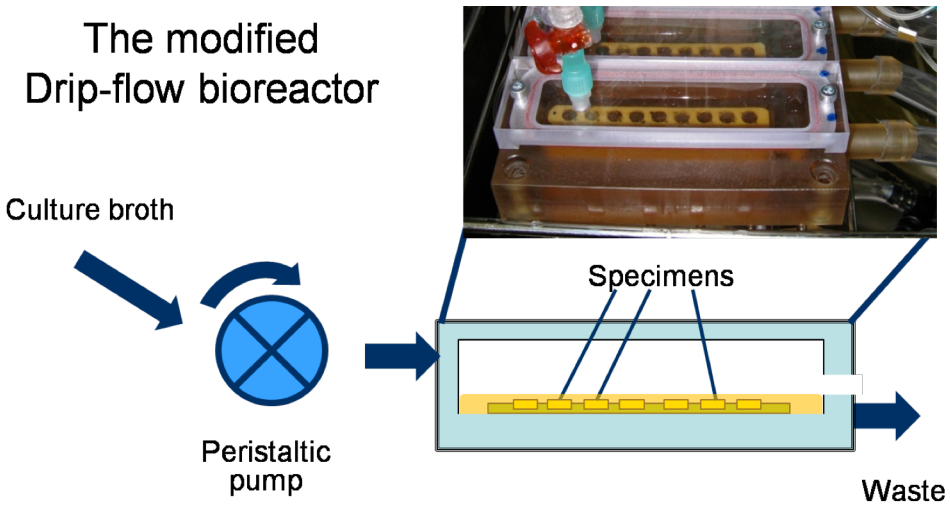

Fig.7: The MDFR device assembled inside the thermostat.

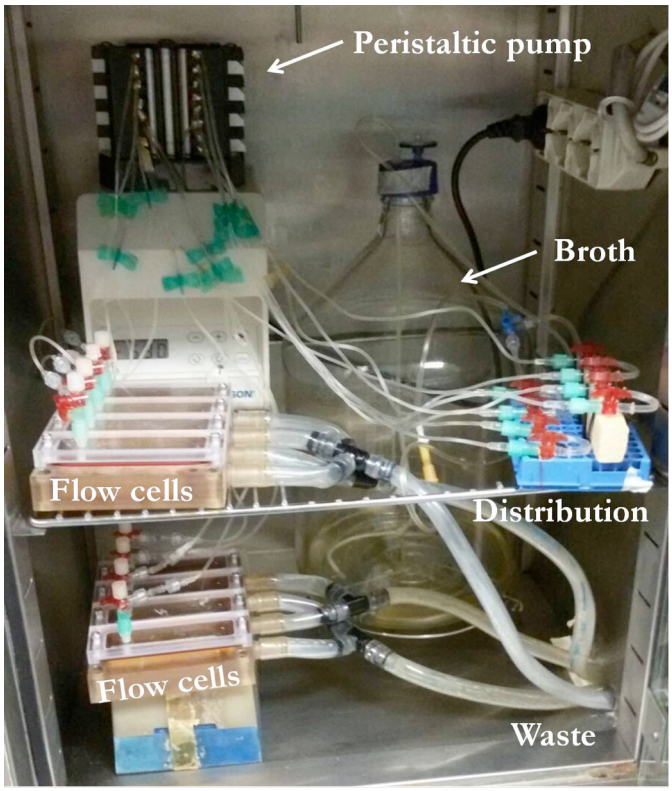

1.4 Strategies to control oral biofilm formation

The development of RBCs that may actively inhibit biofilm formation on their surfaces is a promising approach in contemporary dental materials science.

Extensive research has been devoted in developing new restorative materials able to modulate biofilm formation and therefore prevent the occurrence of secondary caries by protecting hard tissues surrounding the restorations and incorporating different antibacterial agents into resin composite formulations (F. G. Lima, Romano, Correa, & Demarco, 2009). Regarding RBCs, promising strategies include the development of materials with contact-killing surfaces and materials featuring a long-term release of antibacterial agents (S. Imazato, 2009; Wiegand, Buchalla, & Attin, 2007).

Furthermore, biofilm formation on the surface of conventional RBCs can also be modulated by an optimization of their surface properties focused on tailoring non-adhesive surfaces that feature nano-texturing and easy-to-clean properties (M. Hannig, Kriener, Hoth-Hannig, Becker-Willinger, & Schmidt, 2007).

A completely different approach is based on the design of biomimetic materials able to promote the remineralization of natural tooth tissues adjacent to the restoration (Langhorst, O'Donnell, & Skrtic, 2009; Skrtic, Antonucci, Eanes, Eichmiller, & Schumacher, 2000).

1.4.1 Materials featuring a long-term release of antibacterial agents

The development or resin-based materials with controlled release of antimicrobial agents has involved many researchers from all over the world **(Fig. 8-9)**. The design of these materials is frequently characterized by the addition of soluble antimicrobials such as metal ions, quaternary ammonium compounds, chitosan, chlorhexidine or fluoride into the resin matrix of RBCs.

Fluoride has been introduced into resin composites by a variety of compounds (Arends, Ruben, & Dijkman, 1990; Dijkman, De Vries, Lodding, & Arends, 1993). The antimicrobial effects of fluoride can be explained by its ability to inhibit not only the glycolytic enzyme enolase and the proton-extruding ATPase, but also bacterial colonization.

Fluoride release from restorations can provide bactericidal activity and further increase remineralization by the formation of fluoroapatite (Feagin & Thiradilok, 1979). Moreover, an *in vitro* study showed that fluoride ions in high concentrations are also able to inhibits the

metabolism of the two prominent microorganisms involved in dental caries, *S. mutans* and *S. sobrinus* (Seppä, Torppa-Saarinen, & Luoma, 1992).

Several restorative materials are currently available on market, including glass ionomer cements, resin modified glass ionomer cements, polyacid modified resin composites (compomers), resin composites and fissure sealants (Burke, Ray, & McConnell, 2006). However, it appears that the release of fluoride from RBCs is too low to have a significant effect on cariogenic biofilms (Burke et al., 2006). In fact, clinical studies have failed to prove a significant antimicrobial effect of fluoride-releasing dental materials, in spite of the promising *in vitro* results (Wiegand et al., 2007).

Another problem related to the incorporation of antimicrobials into RBCs is an adverse influence on materials mechanical properties (Jedrychowski, Caputo, & Kerper, 1983). This issue is probably due to the disturbance monomers curing or the interference of binding of the filler and matrix phases by the incorporated agent.

Fig. 8: Schematic representation of biofilm formation on a RBC featuring a long-term release of antibacterial agent.

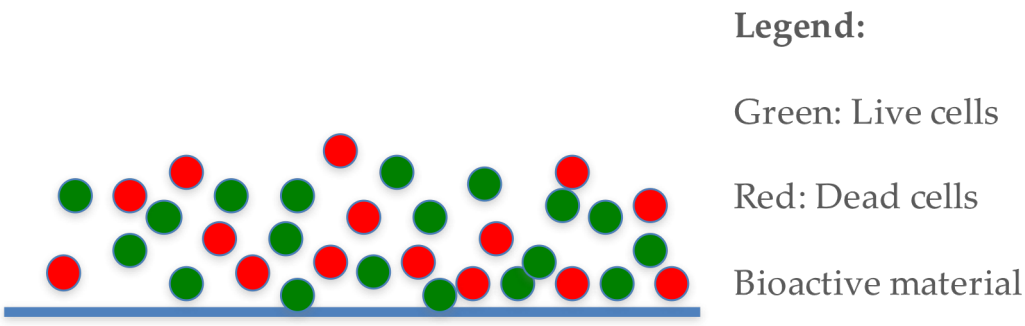

Fig. 9: CLSM image of a biofilm developed on a RBC featuring a long-term release of antibacterial agent. Green represents live bacteria and red represents non-viable, dead bacterial cells. The release of the antibacterial agent cause the presence of a high number of dead bacteria (red) into the biofilm.

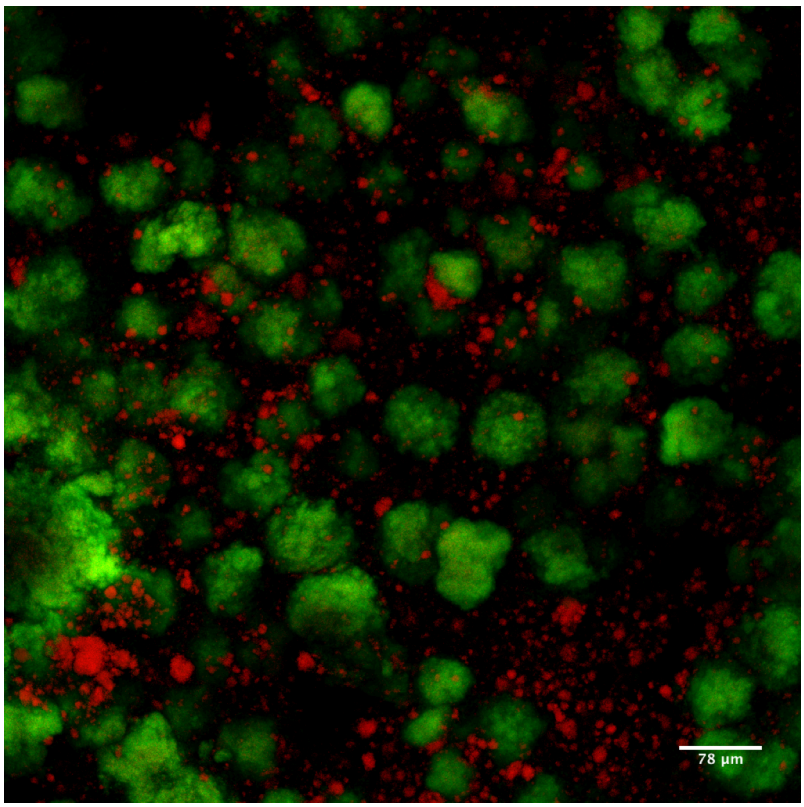

1.4.2 Materials with contact-killing properties

Current strategies also focus on tailoring resin-based materials with contact-killing properties. This is a unique approach to achieve antibacterial composites in which the antimicrobial agent is firmly incorporated within the matrix and is not supposed to be released. For example, materials featuring the inclusion of monomeric cationic quaternary ammonium compounds (QAC) such as MDPB (methacryloyloxydodecylpyridinium bromide) or MAPTAC ([3-(methacryloylamino)propyl] trimethylammonium chloride) have been introduced (Satoshi Imazato, Chen, Ma, Izutani, & Li, 2012; Li Mei, Ren, Loontjens, van der Mei, & Busscher, 2012). Another class of antibacterial composites, incorporating silver (Ag) particles has been recently reported to reduce biofilm viability and inhibit biofilm growth (Wang, Shen, & Haapasalo, 2014).

The antibacterial monomer copolymerizes with other monomers after RBCs curing and is covalently bonded to the polymer network. The immobilized agent does not leach out from the material but acts as a contact inhibitor against the bacteria which attaches to the surface **(Fig.10-11)**.

One of the advantages of RBCs with contact-killing properties is the long-lasting antibacterial effect. It has been shown that no influence on the mechanical properties and curing behavior were other advantages of these materials (S. Imazato & McCabe, 1994). On the contrary, other studies found that incorporation of QAC into the resin composite significantly affects the mechanical properties by increasing water absorption which significantly alters the mechanical properties of the materials (Weng et al., 2011) (Dermaut, Van den Kerkhof, van der Veken, Mertens, & Geise, 2000).

RBCs featuring contact-killing properties show the antibacterial effects only against bacteria which come in contact with the immobilized antibacterial molecules, so its effect is not able to reach the area around the filled composites. Nevertheless, it has been hypothesized that the antibacterial agent may probably leach from the polymer matrix and diffuse on the surface, influencing bacterial activity and growth due to the impossibility of achieving a complete copolymerization of the antibacterial monomer with the other primer ingredients (Eugenio Brambilla et al., 2013).

Furthermore, the effect of the antibacterial component immobilized is mainly bacteriostatic as the agent cannot penetrate through the cell wall or membrane unlike free antimicrobials.

Fig. 10: Schematic representation of biofilm formation on a RBC with contact-killing properties.

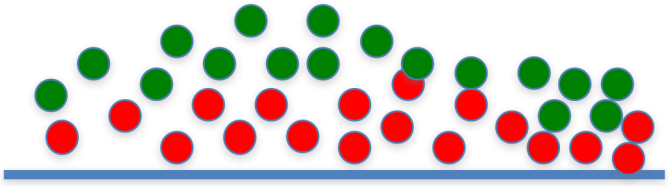

Legend:

Green: Live cells

Red: Dead cells

Bioactive material

Fig11: CLSM image shows biofilm formed on the surfaces of a contact-killing dental material.

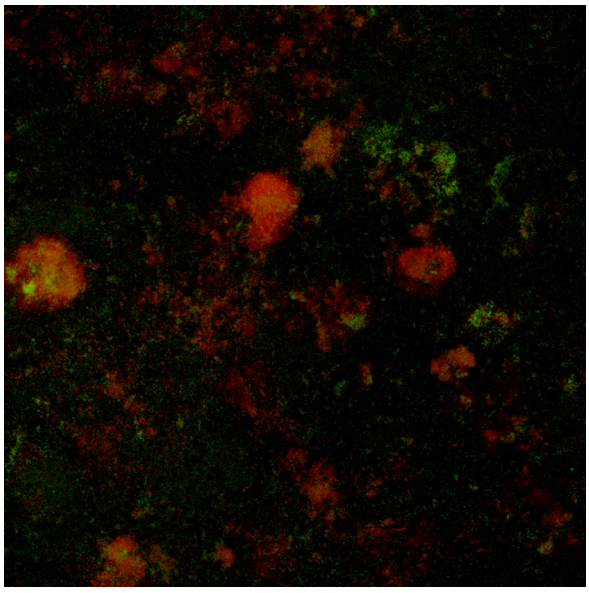

1.4.3 Materials featuring non-adhesive surfaces: optimizing materials formulation without the addition of antibacterial agents

Biofilm formation on the surface of conventional RBCs can be modulated by an optimization of their surface properties without the addition of any antibacterial agent (M. Hannig et al., 2007). It has been show that a reduction of SR and SFE of a dental material may lead to a decrease in microbial adhesion and biofilm formation (Cazzaniga et al., 2015) (Teughels, Van Assche, Sliepen, & Quirynen, 2006). However, modern commercially available RBCs already yield a SR that is by far lower than the commonly accepted threshold value at 0.2 μm (Bollen, Lambrechts, & Quirynen, 1997), suggesting that this parameter does not further impact biofilm formation.

Furthermore, it has been highlighted that commercially available RBCs may present differences in viable microbial biomass, even in presence of similar SR and SFE values (A. Ionescu et al., 2012). This phenomenon has been attributed to different degrees of resin matrix exposure on the surface of the different RBCs. Surface parameters such as the chemical composition and topography might be therefore considered key parameters for optimizing the RBCs surface properties to reduce biofilm formation.

1.4.4 Materials featuring biomimetic properties

The last goal of clinical intervention is the preservation of tooth structure and the prevention of lesions progression with crystallites able promote remineralization and control biofilm formation at the tooth surface.

Recently, the application of nano-scaled hydroxyapatite particles has been shown to affect oral biofilm formation and provide a remineralization capability. Biomimetic approaches are based on the use of hydroxyapatite nanocrystals which allow adsorbed particles to interact with bacterial adhesins, reduce bacterial adhesion and therefore have an impact on biofilm formation (Langhorst et al., 2009).

1.4.5 Considerations on the different approaches

The key to ultimately impacting secondary caries and marginal breakdown may be to effectively control and reduce the growth of cariogenic bacteria at the marginal interface. All the evaluated approaches may show promising possibilities in modulating biofilm

formation on materials surfaces. However, it has been shown that the addition of an antibacterial agent into RBCs formulation may show problems related to a prolong effect on biofilm formation or may alter the mechanical properties of the material.
It has been also highlighted that the optimization of RBCs formulation as well as alteration of surface morphology may have an impact on biofilm formation. Moreover, RBCs surface features and surface chemistry may influence the capability of the material to release an antibacterial agent. The development of biomimetic materials may also represent a good innovation in this field.

1.5 Aims of this PhD thesis

The aim of this PhD thesis was to explore different approaches in order to discriminate the parameters influencing the microbiological behaviour of resin-based dental materials and therefore allow the optimization of materials formulation. Hence, the final aim was to promote the development of materials able to successfully control oral biofilm development and the interactions between the host and biofilms thus preventing the occurrence of secondary caries.

2 EXPERIMENTS

Different promising research field already mentioned in the introduction of the thesis were investigated. Particularly, studies were made to evaluate the optimization of resin-based dental materials formulation and surface features in order to develop an anti-adhesive material. Moreover, the development of a material featuring antibacterial properties or a biomimetic material were analysed.

Considering the first approach, the optimization of the microbiological properties of resin-based dental materials was evaluated from different points of view. Experimental RBCs with different compositions were studied (cf. 2.1), hypothesizing that surface features and nanotexture of the tested materials would have influenced microbial biofilm formation. The anti-adhesive properties of the tested materials were evaluated as a possible effective way to control biofilm formation without the need of antibacterial agents. Conversely, different commercially available RBCs were submitted to diverse finishing and polishing protocols in order to evaluate the influence of these procedures on the surface features and on the microbiological behaviour of each material (cf. 2.2).

Regarding the second research field, the microbiological behaviour of experimental RBCs derived from a commercial formulation including different fractions of fluoride-releasing S-PRG filler particles was evaluated (cf. 2.3).

The third research field evaluated the possibility that biomimetic materials (designed to positively interact with dental hard tissues) may control oral biofilm formation, without the addition of specific antimicrobial agents (cf. 2.4).

2.1 Optimization of RBCs microbiological properties without the addition of antibacterial compounds

Biofilm formation on the surface of conventional RBCs can be modulated optimizing their surface properties. It has been therefore suggested that surface parameters such as the chemical composition and topography might be key parameters for optimizing the surface properties of RBCs in order to reduce biofilm formation on their surfaces.

Thus, the aim of the present study was to analyse the formation of biofilms on the surface of experimental RBCs differing in matrix composition and filler fraction, hypothesizing that biofilm formation on the experimental RBCs shows a dependency on the resin matrix composition (1) and filler fraction (2) employed.

2.1.1 Materials and methods

Specimens preparation

Eight experimental RBC formulations differing in resin matrix chemistry and filler fraction **(Table 1)** were prepared by VOCO (Cuxhaven, Germany). For preparation of a single specimen, a standardized amount of uncured RBC was packed into a custom-made steel mould with a diameter of 6.0 mm and a height of 1.5 mm, condensed against a glass plate covered by a cellulose acetate strip to prevent the formation of an oxygen-inhibited layer, and light-cured in direct contact for 40 sec using a hand-held light-curing device (LCU; SDI Radii plus, SDI, Bayswater, AUS; 1500 mW/cm2). All specimens were subjected to a standardized polishing protocol, including polishing with 1000/4000-grit grinding paper (Buehler, Lake Bluff, IL, USA) and a polishing machine (Motopol 8; Buehler, Düsseldorf, Germany) as well as final manual finishing with a polisher designed for RBC materials (Dimanto, VOCO). All specimens were stored under light-proof conditions in distilled water for six days at 37±1°C for minimizing the impact of residual monomer leakage on cell viability and were subsequently carefully cleaned using ethanol (70%) and applicator brush tips (3M ESPE, Seefeld, Germany) prior to further processing.

Anterior human teeth extracted for clinical reasons were obtained from the Oral Surgery Unit at the Department of Health Sciences (Milan, Italy). Round enamel-dentin slabs with a diameter of 6.0 mm and a thickness of 2.5 mm were cut from the labial surfaces using a water-cooled trephine diamond bur (INDIAM, Carrara, Italy). Dentin bottoms were removed, and the enamel surfaces were polished with a diamond bur (Intensiv SA, Grancia, Switzerland).

Table 1: Experimental RBCs employed in this study and their composition.

Label	**Matrix blend**	**Filler**
Phi1	BisGMA/ TEGDMA 7/3	coarse 65% wt. dental glass mean particle size 7 µm
Phi2	BisGMA/ TEGDMA 7/3	fine 65% wt. dental glass mean particle size 0.7 µm
Phi3	BisGMA/ TEGDMA 7/3	nano 65% wt. SiO_2 mean particle size 20 nm
Phi4	BisGMA/ TEGDMA 7/3	neat resin blend
Pho1	UDMA/ aliphatic dimethacrylate 1:1	coarse 65% wt. dental glass mean particle size 7 µm
Pho2	UDMA/ aliphatic dimethacrylate 1:1	fine 65% wt. dental glass mean particle size 0.7 µm
Pho3	UDMA/ aliphatic dimethacrylate 1:1	nano 65% wt. SiO_2 mean particle size 20 nm
Pho4	UDMA/aliphatic dimethacrylate 1:1	neat resin blend

Surface analysis

Surface roughness

Peak-to-valley surface roughness (Ra) was determined on four randomly selected specimens for each material using a profilometric contact surface measurement device (Perthen S6P, Feinprüf-Perthen, Göttingen, Germany)**(Fig.12)**. A distance of 1.75 mm was measured in one single line scan perpendicular to the expected grinding grooves using a standard diamond tip (tip radius 2 µm, tip angle 90°) and a cut off level of 0.25. For high-resolution visualization of the surface topography, two specimens for each material were imaged with an atomic force microscope (AFM). Images with a size of 2 µm x 2 µm were recorded with a noncontact atomic force microscope using qPlus force sensors (Giessibl, 2000; D. S. Wastl

et al., 2013; Wastl, Weymouth, & Giessibl, 2013). The imaging technique was frequency modulation AFM (Albrecht, Grütter, Horne, & Rugar, 1991).

Fig.12: Schematic representation of a profilometric contact surface measuerement device

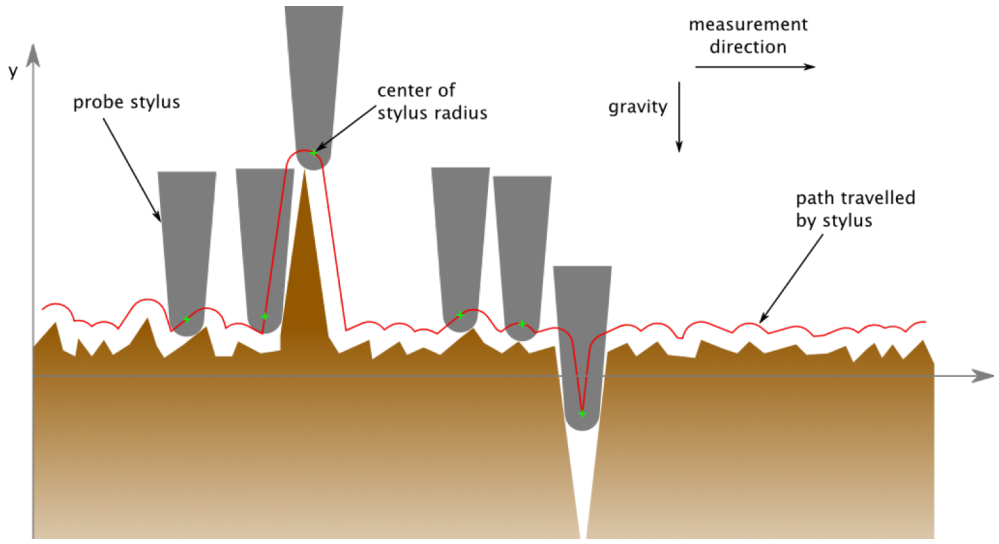

Surface free energy

Contact angles of bidistilled water, diiodomethane, and ethylene glycol were determined using the sessile drop method and a computer-aided contact angle measurement device (OCA 15plus, DataPhysics Instruments GmbH, Filderstadt, Germany). Ten drops of each liquid with a drop volume 0.2 µL were analysed on each of three randomly selected specimens for each material. The surface free energy was calculated according to an approach introduced for the description of polymeric surfaces by Owens and co-workers (Owens & Wendt, 1969). Data were indicated as total SFE, given by the summation of its disperse and polar contribution.

Energy-dispersive X-ray Spectroscopy (EDS)

Five randomly selected specimens for each material were subjected to surface analysis (EDAX Genesis 2000, Ametek GmbH, Meerbusch, Germany) for determination of surface chemistry and composition.

Bacteria

Monospecies *S. mutans* biofilm formation (n = 8) was simulated as described previously (A. Ionescu et al., 2012). In brief, a wild strain of *S. mutans* was isolated from human dental plaque and cultured on Mitis salivarius bacitracine agar. In order to confirm the isolated strain type, biochemical identification was performed with an automatic device (Vitek, BioMerieux; Marcy-L'Etoile, France) using specific single-use cartridges for *S. mutans* identification. A single colony of the isolated *S. mutans* strain was cultured in Trypticase soy broth (TSB) for 24 h at 37 °C in a 5 % supplemented CO_2 environment. Cells were harvested by centrifugation (2,200 rpm, 19 °C, 5 min), washed twice with sterile phosphate buffered saline (PBS), and were then resuspended. The optical density of the cell suspension was adjusted to 0.3 OD units at 550 nm (Genesys 10-S, Thermo Spectronic, Rochester, USA), corresponding to a microbial concentration of 3.6×10^8 cells/mL.

Multispecies biofilm formation (n=8) was simulated in accordance with a previously published protocol (Ledder, Madhwani, Sreenivasan, De Vizio, & McBain, 2009). Briefly, human whole saliva was collected by expectoration from two healthy volunteer donors who gave their informed consent to participate. The donors refrained from oral hygiene for 24 h, did not have any active dental disease, and had refrained from consumption of antibiotics for at least three months prior to the experiments. The saliva was collected during a single occasion within 30 min; the saliva samples were subsequently pooled prior to further processing.

Modified drip-flow biofilm bioreactor (MDFR)

Biofilm formation was simulated under continuous flow conditions using a modified commercially available drip-flow reactor (MDFR; DFR 110, BioSurface Technologies, Bozeman, MT, USA).

The modified design enabled the placement of customized specimen-trays on the bottom of the flow cells and the complete immersion of the surfaces of the specimens into the surrounding flowing medium **(Fig. 6-7)**. All remaining specimens were placed in Teflon trays which fixed the specimens tightly and exposed their surfaces to the surrounding medium; the trays were fixed on the bottom of each flow chamber of the MDFR. All tubing and specimen-containing trays were sterilized before the beginning of biofilm formation using a chemiclave with hydrogen peroxide gas plasma technology (Sterrad; ASP, Irvine,

CA, USA). By limiting the maximum temperature to 45°C, heat-related damages of the specimens or their coating were avoided.

The whole apparatus was then assembled under a sterile hood and transferred into an incubator in order to operate with a temperature of 37°C. Each chamber of the MDFR was inoculated with 10 mL of *S. mutans* suspension in early log phase to allow bacterial adhesion. After 4 h, a constant flow of nutrient broth (TSB, 1.2 g/L supplemented with 1 % sucrose (Klein et al., 2010)) with a flow rate of 9.6 mL/h was provided using a multichannel, computer-controlled peristaltic pump (RP-1; Rainin, Emeryville, CA, USA).

In the multispecies biofilm model, after assembly of the MDFR, it was inoculated with sterile culture medium including 2.5 g/L mucin (type II, porcine gastric), 2.0 g/L bacteriological peptone, 2.0 g/ L tryptone, 1.0 g/L yeast extract, 0.35 g/L NaCl, 0.2 g/L KCl, 0.2 g/L CaCl2, 0.1 g/L cysteine hydrochloride, 0.001 g/L hemin, and 0.0002 g/L vitamin K1. After 24 h, 5 mL of pooled saliva were inoculated into each flow-cell and microbial adherence was allowed for 4 h. Subsequently, a constant flow of culture medium was provided, employing a flow rate of 9.6 mL/h.

Viable biomass assessment (MTT assay)

Viable biomass adherent to the specimens was analysed using a MTT-based assay.

Test reagents for the MTT assay were prepared as follows: two starter MTT stock solutions were prepared by dissolving 5 mg/mL 3-(4,5)- dimethylthiazol-2-yl-2,5-diphenyltetrazolium bromide in sterile PBS, and 0.3 mg/mL of N- methylphenazonium methyl sulphate (PMS) in sterile PBS. The solutions were stored at 2°C in light-proof vials until the day of the experiment, when a fresh measurement solution (FMS) was made by mixing 1 mL of MTT stock solution, 1 mL of PMS stock solution and 8 mL of sterile PBS. A lysing solution (LS) was prepared by dissolving 10% v/v of sodium dodecyl sulphate (SDS) and 50% v/v of dimethylformamide (DMF) in distilled water and stored at 2°C until the day of the experiment, when it was warmed at 37°C for 2 h before use.

After 48 h, the continuous flow of nutrient broth was halted; the specimen carriers were then carefully removed from the flow chambers and the specimens were carefully detached from the tray using a pair of sterile tweezers, passed into a dish containing sterile PBS at 37°C in order to remove non-adherent cells, and finally placed into the wells of sterile 96-well plates. MTT test solutions were added, then 80 μL of the final aliquots were transferred to 96-well plates and the absorbance was measured using a spectrophotometer (Genesys 10-S) at a

wavelength of 550 nm; results were displayed as optical density (OD) units, which are directly proportional to the number of viable adherent cells.

Statistical analyses

Statistical analyses were performed using JMP 10.0 software (SAS Institute, Cary, NC, USA). Homogeneity of variances was preliminarily checked and verified using Bartlett‘s test. One- way ANOVA was employed to investigate differences in surface roughness and surface free energy between the various materials, guided by subsequent post-hoc analysis using the Tukey-Kramer multiple comparison test where appropriate. Two-way ANOVA was employed to investigate differences in biofilm formation regarding filler fractions and resin matrix blend as fixed factors. Student–Newman–Keuls post-hoc test was employed to analyse significant differences where appropriate. The level of significance (α) was set to .05.

2.1.2 Results

Surface roughness

One-way ANOVA identified significant differences between the different materials (P<.001). Phi1 and pho1 showed significantly higher surface roughness than all other materials (P<.018). Intermediate surface roughness was identified for phi4 and pho4 as well as enamel; significantly lowest values were identified for the RBCs with nano-scaled and fine filler particles **(Table 2)**. AFM images **(Fig.13)** highlighted differences in surface topography in dependence on the different filler fraction.

Surface free energy

Surface free energy data for the different experimental RBCs is displayed in **Table 2**. One-way ANOVA identified significant differences in total surface free energy between the different materials (P<.001); significantly lowest values were identified for enamel (P<.001), and significantly highest values for pho4 (P<.008). Regarding the disperse contribution to the total surface free energy, significant differences between the materials were identified (P<.001), suggesting the lowest disperse contribution for enamel and the significantly

highest disperse contribution for pho4 (P<.004). No significant differences in the polar contribution to total surface free energy were identified between the various materials (P=.333).

Energy-dispersive X-ray Spectroscopy (EDS)

EDS data for the different experimental RBCs is displayed in **Table 2.** EDS analysis indicated pronounced differences in the chemical surface composition. Incorporation of filler particles led to a general decrease in the carbon content and an increase in the silicon content of the RBC surfaces.

Table 2 : Surface features of the experimental RBCs tested. Means and standard deviations (SD) are shown for surface roughness and surface free energy. Chemical surface composition data as assessed by EDS are indicated (%).

Exp. RBC label	**R_a (μm)**	**Surface Free Energy (mJ/m^2)**			**EDS (%)**			
		Total	**Disperse**	**Polar**	**C**	**O**	**Si**	**Al**
Phi1	.11 (.00)	41.7 (1.9)	38.9 (1.8)	2.8 (2.0)	51.6	33.1	9.7	1.5
Phi2	.04 (.00)	42.5 (1.7)	40.0 (1.1)	2.3 (.8)	46.0	36.3	9.8	2.1
Phi3	.05 (.02)	42.5 (1.8)	40.3 (2.3)	2.2 (1.1)	36.8	41.0	22.2	-
Phi4	.08 (.03)	43.4 (2.8)	40.2 (2.3)	3.2 (1.8)	81.3	17.9	.6	-
Pho1	.21 (.03)	44.1 (1.5)	42.0 (2.0)	2.2 (1.9)	51.8	36.0	8.1	1.3
Pho2	.04 (.00)	41.2 (3.1)	40.0 (3.2)	2.2 (1.1)	44.6	47.7	5.4	1.2
Pho3	.04 (.00)	42.2 (2.0)	39.8 (1.9)	2.4 (1.8)	46.2	45.2	8.3	.15
Pho4	.08 (.03)	47.6 (2.8)	44.5 (2.3)	3.0 (2.1)	83.8	14.9	.4	-
Enamel	.07 (.02)	36.9 (2.4)	35.9 (2.3)	.9 (.7)	7.5	36.4	-	-

Fig. 13: Atomic force microscopic images of the surfaces of the different RBCs employed in the present study. Green shades (2a-2d) show the experimental composites with hydrophilic resin matrix; red shades (2e-2h), the experimental composites with hydrophobic resin matrix; the yellow shade display the human enamel surface (2i).

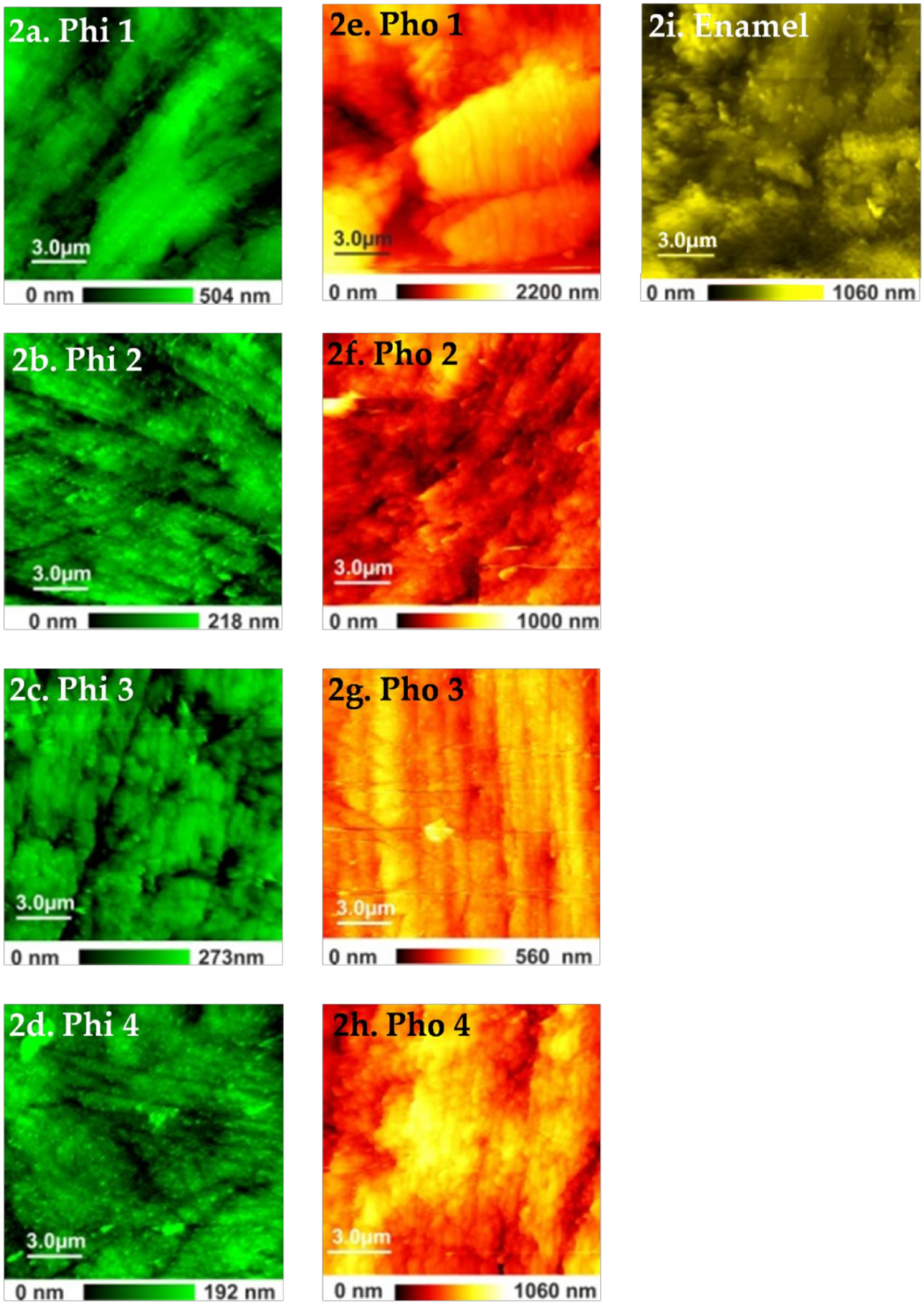

Monospecies biofilm formation.

S. mutans monospecies biofilm formation results are displayed in **Fig.14**. Highest biofilm formation was identified for phi2 and pho2. Significantly lower biofilm formation was identified for phi4 and pho4 in comparison to RBC formulations including coarse and fine filler particles (P<.01), and for phi3 and pho3 in comparison to RBCs including fine filler particles (P<.01).

Fig. 14: Monospecies biofilm formation. Means and standard deviations are indicated; identical letters indicate no statistically significant differences for α=.05.

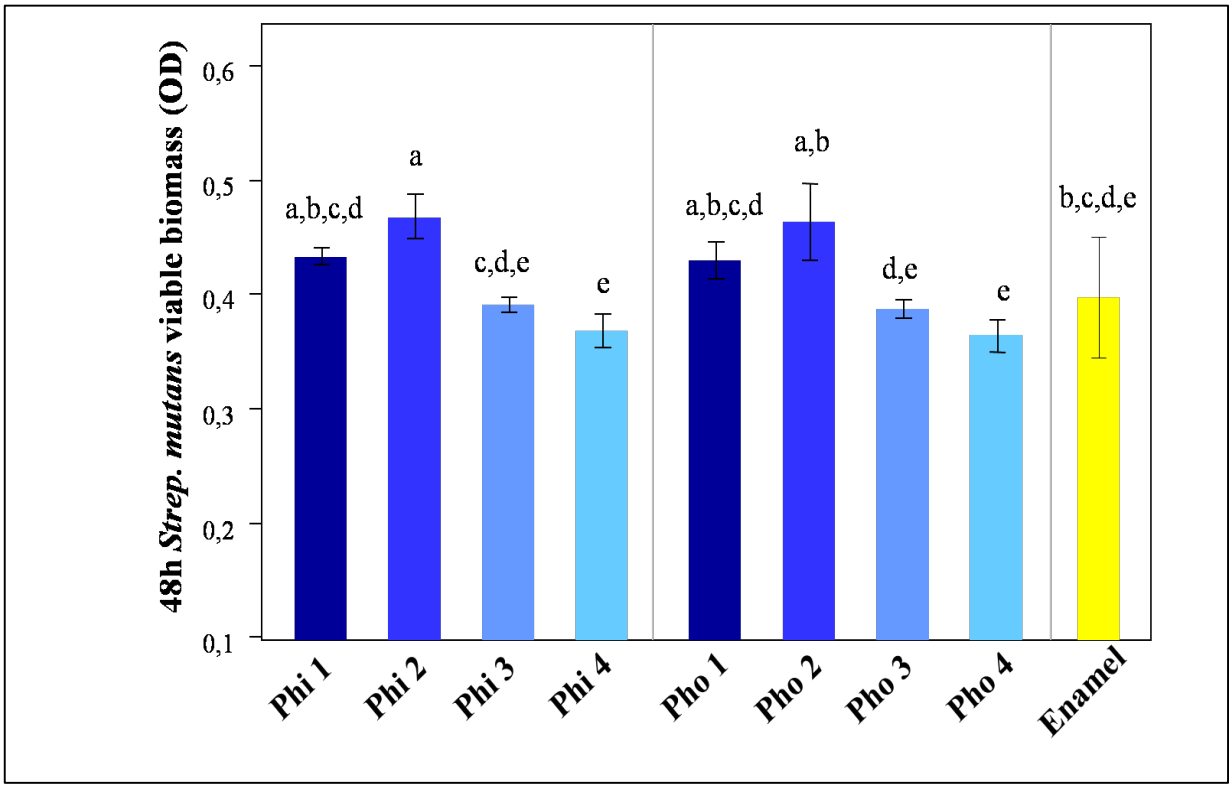

Multispecies biofilm formation

Multispecies biofilm formation results are displayed in **Fig.15**. Significantly highest biofilm formation was identified for pho1 than for all other experimental RBC formulations (P<.013). Significantly higher biofilm formation was identified for pho2 than for phi2 (P<.0001), and for pho4 than for phi4 (P=.007). No significant differences in biofilm formation were identified between phi3 and pho3 (P=.396).

Fig.15: Multispecies biofilm formation. Means and standard deviations are indicated; identical letters indicate no statistically significant differences for α=.05.

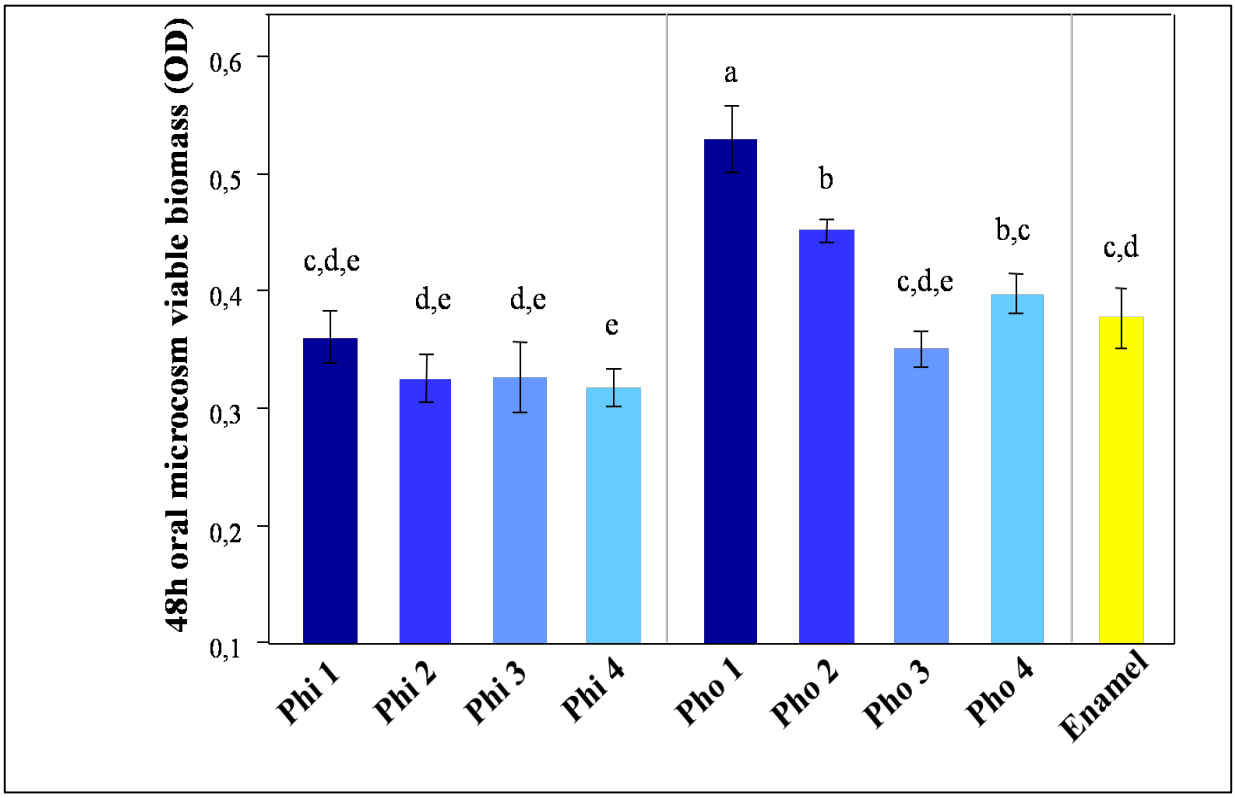

2.1.3 Discussion and conclusions

The results of the present study do not allow simple acceptance or rejection of the research hypothesis, suggesting that biofilm formation on the surface of RBCs is a complex phenomenon that cannot be easily predicted.

Several *in vitro* studies investigating biofilm formation on RBCs employed monospecies biofilm models. However, the comparability between those studies is poor due to the different experimental conditions applied, which is one reason why no proper estimation of the relation between the physical data of a RBC surface and biofilm formation could be established to date. With regard to this aspect, the authors employed two distinct biofilm models to clarify whether differences in biofilm formation occur depending on the model applied. In the monospecies model, *S. mutans* biofilm formation was simulated without prior salivary pellicle formation. This procedure represents an oversimplified approach, as in the oral cavity all interfaces are immediately covered by the salivary pellicle and *S. mutans* is not usually counted among the early-colonizing bacteria (Kindblom, Davies, Herzberg, Svensater, & Wickstrom, 2012). However, it has been reported that *S. mutans* binds better to surfaces which are not coated by saliva (E. M. Lima, Koo, Vacca Smith, Rosalen, & Del Bel Cury, 2008); moreover, *S. mutans* is an acidogenic and acidotolerant species (Philip D. Marsh, Moter, & Devine, 2011) and an important etiological agent in the development of dental caries (Busscher, Rinastiti, Siswomihardjo, & van der Mei, 2010; Sbordone & Bortolaia, 2003), which are considerations that justify its selection as strain for the monospecies biofilm model of the present study. The multispecies biofilm model employed freshly collected and pooled human saliva from at least two distinct donors, which is a more elaborate and comprehensive approach towards the analysis of biofilm formation on the surface of RBCs, as it included the multitude of microbial species available in the oral cavity. The results suggested that the influence of the biofilm model employed cannot be neglected. For the monospecies biofilm model, we could show that the differences in filler fractions overruled the impact of the matrix formulation on biofilm formation. However, this phenomenon could not be supported by the data gathered in the multispecies biofilm model, where a significant impact of the resin matrix blend on biofilm formation was identified. Except for RBC formulations including nano-sized filler particles, RBCs with a UDMA/aliphatic dimethacrylate matrix blend showed significantly higher biofilm formation on their surfaces than specimens with a BisGMA/TEGDMA matrix blend and analogous

filler fraction, suggesting that in this model, the impact of the resin matrix blend overruled the influence of filler particle size on biofilm formation.

As all materials used in this study featured Ra values lower or ranging around the threshold value at 0.2 μm, it is unlikely that the discrepancies observed in biofilm formation can be attributed to differences in surface roughness. However, it is even more complex to identify correlations between the surface free energy of RBCs and biofilm formation, as due to their inhomogeneous composition with hydrophilic filler particles and hydrophobic resin matrix, RBCs do never yield homogeneous surfaces. We identified only few significant differences in surface free energy between the different RBCs, which relates to the poor correlations observed between surface free energy and biofilm formation. In the recent time, surface free energy has been associated with the very initial adhesion of microorganisms rather than biofilm formation, suggesting that the influence of original differences between substrata regarding SFE gradually diminishes (Busscher et al., 2010). Apart from surface free energy, recent studies identified a relation between surface carbon content and biofilm formation on the surface of RBCs (A. Ionescu et al., 2012), yet in the present research, a pronounced decrease in surface carbon was identified with decreasing filler particle size for RBCs with a BisGMA/TEGDMA matrix blend, whereas it was less pronounced for RBCs with UDMA/alphatic dimethacrylate matrix blend. It appears unlikely that the differences observed in prolonged biofilm formation can be accounted to differences in surface composition, although the authors have previously identified an impact of the resin matrix blend on the very initial phases of microbial adhesion (Hahnel, Rosentritt, Burgers, & Handel, 2008). All specimens were kept in distilled water for six days for allowing the elution of residual monomers prior the experiments, also according to protocols used in previous studies (E. Brambilla et al., 2014; A. Ionescu et al., 2012), yet it cannot be completely excluded that differences in the release of residual monomers from the two distinct matrix formulations employed may account for differences in subsequent biofilm formation. However, different previous studies support the assumption that the release of residual monomers is almost complete within a 24h period and decreases significantly within one week of storage (Polydorou, Hammad, Konig, Hellwig, & Kummerer, 2009). Significant differences in biofilm formation were identified particularly between RBCs including fine and nano-scaled filler particles, and as surface roughness, surface free energy and chemical surface composition did not differ significantly, it is possible that differences in surface topography of the materials may have accounted for the differences observed in biofilm formation. AFM images proved the presence of a more homogeneous surface topography of

RBCs including nano-scaled filler particles, suggesting that in cases of similar surface roughness and surface free energy as well as chemical surface composition, differences in surface topography may be responsible for differences in biofilm formation.

It is therefore possible to conclude that experimental RBCs employed in this study do not completely answer to the complexity of the hybrid materials which are currently available on the market. These results however suggest that more scientific attention should be drawn to the surface features of contemporary RBCs, implying that an optimization of RBCs surfaces may help in reducing biofilm formation.

2.2 Optimization the microbiological properties of RBCs submitted to different surface finishing/polishing protocols

It has been shown that RBCs surface chemistry and topography may influence materials microbiological behaviour. Nevertheless, another important aspect to consider is that no resin composite material can reach a complete polymerization or even get close to full conversion and this negatively influences its microbiological behaviour (Rueggeberg, 2005; Takahashi, Imazato, Russell, Noiri, & Ebisu, 2004).

The finishing and polishing (F/P) procedures adopted after a RBC restoration placement are used to decrease SR and to obtain a smooth and glossy surface (Avsar, Yuzbasioglu, & Sarac, 2014). They are useful in order to refine surface anatomy and remove the oxygen-inhibited layer that promotes bacterial adhesion and colonization. For these purposes, a great variety of F/P instruments and techniques are available.

This study investigated the influence of different surface treatment protocols on both surface characteristics and biofilm formation of different commercial RBCs used for direct restorations.

The aim of this *in vitro* study was therefore to evaluate the effect of 6 different F/P protocols on SR, gloss, chemical composition and *S. mutans* biofilm formation on the surfaces of 4 commercially available RBCs using a continuous-flow bioreactor model.

2.2.1 Materials and methods

The following factors were considered:

- Tested RBCs
    - A - microhybrid (Enamel Plus HFO, Micerium, Avegno, GE, Italy)
    - B - nanohybrid (Estelite Asteria, Tokuyama, Kasumigaseki, Chiyoda-ku, Tokyo, Japan)
    - C - nanofilled (Filtek Supreme XTE, 3M, Maplewood, Minnesota, USA)
    - D - bulk-fill (Sonicfill 2, Kerr Corporation, Orange, California, USA)
- F/P procedures
    - Group 1 - light-curing with no-finishing (surface open to air)
    - Group 2 - light-curing against Mylar strip
    - Group 3 - light-curing against Mylar strip, then finishing with aluminum oxide discs (Sof-lex, 3M, Maplewood, Minnesota, USA)

- Group 4 - light-curing against Mylar strip, then finishing with one-step rubber points (Opti1Step, Kerr Corp., Orange, California, USA)
- Group 5 - light-curing against Mylar strip, then finishing with diamond bur 8862.314.012 followed by 862EF.314.012 (Komet, Gebr. Brasseler GmbH & Co. KG, Lemgo, Germany)
- Group 6 - light-curing against Mylar strip, then finishing with multi-blade carbide bur H48L.Q.314.012 followed by H48L.UF.314.012 (Komet, Gebr. Brasseler GmbH & Co. KG, Lemgo, Germany).

The experimental design included standardized composite specimens subjected to different F/P procedures. *S. mutans* biofilm formation was evaluated after 24h with the MTT assay. A morphological evaluation of the specimens was performed with confocal laser scanning microscopy (CLSM). SR of the specimens surface was determined with a profilometer and a small-area glossmeter was used to assess surface gloss. Energy-dispersive X-ray spectroscopy (EDS) was performed in order to study surface chemical composition before and after biofilm formation.

Specimens preparation

Ten syringes of each RBC (A3 shade) were used in this study. A total of one hundred and eight specimens were prepared for each of the tested RBCs by packing an excess of uncured RBC into a custom-made polytetrafluoroethylene (PTFE) mold with a diameter of 6.0 mm and a height of 1.5 mm. The material was covered with a Mylar strip placed on the top and bottom surfaces of the PTFE mold and condensed against a glass plate. The specimens were then irradiated for 80 s by placing the light emitting diode of a hand-held light-curing unit (Spectrum 800, Dentsply International Inc., York, PA, USA) into direct contact with the Mylar strip.

The specimens belonging to Group 1 (n=18) were prepared by condensing RBC against the glass plate using a PTFE strip, then the PTFE strip was removed and the specimens were irradiated by placing the light emitting diode of a hand-held light-curing unit at 1 mm distance from the surface for 80 s (Spectrum 800, Dentsply International Inc., York, PA, USA).

Specimens belonging to the other 5 Groups were randomly divided (n=18) depending on the finishing and polishing treatment. Specimens of Group 3 were finished and polished with a sequence of three aluminum oxide discs (medium, fine, superfine) for 30 seconds each at

20,000 rpm under water irrigation. At each disc exchange, the specimen's surface was washed and air dried for 10 seconds. A new disc was used after every three samples. Specimens of Groups 4, 5 and 6 were treated for 30 seconds at 20,000 rpm under water irrigation and a new point/bur was used after three samples.
All specimens were stored under light-proof conditions in distilled water for 6 days at 37 ± 1°C in order to minimize the impact of residual monomer extraction on cell viability and were subsequently carefully cleaned using an applicator brush tip (3M, Maplewood, Minnesota, USA) soaked in ethanol (70%) prior to any further processing.

Surface roughness

Surface roughness was evaluated as described previously (cf. 2.1.1).

Gloss

Gloss measurements, expressed in gloss units (GU) were performed using a small-area glossmeter (MG6-SA, KSJ, Quanzhou, China) with a square measurement area of 2 mm x 2 mm and 60 degrees geometry to determine the baseline gloss of the samples. A black opaque plastic mold was placed over the specimen during measurements to eliminate the influence of the ambient light and maintain the exact position of the sample for the repeated measurements. Five specimens per group were examined, three measurements were performed for each of them.

Scanning Electron Microscopy (SEM)and EDS analysis

Two specimens per group were subjected to SEM analysis and surface chemical composition assessment using a TM3030Plus Tabletop SEM (Hitachi, Schaumburg, IL, USA) equipped with an EDS probe (SwiftED3000 Oxford Instruments Analytical Ltd., Abingdon, Oxfordshire, UK). SEM micrographs at 5000x magnification were performed to have a morphological evaluation of the tested RBCs surfaces after application of the different F/P procedures. Specimens were placed in a 2% glutaraldehyde fixative solution (pH 7.4) (Sigma-Aldrich). The specimens were dehydrated in 70%, 80%, 85%, 90%, and 95% (v/v) ethanol solutions for 24 h each, and finally in a 100% ethanol solution for 48 h (Sigma-Al-

drich). Finally, the specimens were subjected to critical- point drying (Critical-point Dryer 850, EMS; Hatfield, PA, USA), and observed with SEM.

Three randomly selected 300 x 300 μm fields were analyzed for each specimen in full-frame mode using a 150 s acquisition time and 5 or 15 KV accelerating voltage. Analysis was repeated on 2 randomly selected specimens for each group after biofilm formation. Specimens were rubbed clean of biofilm using a microbrush, then sonicated for 10 min in distilled water.

Saliva collection

Paraffin-stimulated whole saliva was collected from three healthy volunteer donors in accordance with the protocol published by Guggenheim et al. (Guggenheim, Giertsen, Schupbach, & Shapiro, 2001). Briefly, saliva was collected in chilled test-tubes, pooled, heated to 60°C for 30 min to inactivate endogenous enzymes and was then centrifuged (12,000 x g) for 15 min at 4°C. The supernatant was transferred into sterile tubes, stored at -20°C, and thawed at 37°C for 1 h prior to the experiments.

Microbiological procedures

Culture media were obtained from Becton-Dickinson (BD Diagnostics-Difco, Franklin Lakes, NJ, U.SA) and reagents were obtained by Sigma–Aldrich (Sigma–Aldrich, St. Louis, MO, U.S.A.). Mitis Salivarius Bacitracin agar (MSB agar) plates were inoculated with *S. mutans* (ATCC 35668) and incubated at 37°C for 48 h in a 5% CO_2 supplemented environment. A pure culture of the microorganism in Brain Heart Infusion broth (BHI) was obtained from these plates after incubating at 37°C for 12 h in a 5% supplemented CO_2 environment. Cells were harvested by centrifugation (2,200 rpm, 19°C, 5 min), washed twice with sterile PBS and resuspended in the same buffer. The cell suspension was subsequently subjected to sonication (Sonifier model B-150; Branson, Danbury, CT, USA; operating at 7W energy output for 30 s) in order to disperse bacterial chains. Finally, the suspension was adjusted to a McFarland scale 1.0 optical density, corresponding to a concentration of approximately 3.0 x 10^8 cells/mL.

MDFR procedures

S. mutans biofilm formation was simulated under continuous flow conditions using the MDFR bioreactor as described previously (cf. 2.1.1).

In this study salivary pellicle formation was allowed by placing 10 ml of sterile saliva into each flow cell then the MDFRs incubated at 37 °C for 24 h (A. Ionescu et al., 2012). After this incubation period, saliva was removed by gentle aspiration and each flow cell was inoculated with 10 ml of *S. mutans* suspension to allow bacterial colonization of the RBCs surfaces. After 4 h, a multichannel, computer-controlled peristaltic pump (RP-1; Rainin, Emeryville, CA, USA) was turned on to provide a constant flow of nutrient medium through the flow cells. Sterile culture medium including 2.5 g/L mucin (type II, porcine gastric), 2.0 g/L bacteriological peptone, 2.0 g/ L tryptone, 1.0 g/L yeast extract, 0.35 g/L NaCl, 0.2 g/L KCl, 0.2 g/L CaCl2, 0.1 g/L cysteine hydrochloride, 0.001 g/L hemin, and 0.0002 g/L vitamin K1 supplemented with 1% sucrose was used; the flow rate was set to 9.6 ml/h. Viable biomass was assessed 24 h after starting the pump on 16 specimens per group, while biofilm morphology was assessed using CLSM microscopy for 2 specimens per group.

MTT assay

Viable biomass adherent to the specimens was analysed using a MTT-based assay as reported previously (cf. 2.1.1)

After 24 h of incubation, the medium flow was stopped, the flow cells were opened, the trays containing the specimens were carefully removed and placed into Petri plates containing sterile PBS at 37°C. Specimens were gently removed from the trays, washed three times with sterile PBS to remove non-adhered cells and finally placed inside the wells of 48-well plates. The MTT assay was performed as follows (Andrei Ionescu et al., 2015; A. Ionescu et al., 2012): briefly, 300 µl of FMS were placed in each well, then the plates were incubated for 3 h in light proof conditions at 37◦C. During incubation, electron transport across the microbial plasmatic membrane and, to a lesser extent, microbial redox systems, converted the yellow MTT salt to insoluble purple formazan. The conversion at the microbial membrane level was facilitated by the intermediate electron acceptor (PMS). The FMS was then gently removed by aspiration and the intracellular formazan crystals were dissolved by adding 300 µl of lysing solution to each well and incubating again for 1h at room temperature in light proof conditions. One hundred µl of suspension were transferred from each well to

96-well plates and optical density (550 nm) was measured with a spectrophotometer (Genesys 10-S, Thermo Spectronic, Rochester, NY, USA). Results are displayed as OD units.

Confocal laser scanning microscopy (CLSM)

Two disks for each of the experimental groups were analyzed using CLSM. After the 24 h incubation time the biofilm growing on the disks was gently washed three times with PBS to remove non-adherent cells and stained using the FilmTracer live/dead Biofilm Viability Kit (Invitrogen, Carlsbad, California, USA) for microscopic examination. The fluorescence from live stained cells adherent to the test samples was observed using a CLSM (Leica TCS SP2, Leica Microsystems, Wetzlar, Germany). Three randomly selected image stack sections were recorded for each specimen. Confocal images were obtained using a dry 20× (NA 0.7) objective and digitalized by using the Leica Application Suite Advanced Fluorescence Software (LAS AF, Leica microsystems, Wetzlar, Germany), at a resolution of 1024 × 1024 pixels, with a zoom factor of 1.0. For each image stack section 3D-rendering reconstructions were obtained using Drishti 3D software (Limaye).

Statistical analysis

Data were analyzed using statistical software (JMP 12 Pro, SAS, Cary, NC, USA). Normality of data distribution was preliminarily checked using Shapiro-Wilk's test and homogeneity of variances was verified using Barlett's test. Adherent biomass data were statistically analyzed using two-way ANOVA considering RBC and surface finishing as fixed factors. Tukey post-hoc test was used to assess differences between groups. The level of significance was set to $p<0.05$. Surface roughness and gloss data were statistically analyzed using Wilcoxon on each pair since they didn't show a normal distribution or homogeneous variances.

The statistical analysis displayed the presence of an outlier group (Group 1) for gloss and SR data: the results of that group were the highest and showed a huge standard deviation thus concealing the differences among groups. The statistical analysis was therefore repeated after the exclusion of the outlier group.

2.2.2 Results

Surface roughness

Mean Ra ± SE values are shown in **Fig.16,** while **Fig.17** presents the results after excluding the outlier group. The non-parametric test showed that SR was significantly influenced only by the tested F/P procedures. Group 2 showed the lowest SR values ($p<0.001$) when compared to all the other Groups. Group 3 presented lower SR values than Groups 4, 5 and 6 ($p<0.001$). No statistically significant differences were found in SR results among Groups 4, 5 and 6. **Panel 1** shows SEM micrographs of the different surfaces at 5000x magnification. No differences could be seen between Groups 1 and 2, between Groups 3 and 4 and between Groups 5 and 6. Groups 1 and 2 showed very smooth surfaces where filler particles were surrounded by a coating layer of resin matrix; fillers of C - nanofilled RBC could not be observed at this magnification. All other groups showed superficial grooves left by the F/P procedures. The grooves were almost non-noticeable in Group 3, which overall appeared as the F/P procedure leaving the smoothest surface, confirming SR data. F/P procedures exposed more filler to the surface compared to Groups 1 and 2, and especially the bulk fill RBC surface changed significantly, by exposing macro-sized filler particles.

Fig.16 Surface roughness of the tested finishing/polishing groups and RBCs. Mean Ra ± SE values are displayed.

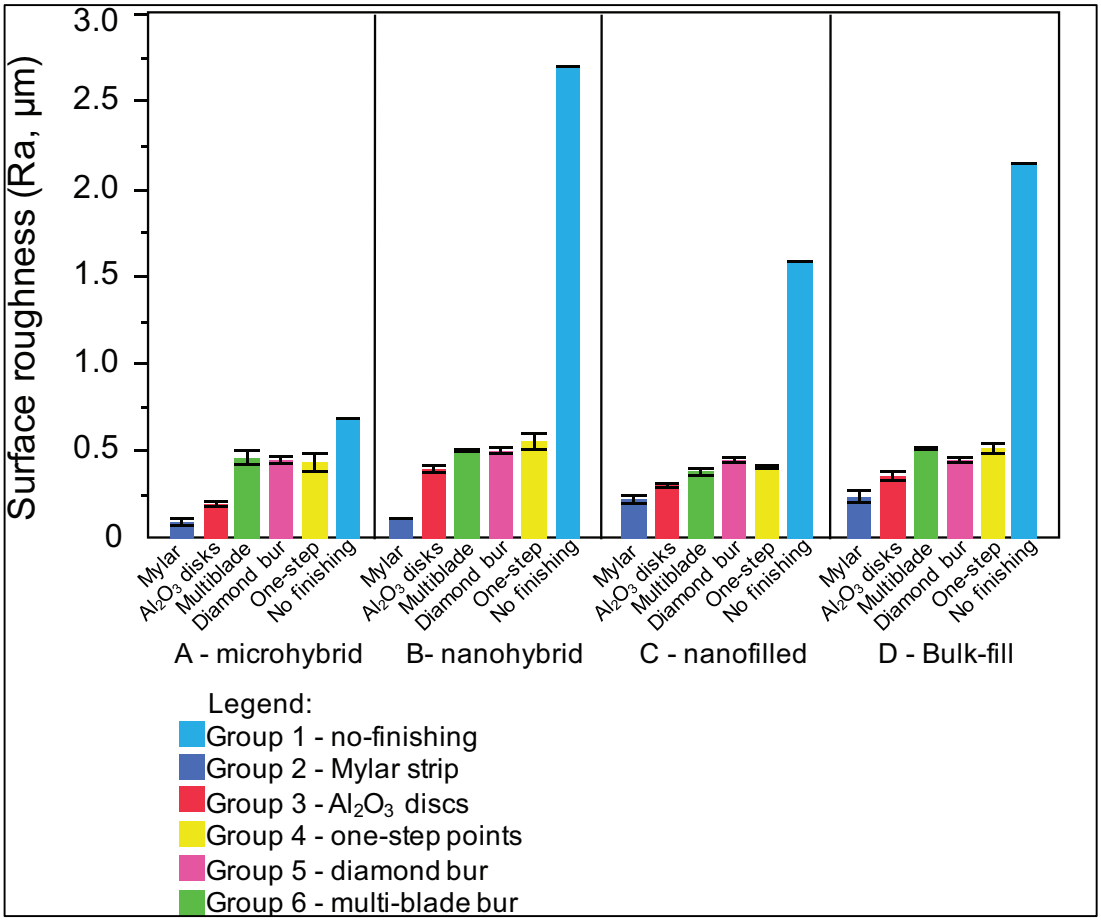

Fig.17: Surface roughness of the tested finishing/polishing groups and RBCs. Mean Ra ± SE values are displayed, the outlier (Group 1) was excluded and the roughness values rescaled for better comparison among groups.

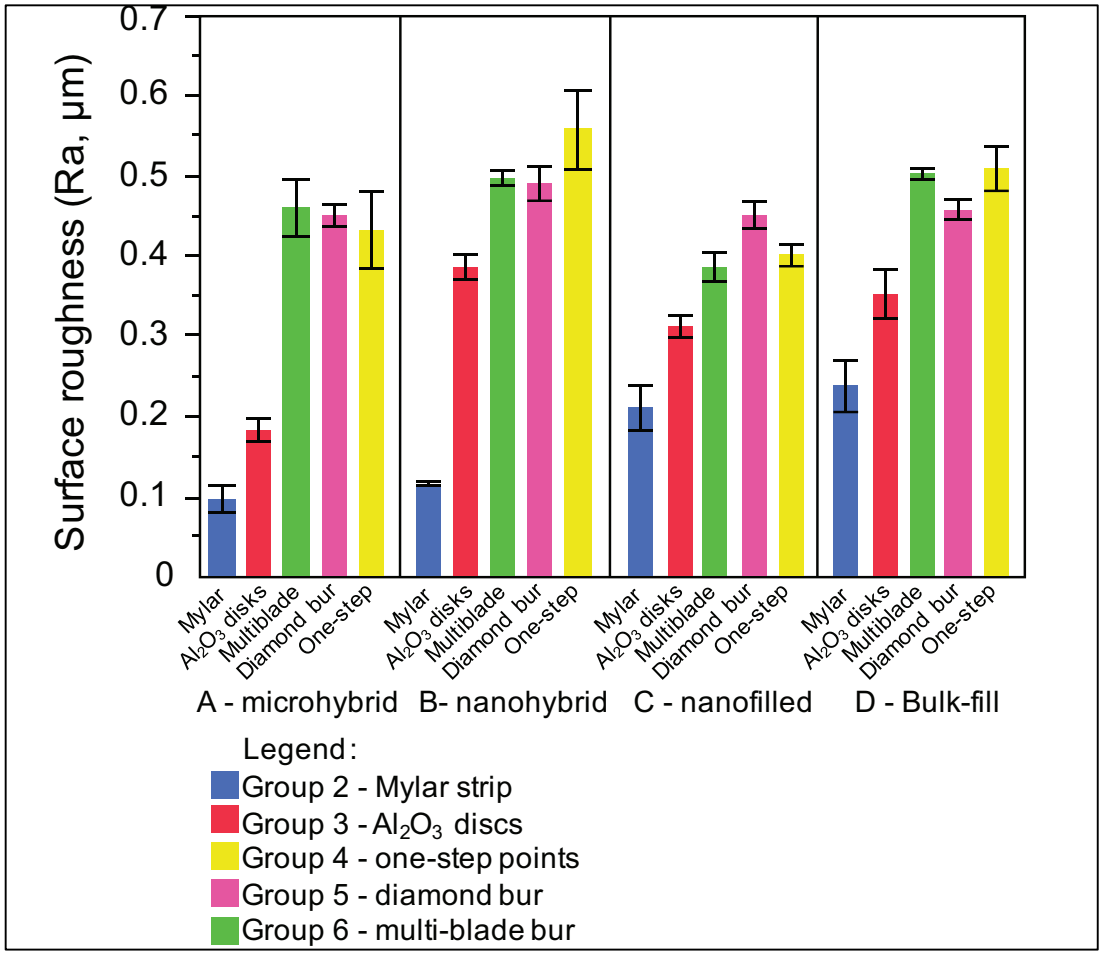

Panel 1: SEM micrographs of the tested RBC surfaces after application of the different F/P procedures at 5000x magnification.

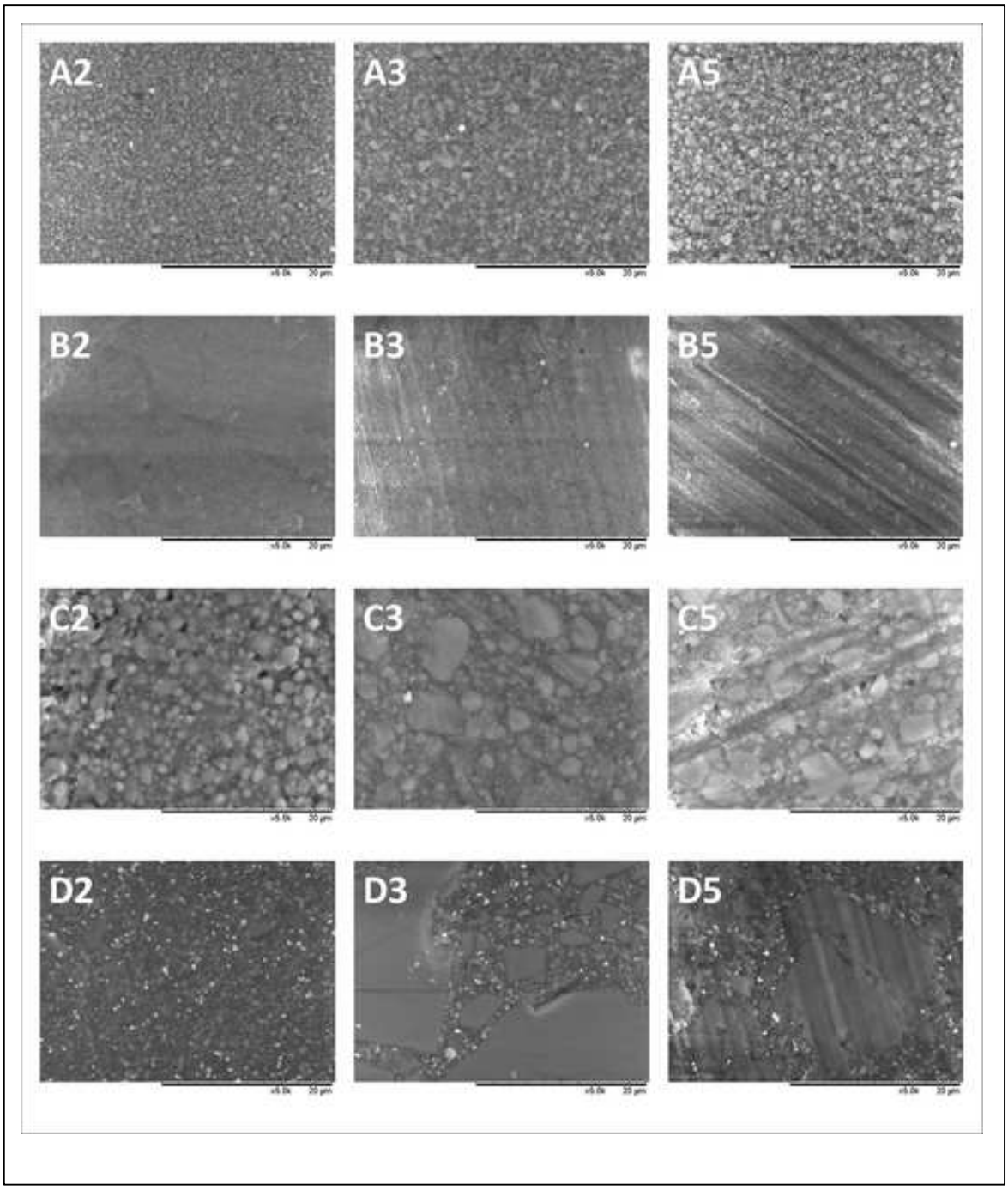

Gloss

Mean GU ± SE are shown in **Fig.18**. The non-parametric test showed a significant effect of F/P procedures ($p<0.001$) on surface gloss. Group 2 showed the highest gloss values while Groups 5 and 6 showed the lowest ones. Groups 3 and 4 showed gloss values lower than Group 2 but higher than Groups 5 and 6.

Fig.19 shows the regression graphs obtained confronting gloss and SR data for each tested RBC. A significant ($p<0.01$) inverse correlation could be found for each RBC, but the goodness of fit was best for D - bulk fill RBC and worst for the A - micro hybrid RBC.

Fig. 18: Gloss of the tested finishing/polishing groups and RBCs. Mean gloss units (GU) ± SE values are displayed.

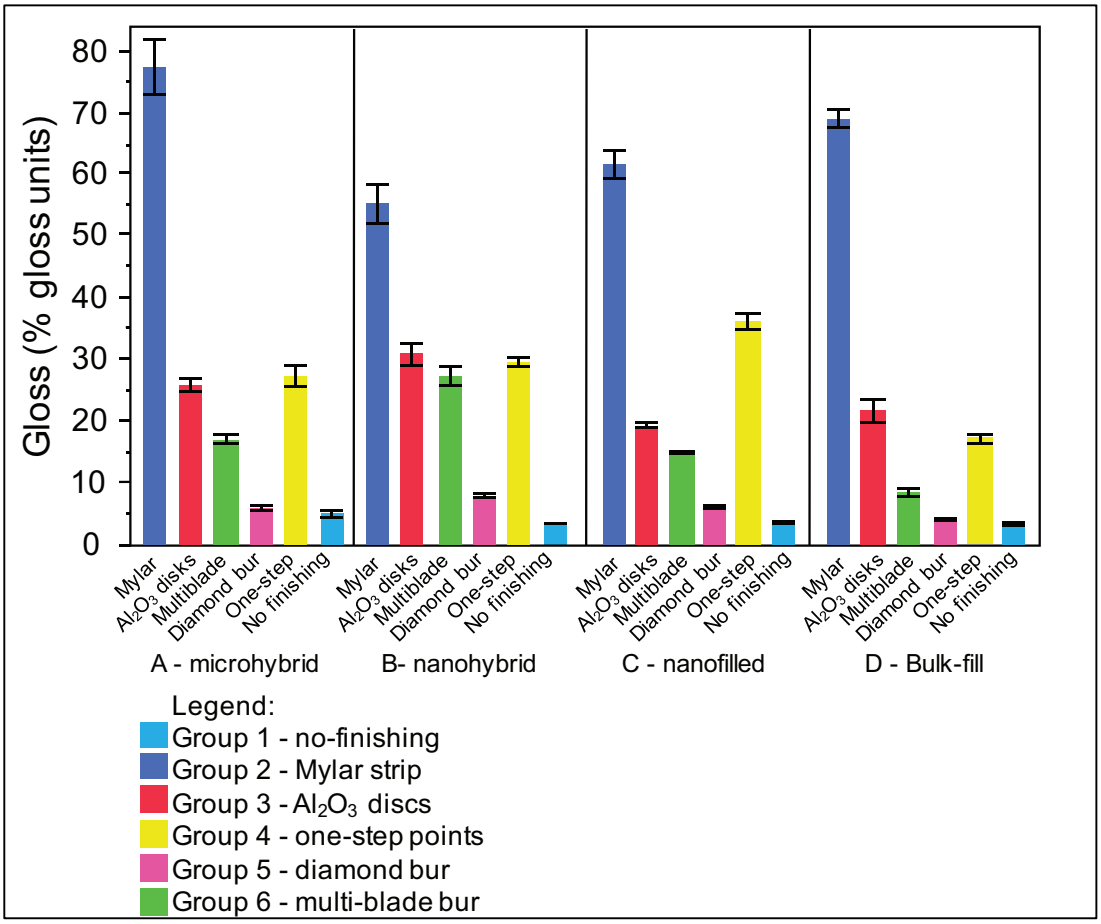

Fig. 19: Regression graphs obtained confronting Gloss and SR data for each tested RBC. A significant ($p<0.01$) reciprocal relationship could be found for each RBC, but the goodness of fit was best for the bulk fill material and worst for the micro hybrid RBC.

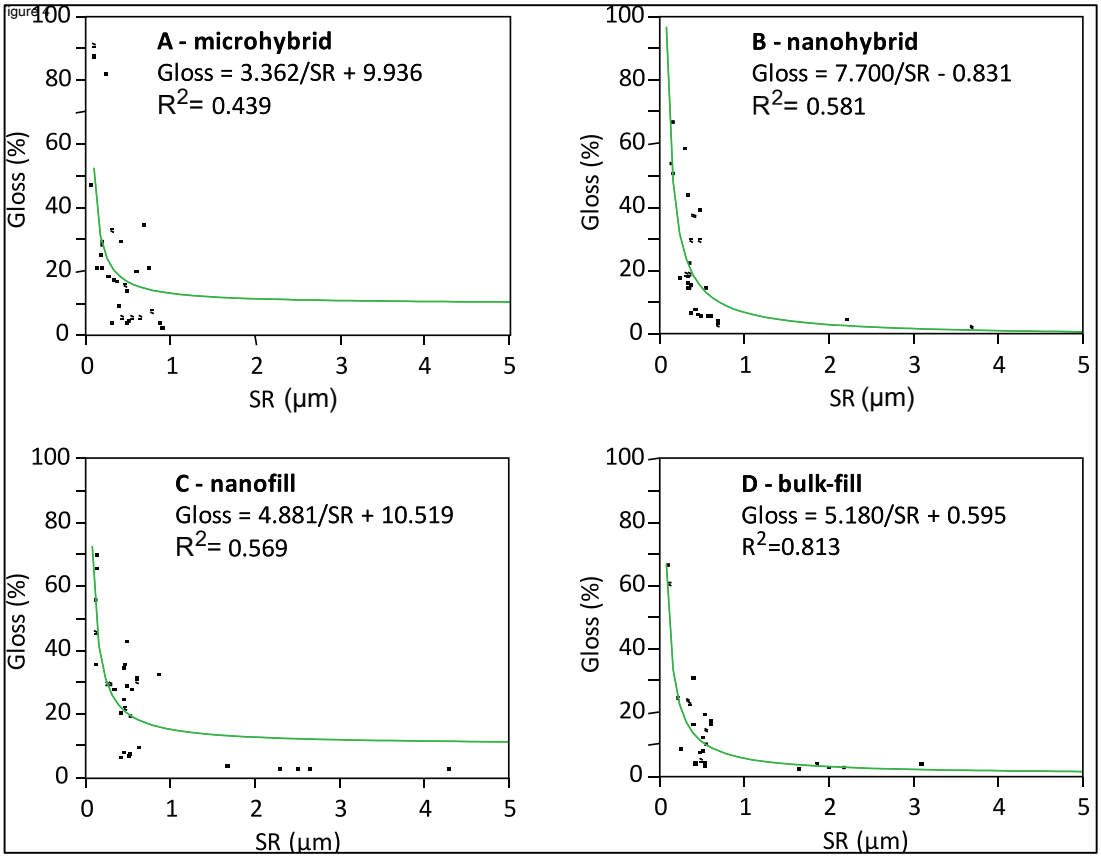

EDS

EDS analysis showed high differences in the composition of the tested RBCs (**Table 3**, data belong to Group 2). In order to compare the influence of the different surface treatments and materials on surface chemical RBCs composition, all the elements belonging to the inorganic fraction were summed whereas the organic fraction was represented by carbon. Oxygen was not considered being representative of both the organic (polymers) and the inorganic (oxides) fractions. No evidence of foreign elements on the RBCs surfaces after the finishing procedures due to contamination from the finishing disks, rubbers or blades was found. A significant ($p<0.001$) negative linear relationship was found between the organic and inorganic fractions both before (Organic = 69,424 - 1,297*Inorganic, R^2=0.831) and after biofilm formation (Organic = 69,609 - 1,150*Inorganic, R^2=0.561).

Fig. 20 shows the pattern of organic and inorganic fractions as representative of the resin matrix and filler belonging to the ≈1 micrometer superficial layer from which electrons were extracted by the 15KV accelerated beam in relation to the different surface treatments and the tested RBCs. Group 1 (no finishing) specimens surface exposed a higher amount of organic matrix than inorganic filler in all the tested RBCs save for RBC C (Filtek Supreme XTE). The latter showed a higher proportion of inorganic filler on the surface, independent of the F/P procedures. Groups 3 and 4 presented a similar pattern, showing a higher amount of inorganic filler in all the tested RBCs except for RBC B (Estelite Asteria), in which inorganic and organic fractions were present in comparable amounts. Groups 5 and 6 showed a similar behavior. In particular, RBCs A (Enamel plus HFO) and B (Estelite Asteria) displayed a similar amount of organic and inorganic fractions, RBCs C (Filtek Supreme XTE) and D (Sonicfill 2) showed a higher amount of inorganic fraction compared with the organic component. Finally, considering Group 2, RBCs A (Enamel plus HFO) and B (Estelite Asteria) displayed a similar proportion of organic and inorganic fractions, RBC D (Sonicfill 2) showed a higher organic fraction while the opposite was found for RBC C (Filtek Supreme XTE).

Fig. 21 shows the pattern of organic and inorganic fractions in relation to the different surface treatments and RBCs as assessed by EDS after biofilm formation. Compared to data acquired prior to biofilm formation, a relative increase in carbon content could be observed in every group independently of the RBC or the F/P procedure applied.

Fig. 22 shows an example of the exopolysaccharide matrix produced by the biofilm and still attached to the RBC surfaces. All specimens observed at SEM and EDS after biofilm formation showed similar features: they appeared sputtered with dark-grey islets measuring several tens of microns of homogeneous material, without any evidence of bacterial cells. The acquired elemental maps (Fig. 22-c and 22 –d) showed that the islets were composed by carbon and traces of other elements (mostly N, but also Na, Ca, P), confirming that they are residues of exopolysaccharide matrix still firmly attached to the surface.

Table 3: Mean composition (%wt) of the superficial layer (≈1µm) of the tested RBCs after light-curing against Mylar strips, as assessed by quantitative fullframe EDS. The sum of the elements composing the inorganic fraction is shown.

RBC	C (organic fraction)	Si	Al	Zr	F	Br	Ba	Yb	Na	W	Inorganic fraction
A - microhybrid	**30,37**	14,58	3,43	0,00	0,00	0,00	0,49	0,00	0,00	11,41	**29,92**
B - nanohybrid	**29,06**	20,48	0,00	10,45	0,00	0,00	0,00	0,00	0,58	0,00	**31,51**
C - nanofilled	**22,62**	21,80	0,00	13,02	0,00	0,00	0,00	0,00	0,00	0,00	**34,82**
D – bulk fill	**36,55**	16,52	0,00	3,29	0,87	1,56	3,50	2,78	0,00	0,00	**28,51**

Fig.20: Results from EDS analysis of surface chemical composition, displayed as % of organic fraction (carbon) and inorganic fraction (sum of all elements present as fillers in the RBC compositions).

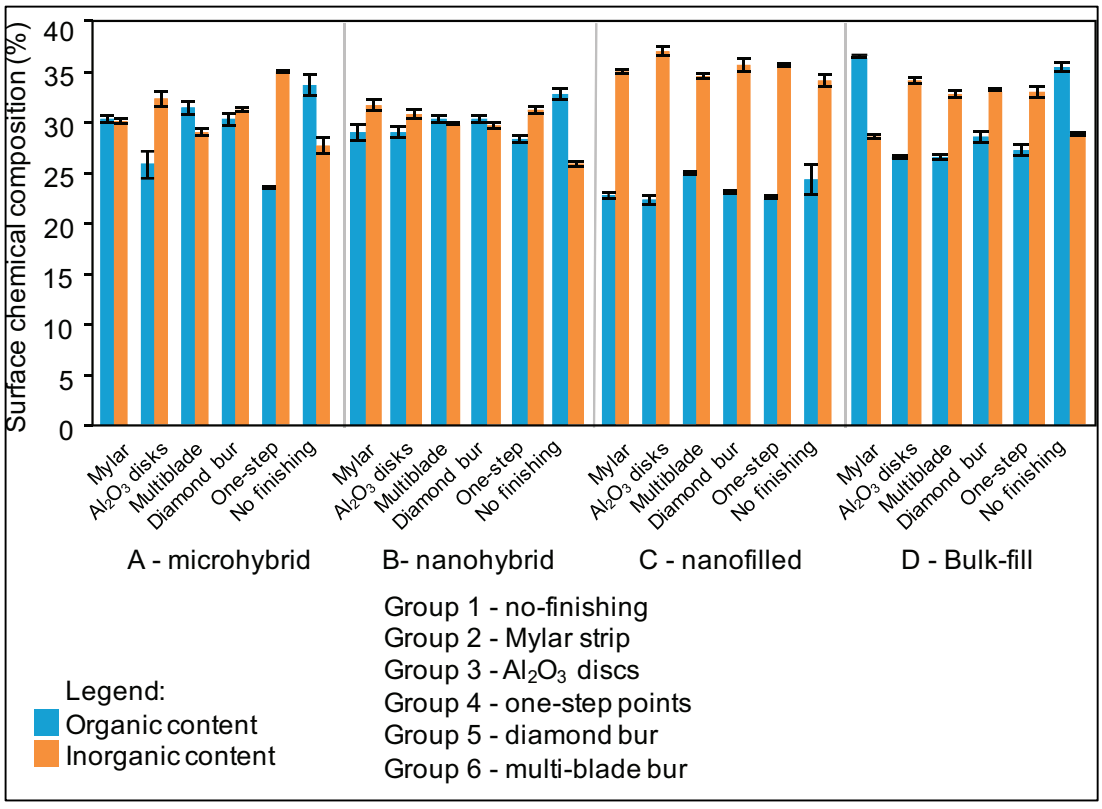

Fig.21: Results from EDS analysis after biofilm challenge and specimen cleansing (surface rubbing with microbrush and sonication). The surface chemical composition is displayed as % of organic fraction (carbon) and inorganic fraction (sum of all elements present as fillers in the RBC compositions). It is noteworthy that carbon content refers to the sum of signals from the RBC resin matrix and the residual biofilm exopolysaccharide matrix, which explains the increase in organic fraction for all groups compared to EDS data before biofilm challenge.

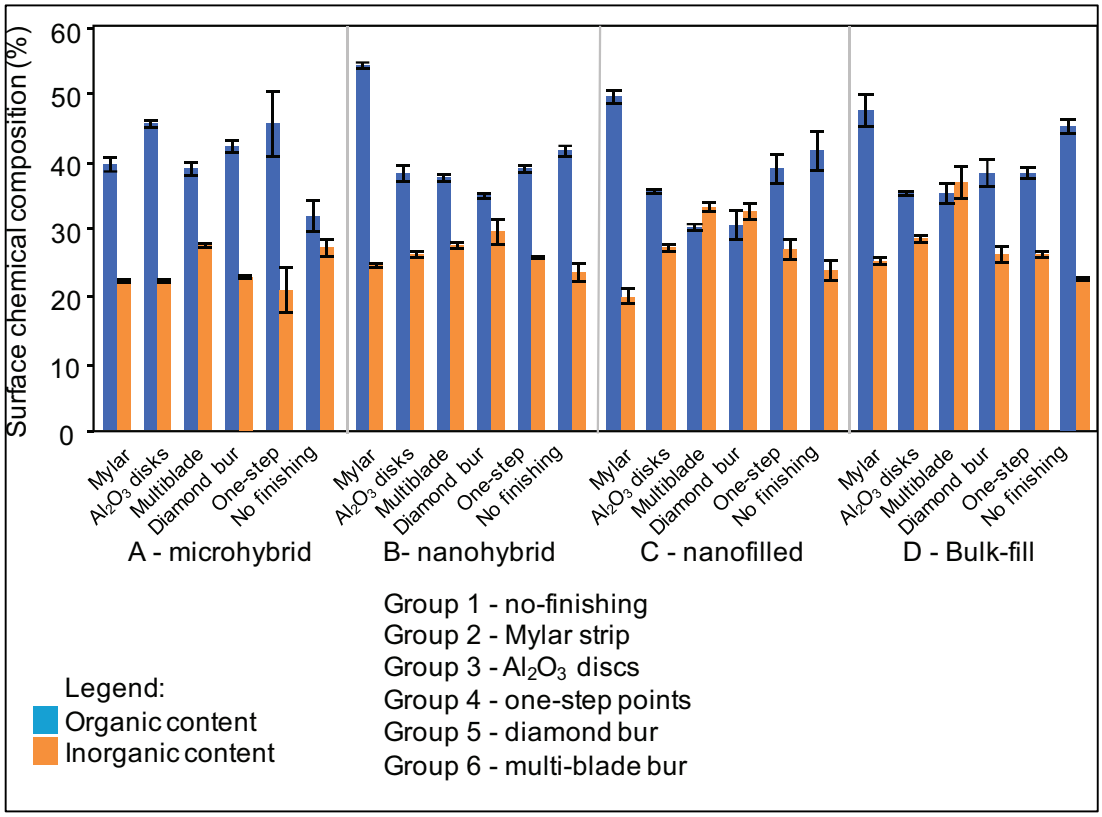

Fig.22: Fields acquired for the bulk fill material from Group 5. Pictures 22a and 22b display the surface at 500x magnification and 5 or 15kV acceleration voltage, respectively, showing thus information from the first 0.5 µm surface layer or from more in-depth (≈1 µm). All specimens observed after biofilm formation showed similar features: they appear sputtered with dark-grey islets measuring several tens of microns of homogeneous material, without any evidence of bacterial cells. Pictures 22c (5kV) and 22d display an elemental map acquired from EDS superimposed to the SEM images of the same field. Carbon is shown in red, and silicon channel in blue, standing, respectively, for organic and inorganic fractions. Nitrogen signal is also displayed in green. Maps show that the islets were composed by carbon and traces of other elements (N, Na, Ca, P), suggesting that, most likely, they are residues of exopolysaccharide matrix produced by the biofilm and still firmly attached to the surface.

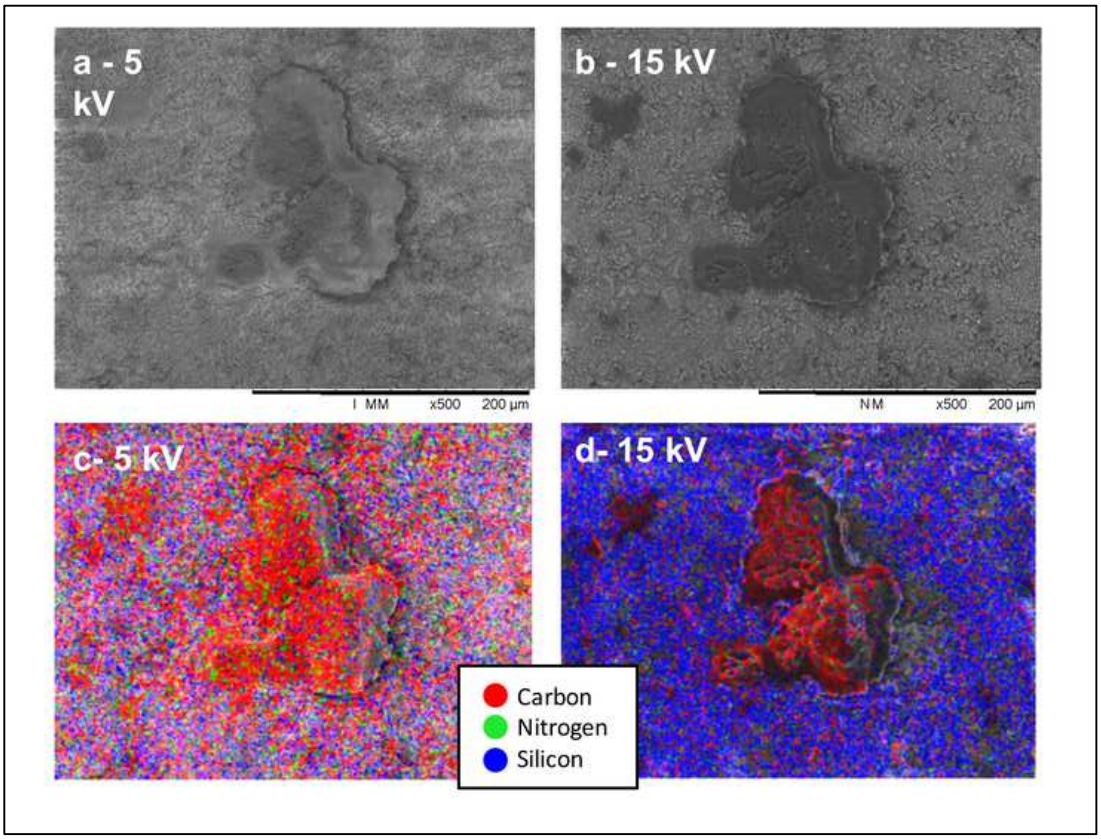

Biofilm formation

Biofilm formation on RBCs discs, expressed as mean OD ± SE, is reported in **Fig. 23**. Two-way ANOVA demonstrated the existence of a significant influence of the tested material ($p < 0.01$) on biofilm formation. Tukey HSD post-hoc test showed that RBC A (Enamel Plus HFO) and RBC C (Filtek Supreme XTE) presented the lowest OD values when compared to the other tested composites. No significant differences were found between RBCs A and C ($p=0.9675$) and between RBCs B and D ($p=0.9999$). Considering the different F/P procedures tested, no significant effect ($p = 0.31$) on biofilm formation could be found for RBCs B, C and D. For RBC A, Group 1 showed significantly more biofilm formation than Groups 2 and 3 ($p= 0.0049$ and $p= 0.0141$, respectively). 3D reconstructions of the biofilms obtained by CLSM are shown in **Panel 2**.

Fig. 23: *S. mutans* biofilm formation expressed as mean OD± SE. The OD values were rescaled to allow for better comparison among experimental groups.

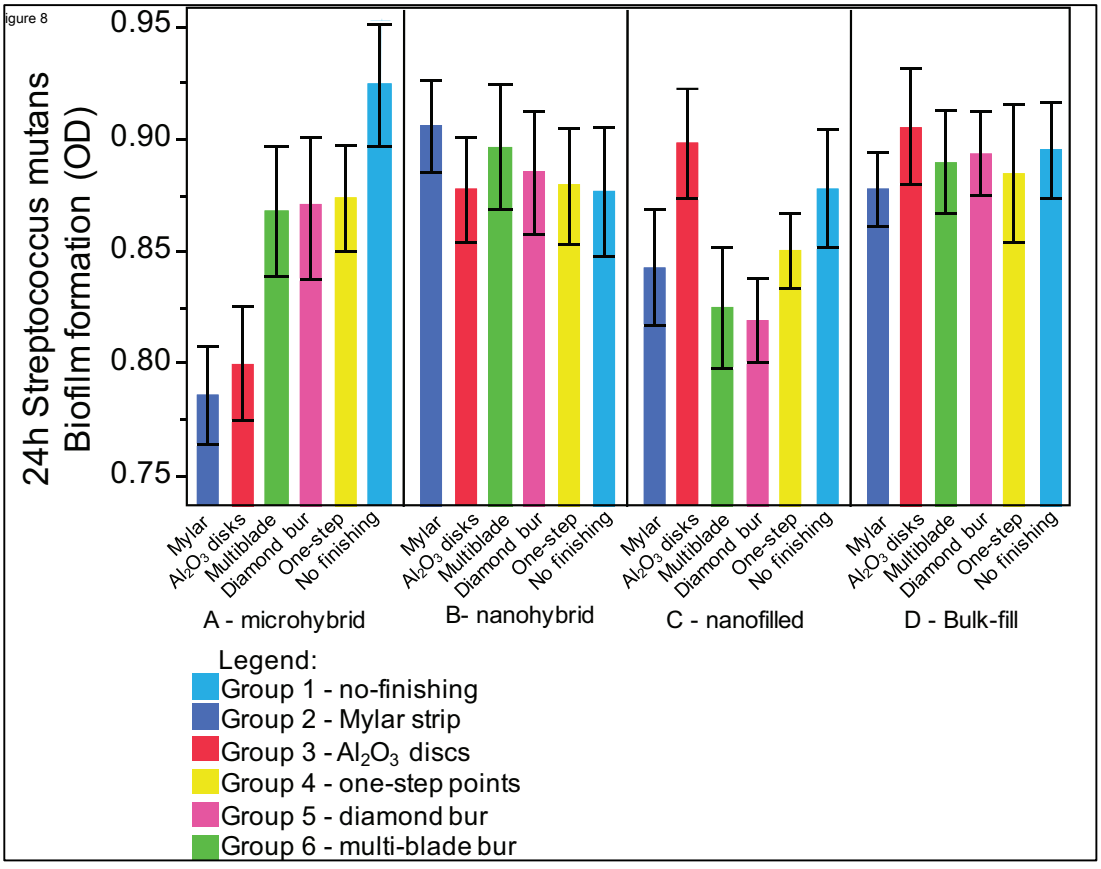

Panel 2: 3D reconstructions of the biofilms obtained by CLSM. LIVE/DEAD dyes stained viable bacterial cells in green while nonviable, dead cells are displayed in red. No significant morphological differences in biofilm formation or in its viability could be observed among the different F/P groups or RBC materials, here a field for each RBC from Group 3 is provided. All fields showed mature, compact biofilm structures covering most part of the specimen surfaces with a prevalence of viable cells.

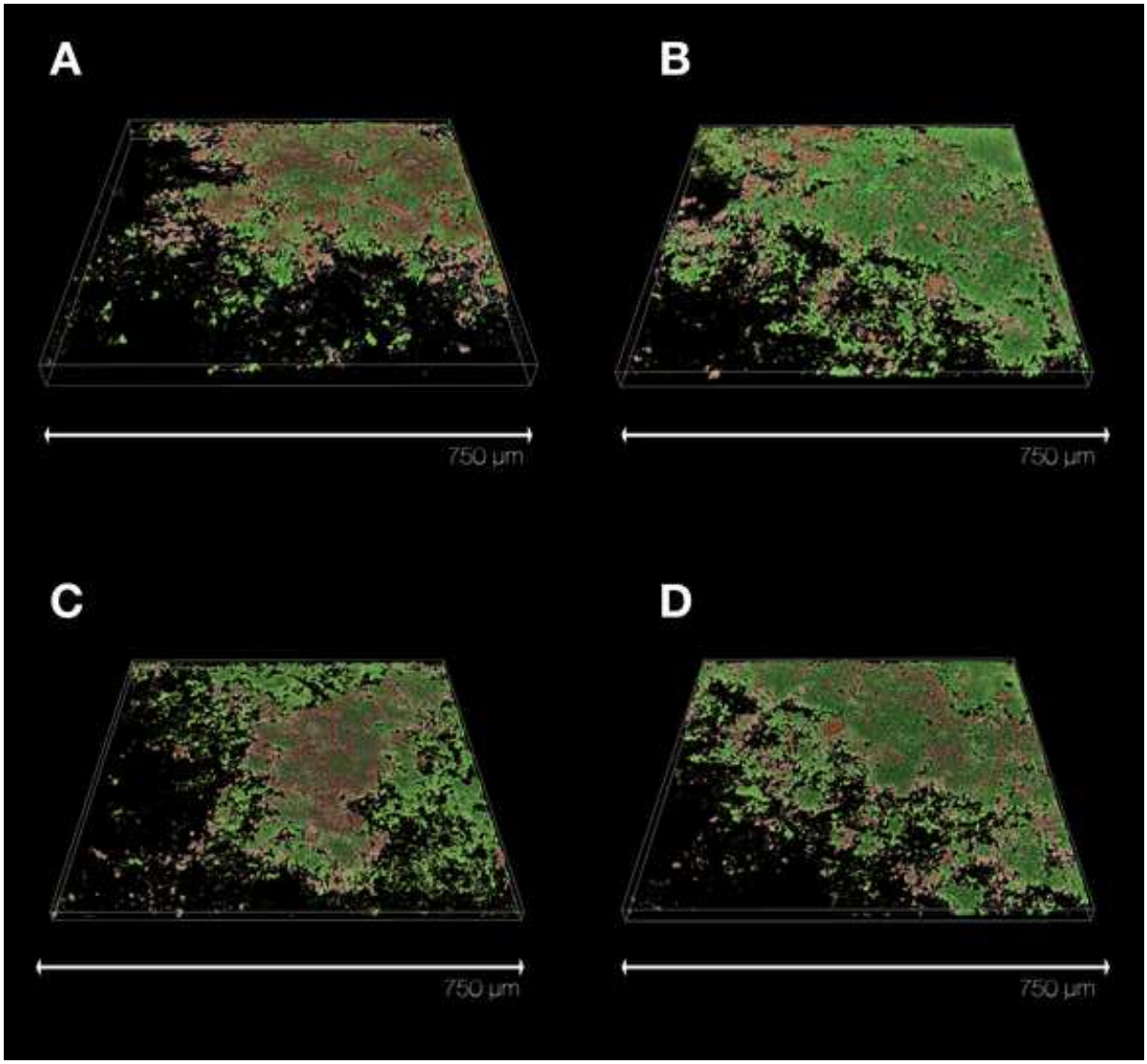

2.2.3 Discussion

A variety of F/P procedures is used in clinical practice to guarantee excellent aesthetic performances of composite restorations (Baseren, 2004). Nevertheless, there is still no clear evidence of the influence of these procedures on the biological interactions of RBCs with oral biofilms. Therefore, the aim of this study was the *in vitro* evaluation of *S. mutans* biofilm formation on four commercially available RBCs treated with six standardized F/P procedures.

The study was performed using *S. mutans* as test microorganism since it is directly involved in the etiology of dental caries (Forssten et al., 2010; Metwalli, Khan, Krom, & Jabra-Rizk, 2013; Michalek, Katz, Childers, Martin, & Balkovetz, 2002). The evaluation of *S. mutans* interactions with the tested surfaces could therefore be of great interest in preventing cariogenic biofilm formation and increasing restorations longevity. This experimental setup promotes the formation of biofilm under dynamic conditions more closely simulating *in vivo* ones, thus allowing a standardized evaluation of the tested parameters on a structured, multilayered microbiological community.

In order to provide a broad perspective of the possible clinical situations, the study was performed on four classes of RBCs currently used in daily practice. The tested RBCs, characterized by differences in filler particles and matrix chemical composition, included a microhybrid, a nanohybrid, a nanofilled and a bulk-fill composite.

Each material was submitted to surface treatments chosen to simulate clinical operative procedures. Among the tested F/P procedures, a "no surface treatment" group (Group 1) was introduced to simulate restoration areas difficult to reach and therefore not involved in F/P procedures. This group is characterized by the presence of an oxygen-inhibited layer. In contrast, one group (Group 2) was made of specimens cured against Mylar strips that are frequently used to build proximal areas, especially of anterior teeth. This methodology allowed to test a resin composites surface cured in an oxygen-free environment and with the smoothest surface achievable. The other remaining groups were representative of some of the surface treatments commonly performed by clinicians. Aluminum oxide discs (Group 3) usually represent a standard protocol to obtain smooth surfaces on a variety of RBCs (Lu, Roeder, & Powers, 2003) and the one-step polishing system (Group 4) was chosen as a fast way to obtain a smooth surface with a single instrument (Bashetty & Joshi, 2010; Costa, Ferracane, Paravina, Mazur, & Roeder, 2007; Ozel, Korkmaz, Attar, & Karabulut, 2008). Diamond burs (Group 5) were used to mimic procedures applied to shape the anatomy of restorations thanks to their high cutting efficiency while multi-blade carbide burs (Group 6),

showing a lower cutting efficiency, are best suited for smoothing and finishing (Jung, 1997). In this study, specimens were submitted to a manual preparation in order to better simulate clinical conditions. Since it is generally accepted that surface preparation under varied conditions could modify surface quality, F/P procedures were performed by a single expert operator in order to remove the possible bias related to variations in operators' experience and skills.

The structure and features of F/P instruments are usually responsible of changes in RBCs surface properties. In particular, SR is considered of high importance and is therefore one of the most studied variables (Reis, Giannini, Lovadino, & Ambrosano, 2003; Song, Koo, & Ren, 2015).

From materials point of view, it is generally believed that the possibility to finish and polish RBC surfaces depends on their filler particle size. Several studies in the literature showed that F/P procedures applied on RBCs with smaller filler particles size create smoother surfaces than on RBCs with larger filler particles (Buchgraber, Kqiku, Allmer, Jakopic, & Städtler, 2011; Ergücü & Türkün, 2007). The results of our study disagree with these observations since SR was not significantly different among the tested RBCs, despite their different filler sizes (as seen in **Panel 1**: nanoparticles in the nanofilled material, nanoparticles and clusters in the nanohybrid, macroparticles in the bulk-fill and micrometer and sub-micrometer size particles in the microhybrid). Considering F/P procedures, the profilometric analysis displayed a clear influence on SR. These findings agree with some studies demonstrating that this parameter is not necessarily influenced by RBCs filler particles size (Da Costa, Goncalves, & Ferracane, 2011). Moreover, it has been demonstrated that different F/P procedures can lead to surfaces with different SR values, strongly related to the procedure and not to the composition of the material (Botta, Duarte Jr, Paulin, Gheno, & Powers, 2009).

As already shown in the literature, and confirmed in our study, the smoothest RBC surfaces were obtained by curing specimens against Mylar strips (Group 2) (Baseren, 2004; Yap, Yap, Teo, & Ng, 2004). Of the different F/P procedures, Group 3 (aluminum oxide discs), showed the lowest overall SR values among the tested materials while Groups 4, 5 and 6 influenced SR in all RBCs classes in a comparable way. The high efficacy of aluminum oxide discs in reducing SR was probably due to their protocol which includes treatment with four different disks with progressively finer grit size to abrade both resin matrix and filler leaving smooth, almost groove less surfaces as also seen in **Panel 1**.

Gloss is commonly used to measure the surface shine and could therefore influence the

esthetic appearance of composite restorations. Several studies revealed the existence of a strong correlation between SR and gloss (Antonson, Yazici, Kilinc, Antonson, & Hardigan, 2011; Ereifej, Oweis, & Eliades, 2012). Our evaluations highlighted the existence of a reciprocal relationship between these two factors in all the tested groups except for Group 4, and for all the tested RBCs. The one-step system (Group 4) showed the highest gloss values among the surface treatments except for specimens cured against Mylar strips (Group 2). Moreover, the one-step system showed high performances in all the tested groups independent of their surface chemistry or filler particle size. The correlation between SR and gloss, although significant for all RBCs tested, was material-dependent since the goodness of the reciprocal fit was highest for the bulk-fill material and lowest for the micro hybrid.

The experimental design of this study allowed the evaluation of the effect of the tested F/P procedures on the above-mentioned surface properties and to correlate these observations with the RBC's microbiological behavior. The data showed that *S. mutans* biofilm formation was significantly influenced by the material ($p< 0.01$) but not by F/P procedures ($p=0.72$). These results are in agreement with those of Ono and coworkers (Ono et al., 2007) demonstrating that different F/P procedures do not influence the microbiological behavior of different RBCs. In our study, no correlation between *S. mutans* biofilm formation and SR was demonstrated except for the micro hybrid RBC (RBC A). This material showed a biofilm formation trend reproducing that of SR. The correlation was significant ($p<0.01$), however the goodness of fit was rather low ($R2= 0.052$). The other groups highlighted a different behavior; for example, the surface of the specimens cured against Mylar strips (Group 2) showed the lowest SR values in all the tested materials but different *S. mutans* biofilm formation.

Our findings therefore disagree with earlier observations on a positive correlation between SR and biofilm formation highlighted by Carlen, Aykent and Pereira. The different experimental design of these studies can explain the different conclusions, for example, in the first case the 1 h incubation period allowed the investigators to study bacterial adhesion and not biofilm formation (Carlen, Nikdel, Wennerberg, Holmberg, & Olsson, 2001). The only paper found in the literature with objectives similar to our study was that of Aykent and co-workers (Aykent et al., 2010), but they unfortunately used an *in vitro* static incubation method instead of a MDFR (Pereira et al., 2011). Moreover, the use of CLSM evaluation alone as performed in Aykent's work, can represent a limit of the study, due to the issues related to this approach. CLSM analysis allows the evaluation of a limited number of small fields which may not present a reliable assessment of the whole biofilm formation on the

tested surfaces. Our study, on the contrary, allowed a quantitative evaluation of *S. mutans* biofilm formation associated with a CLSM morphological analysis (**Panel 2**). CLSM analysis was performed to allow the non-invasive observation of *S. mutans* biofilms fully maintaining their structure and morphology (Brentel et al., 2011). Moreover, this assessment allows a qualitative evaluation of the biofilm thus showing the presence of live (green) and dead (red) bacteria into its architecture. This analysis confirmed the outcomes of the MTT test showing the presence of differences in biofilm formation after 24 h of incubation related to the tested RBCs but not to the F/P procedures. An interesting evaluation supporting our results could be found in the study of Eick and co-workers who investigated biofilms under continuous flow conditions. Results highlighted that no correlation existed between SR and the number of viable *S. mutans* cells determined with plate count (Eick, Glockmann, Brandl, & Pfister, 2004). It has been also highlighted (L. Mei, Busscher, van der Mei, & Ren, 2011) that *S. mutans* adhesion forces are less influenced by composite SR than those of other Streptococci, such as *S. sanguinis*, one of the earlier colonizers. It is therefore possible to hypothesize that F/P procedures may change surface properties such as topography and elemental surface chemical composition; this phenomenon might play an important role in *S. mutans* biofilm formation even exceeding that of SR, especially on a mature *S. mutans* biofilm.

Moreover, the length of incubation time should be considered. Several studies evaluated only adhesion and the first steps of bacterial colonization (Rosentritt et al., 2008). In the present study, the formation of a multilayer biofilm was simulated within the MDFR for 24 h to assess the influence of the tested parameters on a structured, multilayered biofilm. It should be hypothesized that the irregularities due to SR could protect bacteria against shear forces during the early stages of biofilm formation while this parameter seems less important in influencing a fully-grown biofilm.

EDS analysis was also performed to clarify the relationships between the chemical composition of material surface and biofilm formation. The results showed that different F/P procedures may affect surface chemistry depending on the materials and that the influence of each F/P procedure depends on the tested material. A significant negative linear relationship was found between the organic and inorganic fractions both before and after biofilm formation. Since the organic fraction after biofilm formation is composed by composite resin matrix and biofilm exopolysaccharide matrix, one would expect that the negative linear fit would show a homogeneous increase in organic fraction content compared to the data obtained before biofilm formation (i.e. a positive change in the y-intercept of the

linear fits). However, as indicated, the two fits had an almost identical y-intercept and a change in the slope, being less steep. This means that the increase in the organic fraction after biofilm formation, although present in all groups, tended to be higher where a high proportion of inorganic fraction was present. This may either indicate that more exopolysaccharide matrix was present where fillers were exposed, possibly to increase bacterial adhesion to an un-friendly surface, or that exopolysaccharide matrix was more firmly attached and consequently more difficult to remove where a higher proportion of fillers were exposed. This interesting possibility needs confirmation in further studies. Nevertheless, no simple and immediate correlations could be found between the material's surface chemistry and biofilm formation. In a previous study from our group using the same protocol of this study, less *S. mutans* biofilm formation was observed on composite surfaces polished with aluminum oxide discs than on specimens cured against Mylar strips (A. Ionescu et al., 2012). It was therefore supposed that the higher amount of inorganic component on polished specimens might be responsible of their better biological performances. Nevertheless, the experimental set-up of that study evaluated *S. mutans* biofilm formation after 48h and 96h of incubation without the presence of a salivary pellicle. In the present study specimens were coated with artificial saliva to allow the formation of salivary pellicle, in order to simulate oral conditions in a standardized way. It is well known that bacteria in the oral cavity normally coexist with saliva and the adhesion to a salivary pellicle layer on tooth and restoration surfaces is a critical step for oral bacterial colonization (Ikeda, Matin, Nikaido, Foxton, & Tagami, 2007). Thus, differences in the experimental setup of these two studies can explain the different findings, despite two finishing groups and one material being directly comparable.

Others have supported the assumption that surface properties, especially SFE, are transferred through the salivary pellicle layer and therefore are able to influence bacterial growth (Pratt-Terpstra, Weerkamp, & Busscher, 1987). However, it is also likely that those properties play an important role in influencing bacterial adhesion and early colonization, but their influence decrease over time as biofilm formation takes place and bacteria react to one another as opposed to a fresh surface (Dezelic, Guggenheim, & Schmidlin, 2009).

Considering the results gathered from EDS analysis, a reduced biofilm formation would be expected on the surface of the RBC containing fluoride filler particles as antibacterial agent (RBC D) (Ytterbium fluoride, (YbF3) as claimed by the manufacturer and confirmed by EDS). In particular, the higher percentage of inorganic component, including fluoride particles, showed by Groups 3, 4, 5 and 6 would have been responsible of their better

microbiological performances. Nevertheless, the amount of fluoride in material composition or its release were too low to show any significant reduction in biofilm formation. These observations were confirmed by the EDS analysis performed after microbial challenge in which specimens showed a similar amount of YbF3 showing the lack of elution of the antibacterial agent (data not shown).

The results of the present work should be interpreted within the study's limitations since this experimental design does not completely reproduce oral environmental conditions. The main limitation of the *in vitro* approach was the use of a monospecies *S. mutans* biofilm even if, considering its role in caries etiology, represents a useful model of pathogenic biofilm. Further *in vitro* studies are therefore needed to clarify the influence of the tested parameters on the development of a multispecies biofilm in controlled conditions. These preliminary evaluations should be followed by *in situ* and *in vivo* studies essential to confirm *in vitro* results.

It is therefore possible to conclude that a clear and immediate relationship between surface characteristics, such as gloss and roughness, and *S. mutans* biofilm formation could not be established. The influence of the different composite materials themselves on biofilm formation was however significant. Moreover, surface chemistry seems to play an important role in influencing biofilm formation, and may have greater influence than simply surface roughness parameters.

2.3 Evaluation of RBCs featuring antibacterial properties

The development of RBCs that may actively inhibit biofilm formation on their surfaces is a promising approach in contemporary dental materials science. Current strategies focus on tailoring materials with contact-killing surfaces including monomeric cationic quaternary ammonium compounds such as MDPB (methacryloyloxydodecylpyridinium bromide) or MAPTAC ([3-(methacryloylamino)propyl] trimethylammonium chloride) (Satoshi Imazato et al., 2012; Li Mei et al., 2012). Other promising strategies include the design of RBCs that release antimicrobial substances by incorporation of nano- and microparticulate antimicrobial agents such as metal ions, quaternary ammonium compounds, chitosan, (Allaker, 2010) or fluoride (Wiegand et al., 2007).

The antimicrobial effects of fluoride can be explained by its ability to inhibit not only the glycolytic enzyme enolase and the proton-extruding ATPase, but also bacterial colonization (Wiegand et al., 2007).

Currently, some RBCs with fluoride- releasing capabilities are available on the market. One of these commercially available products includes surface pre-reacted glass-ionomer (S-PRG) particles, which are produced in an acid-base reaction of fluoroaluminumsilicate glass with polyacrylic acid. It has been proven that RBCs incorporating S-PRG particles release fluoride and feature a recharging effect (Shimazu, Ogata, & Karibe, 2011). Moreover, recent *in vitro* studies indicated less biofilm formation on the surfaces of an RBC including S-PRG filler particles in comparison to conventional RBC materials (Yoneda et al., 2012).

With regard to the continuous improvement of RBCs and their interaction with oral biofilms, our research group recently proved a dependency of *S. mutans* biofilm formation on the chemical surface composition of RBC materials (A. Ionescu et al., 2012). By tailoring RBC surfaces with either high carbon (matrix-rich) or high silicon (filler-rich) content from several commercially available RBCs that did not include any antimicrobial agent, we observed a correlation between RBC surface carbon content and viable *S. mutans* biomass, suggesting that minimization of resin-matrix exposure might reduce biofilm formation on RBC surfaces. Using experimental RBCs derived from a commercial formulation including different fractions of fluoride-releasing S-PRG filler particles, the aim of this *in vitro* study was to elucidate the impact of surface treatment and surface composition on the release of fluoride and *S. mutans* biofilm formation. As it is clear that the matrix filler-surface ratio changes with increasing filler fractions and depending on the surface finishing protocol applied, the test hypotheses were that i) the release of fluoride from the experimental RBCs

increases as a function of filler fraction and is dependent on the protocol applied for surface treatment; ii) *S. mutans* biofilm formation decreases as a function of filler fraction and release of fluoride, and is also dependent on the protocol applied for surface finishing.

2.3.1 Materials and methods

Specimens preparation

Five experimental resin-based composites (RBCs) with a conventional bis-GMA/TEG-DMA resin matrix blend but different S-PRG filler weight (0/10/30/50/70% w/v) derived from a commercial RBC (Beautifil II) were supplied by Shofu (Kyoto, Japan). Eighty-six standardized specimens were prepared for each RBC by packing an excess of uncured RBC into a custom-made steel mold with a diameter of 6.0 mm and a height of 1.5 mm. The RBC was covered with a cellulose acetate strip (Mylar) placed on the top and bottom surfaces of the steel mold and condensed against a glass plate by centrally applying a load of 1 kg for 20 s. The specimens were then irradiated in one hit for 40 s by placing the light emitting diode of a hand-held light curing unit (SDI Radii plus, SDI; Bayswater, Australia; 1500 mW/cm2) into direct contact with the acetate strip.

Fifty percent of the RBC specimens received no further treatment (MYL, 43/group), whereas the other 50% of the RBC specimens were polished (POL, 43/group) using a standardized polishing procedure with abrasive paper (grain 1000/4000, Buehler; Lake Bluff, IL, USA) in an automated polishing machine (Motopol 8, Buehler; Düs- seldorf, Germany). These specimens were subsequently manually polished to a high gloss using a polishing paste designed for dental materials (Universal Polishing Paste, Ivoclar Vivadent; Schaan, Liechtenstein).

Enamel slabs and polystyrene specimens both with a diameter of 6.0 mm and a height of 1.5 mm were used as reference surfaces. For preparation of standardized enamel specimens, 40 slabs were cut from the labial surfaces of 40 anterior human teeth extracted for clinical reasons in the Oral Surgery Unit of the Department of Health Sciences, S. Paolo Hospital (Milan, Italy). The dentin bottoms of the slabs were removed with diamond burs (Intensiv; Grancia, Switzerland) and the specimens were subsequently polished in accordance with the procedure applied for the RBCs (POL). Forty polystyrene slabs were cut from the lid of a tissue-culture plate (Sigma-Aldrich; St Louis, MO, USA) using a flame-heated stainless steel circular punch. These specimens received no further sur- face treatment. All specimens were

stored under light-proof conditions in distilled water for 6 days at 37 ± 1°C for minimizing the impact of residual monomer leakage on cell viability and were subsequently carefully cleaned using ethanol (70%) and applicator brush tips (3M ESPE; Seefeld, Germany) prior to any further processing.

Surface Characterization

Surface roughness

Peak-to-valley surface roughness (Ra) was determined on the surface of five randomly selected specimens for each material and surface treatment, including the control group as described previously (cf. 2.1.1).

Atomic force microscope (AFM)

For high-resolution analysis of RBC surface topography, two specimens for each RBC and surface treatment were imaged with an atomic force microscope (AFM). Images with a size of 2 µm x 2 µm were recorded with a noncontact atomic force microscope (Giessibl & Trafas, 1994) using qPlus force sensors (Giessibl, 2000) with stiffness k = 1.0 kN/m and 1.28 kN/m and eigen frequencies of f_0 = 38 kHz and 22 kHz. Tips were made from etched tungsten wires and cleaved sapphire splinters. The imaging technique was frequency modulation AFM (FM-AFM)[1] at amplitudes ranging from 0.25 to 0.5 nm and frequency shift set points ranging from +5 to +50 Hz.

Surface-free energy (SFE)

SFE was evaluated on the surface of each of three randomly selected specimens for each material and surface treatment, including the control groups as shown previously (cf. 2.1.1).

Energy Dispersive X-ray Analysis (EDX)

For each experimental RBC and surface treatment, one randomly selected specimen was subjected to EDX analysis (EDX Genesis 2000, Ametek; Meerbusch, Germany) for

determination of surface chemistry and composition. EDX analysis was not performed on control groups.

Fluoride release

The release of fluoride was determined for 16 specimens for each RBC and surface treatment. The specimens were randomly divided into two subgroups, placed into 96-well polystyrene plates and immersed into 200 µl of bidistilled water. For determining the release of fluoride at the end of the biofilm experiments, the wells were covered with Parafilm and stored at 37°C for either 48 h or 120 h (n = 8/each). Each plate was rinsed with bidistilled water twice a day allowing the elution of soluble surface compounds – including fluoride – from the RBCs. Finally, the specimens were immersed in 200 µl of fresh bidistilled water, and the cumulative concentration of fluoride in the supernatant was determined after a period of seven days using the ion-selective electrodes micromethod (E. Brambilla, Felloni, Fadini, & Strohmenger, 1998). In brief, a stock solution with a fluoride concentration of 1000 ppm was appropriately diluted with bidistilled water to obtain fluoride standards with fluoride concentrations ranging from 1.9 to 1000 parts per billion (pbm). A calibration curve was obtained by measuring fluoride standards using a digital pH/mV meter (SA-720, Orion Research; Boston, MA, USA). Sodium acetate buffer 20% v/v with EDTA as ionic strength adjustor was added to each standard prior to analysis. A negative standard (0 pbm fluoride) was prepared by adding 20% v/v of sodium acetate buffer with EDTA to bidistilled water; this solution was also used to rinse the electrodes between the single measurements.

Saliva

Saliva collection was performed as described previously (cf. 2.2.1).

Bacteria

A wild strain of *S. mutans* was isolated and cultured as described above (cf. 2.1.1).

Modified Drip-flow Reactor and Viable Biomass Assessment

S. mutans biofilm formation was simulated under continuous flow conditions using a modified Drip- flow reactor for either 48 h or 120 h (cf. 2.1.1).
Sixteen specimens for each RBC and sur- face treatment as well as each reference material were used and randomly allotted to either 48 h (n = 8) or 120 h (n = 8) biofilm formation.
Viable *S. mutans* biomass was assessed using a MTT- based assay as described previously (cf. 2.1.1).

Statistical Analysis

All statistical analyses were performed using statistical software (Stata v.10, StataCorp; College Station, TX, USA). Homogeneity of variances was preliminarily checked and verified using Bartlett's test. Two-way ANOVA was used to analyse surface roughness, surface free energy, release of fluoride, and viable *S. mutans* biomass, setting the RBC and surface treatment as fixed factors. The analysis indicated no interaction effects between the two factors; thus, data were further analysed using one-way ANOVA models. The Student-Newman- Keuls post-hoc test was used to highlight significant differences. The level of significance (α) was set to 0.05.

2.3.2 Results

Surface Analysis

POL specimens manufactured from the experimental RBC with a filler fraction of 70% showed significantly higher Ra than the other experimental RBCs ($p < 0.01$), whereas no significant differences were identified between the other experimental RBCs and surface treatments ($p > 0.05$; **Table 4**). Qualitative AFM analyses (**Fig 24**) indicated the presence of an increasing amount of filler aggregates on the surface of the experimental RBCs with increasing filler fractions.
Polishing of the different experimental RBCs caused an increase in total SFE; this trend was significant for the RBCs with a 70% filler fraction ($p = 0.004$), which was due to a significant increase in both the disperse and polar contributions to total SFE ($p = 0.0251$ and $p = 0.0295$, respectively). For enamel, a significantly higher total SFE was identified than for all RBCs

and the polystyrene control ($p < 0.001$), which was due to a highly significant increase in the polar contribution to total SFE ($p < 0.001$).

EDX analysis identified a maximum of surface carbon, representing the organic resin matrix, on the surface of neat resins. Alumina and silicon, representing the inorganic filler fractions, were not detected in specimens manufactured from the neat resins. Progressively lower surface carbon contents and progressively higher alumina and silicon contents were identified with increasing filler fractions, except for MYL specimens produced from the RBC with a 30% filler fraction, which showed the highest alumina content.

Table 4: Surface roughness (Ra, µm, 5 specimens/group), surface free energy (erg/cm^2, 3 specimens/group) and EDX analysis (% surface content, 1 specimen/group) of the different experimental RBCs with either MYL or POL surfaces. Means and standard deviations (SD) are indicated. Identical superscript letters indicate no statistical significance for $\alpha = 0.05$.

Filler weight		SR (SD)	Total SFE (SD)	Polar SFE (SD)	Disperse SFE (SD)	EDX: C/O/F/Na/Al/Si surface content
0%	MYL	0.02(0.03)^{d}	42.02 (2.24)^{b,c}	0.11 (0.25)^{c}	41.91 (2.23)^{a,b}	82/16/1/0.2/0/0
	POL	0.07 (0.03)^{c,d}	44.52 (3.05)^{b}	1.44 (1.34)^{b,c}	43.08 (2.75)^{a}	76/22/1/0.4/0/0
10%	MYL	0.04 (0.00)^{c,d}	41.95 (2.34)^{b,c}	0.11 (0.30)^{c}	41.84 (2.32)^{a,b}	78/20/1/0.1/0.5/0.1
	POL	0.03 (0.01)^{c,d}	45.00 (1.49)^{b}	0.98 (0.87)^{b,c}	44.02 (1.21)^{a}	78/19/1/0.3/0.7/0.2
30%	MYL	0.04 (0.00)^{c,d}	42.16 (0.96)^{b,c}	0.19 (0.32)^{c}	41.96 (0.91)^{a,b}	67/28/1/0.1/3.7/0.4
	POL	0.05 (0.02)^{c,d}	43.80 (2.16)^{b}	0.93 (0.73)^{b,c}	42.87 (2.03)^{a}	68/30/1/0/0.8/0.1
50%	MYL	0.04 (0.00)^{c,d}	43.64 (1.73)^{b}	0.33 (0.66)^{b,c}	43.31 (1.60)^{a}	65/32/1/0.1/0.8/0.1
	POL	0.09 (0.03)^{b,c}	45.14 (1.44)^{b}	1.23 (0.79)^{b,c}	43.91 (1.20)^{a}	65/31/2/0.1/0.7/0.2
70%	MYL	0.04 (0.01)^{c,d}	39.86 (1.75)^{c}	0.12 (0.26)^{c}	39.74 (1.73)^{b}	60/36/2/0.2/1.4/0.3
	POL	0.14 (0.31)^{b}	45.29 (2.26)^{b}	1.95 (1.40)^{b}	43.35 (1.77)^{a}	51/38/7/1.0/1.8/1.3
Polystyrene		0.03 (0.02)^{c,d}	44.65 (2.06)^{b}	1.33 (0.68)^{b,c}	43.32 (1.95)^{a}	N/A
Enamel		0.41 (0.61)^{a}	53.68 (2.72)^{a}	14.06 (2.14)^{a}	39.59 (1.68)^{b}	N/A

Fig. 24: AFM analyses. Distributions of S-PRG filler particles on the different experimental RBC surfaces are displayed.

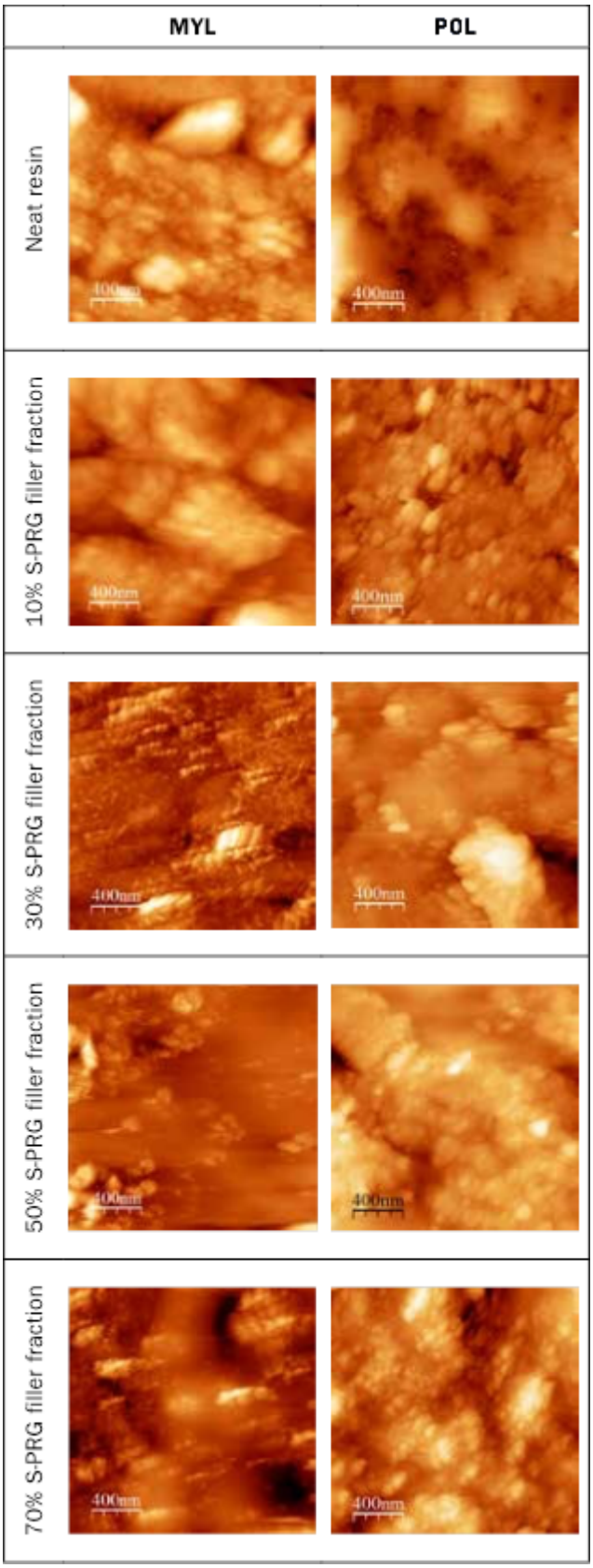

Fluoride Release and Surface Fluoride Content

The calibration curve for the assessment of fluoride release and the equation derived from regression analysis are displayed in **Fig.25.** Data obtained for the release of fluoride after either 48 h or 120 h are displayed in **Fig.26 and Fig.27.**

Data at 48 h showed a significant increase in the release of fluoride with increasing filler fractions. For RBCs with a filler load higher than 30%, a significant dependency on the surface treatment was identified, with POL specimens releasing significantly more fluoride than MYL specimens ($p < 0.001$). After 120 h, RBCs generally released less fluoride than after 48 h. There was a similar tendency regarding fluoride levels and filler fractions, yet for most values, differences did not meet the level of significance. No significant differences in the release of fluoride were identified for RBCs with a filler fraction of 10% and 30% in comparison to specimens produced from neat resin matrix. Significantly higher release of fluoride was identified for RBCs with a filler fraction of 70%, with POL specimens showing a significantly higher release of fluoride than MYL specimens ($p < 0.001$).

For POL RBCs with a filler fraction of 70%, EDX analyses indicated a fluoride surface content of 7%, whereas 1% to 2% fluoride surface content were observed for the other experimental RBCs and surface treatments.

Fig. 25: Calibration curve and linear regression plot for the determination of the release of fluoride.

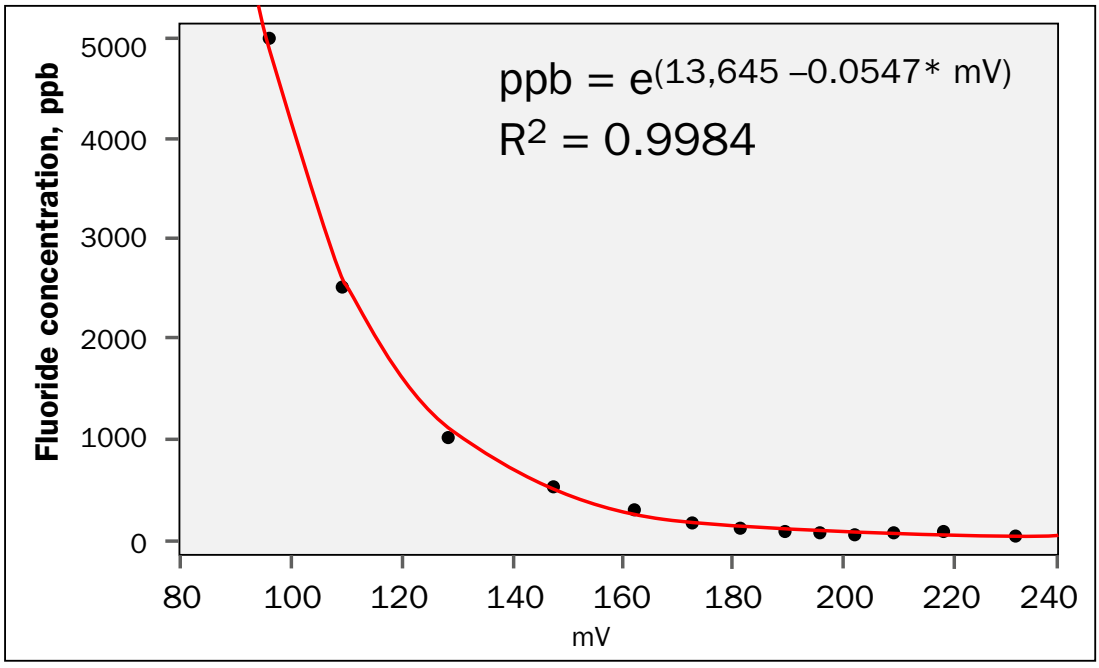

Fig. 26: Release of fluoride (ppm) from the different experimental RBCs after 48 h. Means and standard deviations (SD) are indicated. Identical superscript letters indicate no statistical significance for $\alpha = 0.05$.

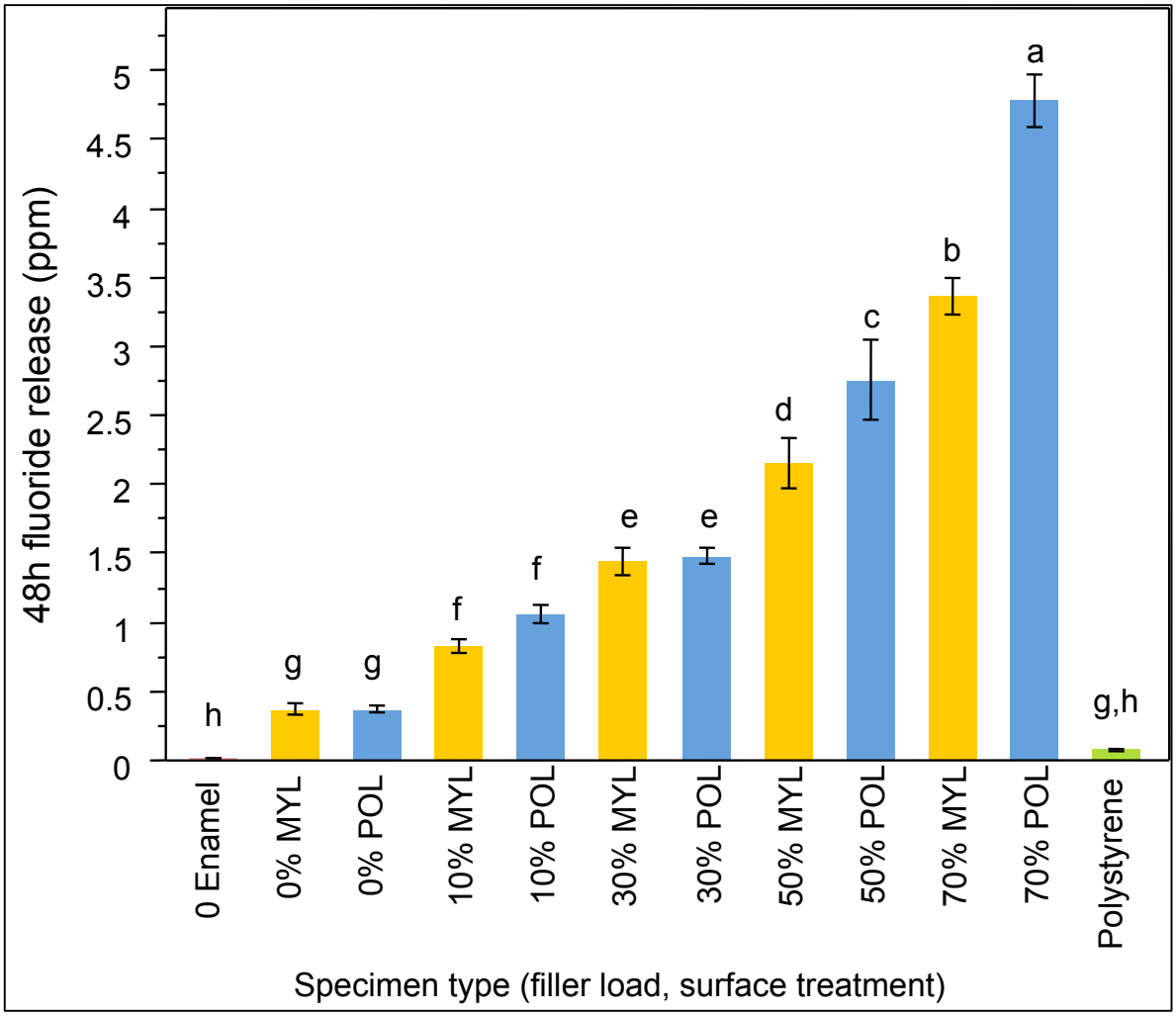

Fig. 27: Release of fluoride (ppm) from the different experimental RBCs after 120 h. Means and standard deviations (SD) are indicated. Identical superscript letters indicate no statistical significance for $\alpha = 0.05$.

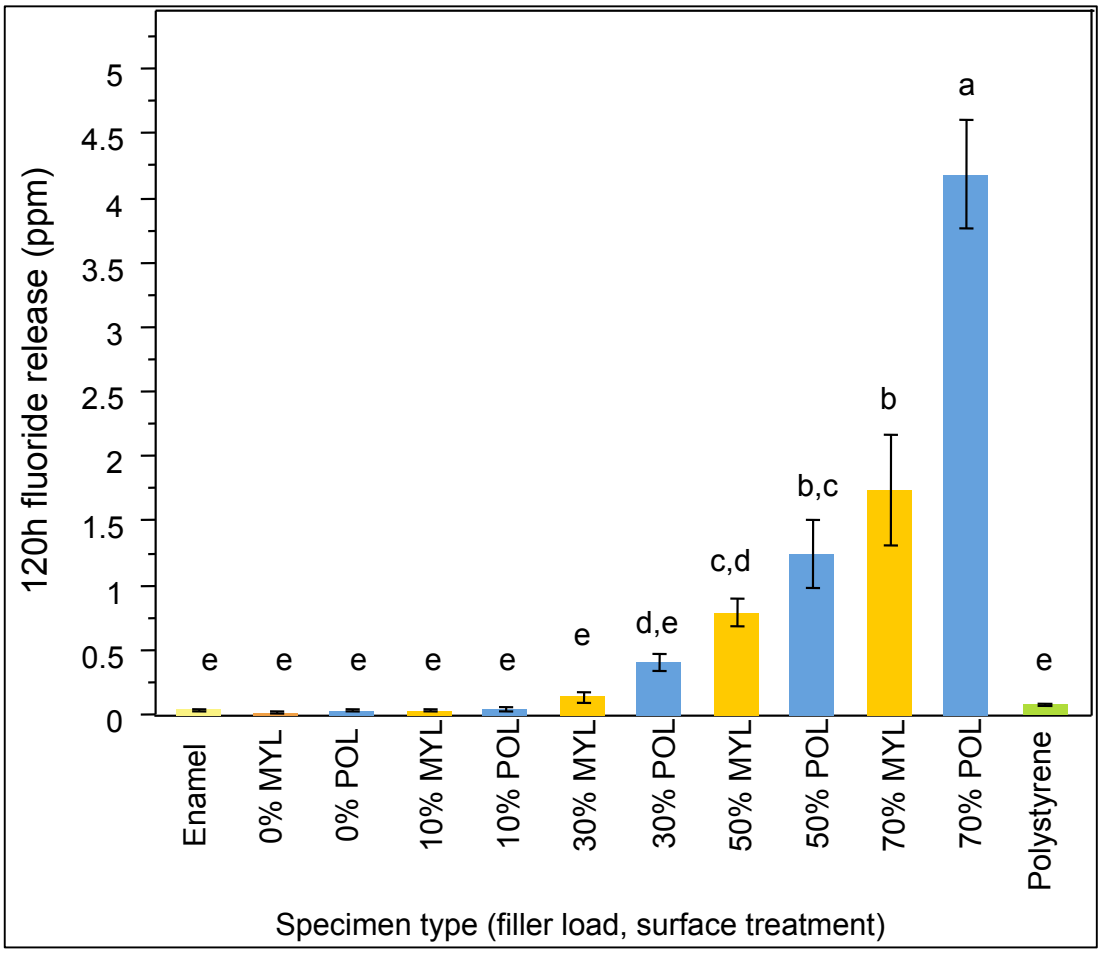

Biofilm formation

Data for viable *S. mutans* biomass after 48 h and 120 h of biofilm formation are displayed in **Fig. 28 and 29**, respectively. After 48 h of biofilm formation, a tendency towards decreasing *S. mutans* biomass with increasing filler fractions regardless of surface treatment was observed. For RBCs with identical filler fractions, no significant differences in *S. mutans* biomass were identified between MYL and POL specimens ($p > 0.25$). Significantly less *S. mutans* biomass was measured on POL specimens with a filler fraction of 70% in comparison to enamel ($p < 0.001$).

After 120 h of biofilm formation, the highest values for *S. mutans* biomass were identified for MYL RBCs with a filler fraction ≥30%. These values were significantly higher than

those measured for enamel ($p < 0.001$). For RBCs with filler fractions of 30% or 70%, POL specimens yielded significantly less *S. mutans* biomass than MYL specimens ($p = 0.002$ and $p = 0.001$, respectively); a similar yet not statistically significant trend was identified for RBCs with a filler fraction of 50% ($p = 0.161$).

Fig.28: Viable biomass assessment after 48 h of *S. mutans* biofilm formation. Data are displayed as mean ± 1 standard error (SE). Identical superscript letters indicate no statistical significance for $\alpha = 0.05$.

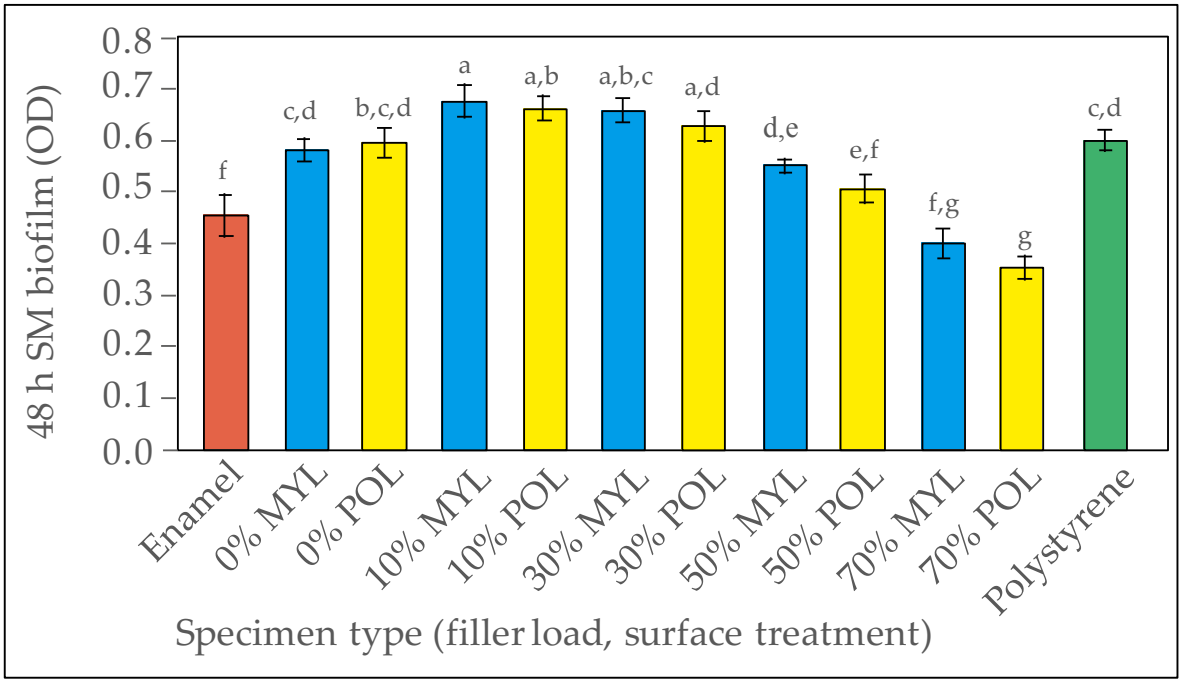

Fig. 29: Viable biomass assessment after 120 h of *S. mutans* biofilm formation. Data are displayed as mean ± 1 SE. Identical superscript letters indicate no statistical significance for $\alpha = 0.05$.

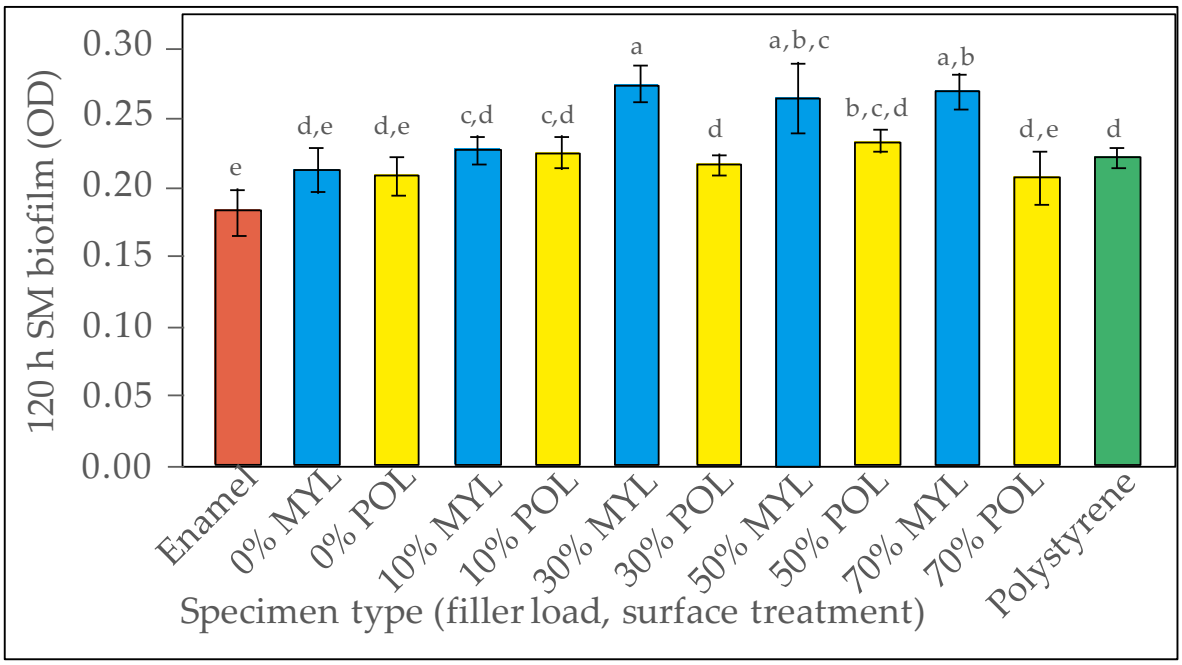

2.3.3 Discussion

The results of this *in vitro* study suggest acceptance of the first research hypothesis, showing that the release of fluoride increases as a function of S-PRG filler fraction. To a lesser extent, the release of fluoride was influenced by the protocol applied for surface finishing of experimental RBCs including S-PRG particles, indicating that polishing of the experimental RBCs causes an increase in the release of fluoride. The data obtained in the present study agree with the results of previous studies, (Kamijo et al., 2009) attesting a significant release of fluoride from S-PRG containing materials in dependence on filler fraction. Studies investigating the kinetics of the release of fluoride from RBCs as a function of time proved the existence of a so-called burst effect, with an initially high release of fluoride that diminishes rapidly with time (Temin & Csuros, 1988). These observations support the results of the present study, where the release of fluoride diminished markedly after five days in comparison to data obtained after two days. The only exception identified was for POL specimens manufactured from the RBC blend with a 70% filler fraction, which showed a similar release of fluoride after two and five days. In addition, EDX analyses showed that for the RBC with a filler fraction of 70%, the fluoride content of the experimental RBC surfaces was approximately 7% for surfaces that had been subjected to polishing (POL), whereas the fluoride content was markedly lower for surfaces without any surface treatment (MYL). These results suggest that optimizing surface finishing protocols for RBCs might help to improve the fluoride-releasing performance of RBCs including S-PRG particles. Regarding this aspect, future studies might focus on elucidating the impact of different surface finishing procedures on the fluoride recharging abilities of S-PRG-containing RBCs. However, the correlations between the release of fluoride, surface fluoride content, and filler fractions included into the experimental RBC formulations did not follow a dose-dependent pattern. This phenomenon is particularly interesting since the data of this study suggest the existence of a threshold value, indicating that exceeding a particular amount of S-PRG filler particles in an RBC formulation causes a significant increase in the release of fluoride and surface fluoride content.

Another interesting phenomenon observed in the present study was the release of fluoride from the control groups made of neat resin, even if the neat resins did not feature any fluoride releasing capacity. A valid explanation for this phenomenon may be that there have been changes in the ionic composition of the solution due to a release of monomers and ions from the surface of the experimental RBCs. These compounds may have influenced the readings

of the electrode despite of the addition of TISAB buffer; this effect might have been reduced by calibrating the electrode against a series of fluoride standards obtained from the solution in which the neat resin specimens were immersed, which is something that should be addressed in future studies. Considering the high surface alumina content observed for MYL specimens produced from the RBC with a 30% filler fraction, this phenomenon may be due to an inhomogeneous distribution of the S-PRG filler particles blended into the different experimental RBCs.

The second research hypothesis can only be accepted in parts, since a correlation between filler fraction, the release of fluoride, and *S. mutans* biofilm formation could be identified after 48 h, but not after 120 h. These results confirm the outcome of a recently published study, indicating that *S. mutans* biomass may be effectively reduced during the early stages of biofilm formation if enough fluoride is released from the substrate surface (Pandit, Kim, Lee, & Jeon, 2011).

Nevertheless, a pronounced influence of surface finishing on *S. mutans* biofilm formation was identified in the present study after 120 h of biofilm formation. Particularly for experimental RBCs with a filler fraction equal to or higher than 30%, significantly less biomass was identified for polished specimens (POL) than for those that had not undergone surface treatment (MYL). These data suggest that the effect of the release of fluoride on viable *S. mutans* biomass decreased over time, whereas the impact of the surface treatment increased with prolonged biofilm formation. It is therefore important to underline that the specific filler composition of the tested materials made them similar to a bioactive material which is barely comparable with conventional RBCs as those evaluated in the previous studies (cf. 2.1).

As the results of this study were obtained *in vitro*, they require careful interpretation within the limitations of the study design, which include the simulation of salivary pellicle formation prior to the simulation of single-species biofilm formation. It is generally quite complicated to provide reproducible laboratory conditions for the development of biofilms that adequately simulate intraoral plaque formation; however, analysis of biofilm formation on a multitude of different experimental materials *in vivo* using intraoral splints is complex, time-consuming and, due to the inter- and intra-individual differences in biofilm formation, hard to standardize. Continuous culture systems as employed in the present study operate under strictly defined experimental conditions; thus, biofilms developed in these systems have a growth rate, composition, and structure that closely resemble their *in vivo* counterparts (Tang, Yip, Cutress, & Samaranayake, 2003). In order to simulate clinical

conditions as far as possible, the authors isolated a wild-type *S. mutans* strain from human dental plaque rather than using a type collection strain. With regard to simulation of biofilm formation *in vitro*, it is commonly accepted that the presence of a salivary pellicle impacts subsequent adhesion and proliferation of bacteria, (C. Hannig & Hannig, 2009) although some researchers support the theory that the original substrate surface properties are transferred even through a protein layer (Pratt-Terpstra et al., 1987) and that the surface free energy of an RBC influences *S. mutans* adhesion irrespective of saliva coating.

Regarding the analysis of RBCs including S-PRG filler particles, Honda et al (Honda, 2004) identified a thin, layer-like interface including high levels of alumina, silicon and strontium on the surface of RBCs supplemented with S-PRG filler particles that had been exposed to saliva, and attributed this phenomenon to a reduced adhesion of *Streptococcus oralis* to these materials. In this study, EDX surface analyses of the various RBCs prior to salivary pellicle formation identified various amounts of alumina and silicon, but no traces of strontium (data not shown).

The techniques applied in this study for tailoring different experimental RBC surfaces (MYL vs POL) simulate typical clinical procedures for improving the aesthetic and functional performance of commercially available RBCs. In the present study, a standardized polishing regime derived from a clinical protocol using silicon carbide papers with decreasing grain sizes was applied for preparing polished specimens (POL). Dental matrices are most commonly applied for shaping the proximal areas of RBC restorations, and frequently these areas require no further surface finishing. Bollen et al (Bollen et al., 1997) recommended compression of resin-based composites against polyester strips as "the optimal way to make composite resins smooth", which justifies its application as a protocol for preparing non polished RBC specimens with a smooth surface (MYL). Using a similar procedure, Carlén et al (Carlen et al., 2001) identified significantly higher surface roughness for polished RBC samples in comparison to their counterparts polymerized against plastic strips. In the present study, a similar phenomenon was observed for the experimental RBC with a filler fraction of 70%, whereas for all other experimental RBCs, no significant differences in surface roughness were identified. Due to the small areas analysed, AFM analyses on heterogeneous materials such as RBCs need to be interpreted carefully by also considering the results obtained with other surface analysis techniques, such as profilometry. In this study, qualitative AFM analyses indicated the presence of an increasing amount of filler particles on the surface of RBCs with increasing filler fractions, whereas visual differences between POL and MYL surfaces were rather subtle. In particular, MYL surfaces were hard to image

due to a high number of tip changes, possibly due to agglomeration of resin matrix. However, the mean Ra for the experimental RBCs was below the 0.2 μm threshold introduced by some researchers in the 1990s, (Bollen et al., 1997)suggesting that lower values do not have a significant impact on biofilm formation. This assumption supports the idea that the differences in surface roughness values observed in this study cannot be responsible for differences in biofilm formation on the different experimental RBCs.

With regard to surface free energy, the literature provides only little evidence on the extent to which changes in surface free energy and surface chemistry influence biofilm formation (A. Ionescu et al., 2012). In the present study, all experimental RBCs with polished surfaces (POL) showed lower total surface free energy than their unpolished counterparts (MYL). However, for neat resins without any S-PRG fillers, a similar phenomenon was observed after polishing, and an increase in filler fraction did not significantly impact surface free energy values. Recent studies have associated the surface free energy of a material with microbial binding forces rather than with the extent of biofilm formation, suggesting that the impact of originally distinct surface free energies gradually disappears as a function of time (Busscher et al., 2010).These considerations might explain why no correlation between surface free energy and viable biomass could be identified in this study. However, as RBCs never yield homogeneous surfaces due to their heterogeneous composition with matrix and filler rich areas on both a micro and nanoscale level, results of contact angle measurements on RBC surfaces should not be overestimated.

The results of the present in vitro study suggest an impact of fluoride-releasing S-PRG filler particles particularly on the early phases of biofilm formation on RBCs. As the release of fluoride diminishes as a function of time, optimizing the fluoride-recharging abilities of RBCs including S-PRG filler particles might help to control biofilm formation for longer periods. The final polishing of RBC restorations may substantially influence the release of fluoride.

2.4 Design of an experimental RBCs featuring bioactive and biomimetic properties

A completely different approach has been introduced with the design of biomimetic materials, which foster the remineralization of natural tooth tissues adjacent to the restoration (Chae, Yang, Ko, & Troczynski, 2014; Chang et al., 2013). There have been attempts to develop RBCs featuring both biofilm-controlling and biomimetic properties by including calcium-phosphate nanoparticles (Cheng et al., 2012; Melo et al., 2013). Dicalcium phosphate dihydrate (CaHPO4*2H2O) nanoparticles (nDCPD) additioned as bioactive fillers in RBCs may release calcium and phosphate ions to areas nearby RBC restorations. These ions may reprecipitate to form hydroxyapatite (Marcela C. Rodrigues, Natale, Arana-Chaves, & Braga, 2015). Regarding a potential antibacterial activity of these nanoparticles, previous studies reported conflicting results (C. Chen et al., 2014) (Moreau, Sun, Chow, & Xu, 2011).

The synthesis of nDCPD particles may include different chemical agents such as methacrylates in order to add specific functionalities (Arcís et al., 2002). Recently, it has been reported that the functionalization of nDCPD with triethyleneglycol dimethacrylate (TEGDMA) reduces agglomeration of the nanoparticles and improves their compatibility with RBCs (Marcela Charantola Rodrigues, Hewer, de Souza Brito, Arana-Chavez, & Braga, 2014).

The aim of this study was to evaluate biofilm formation on the surface of an experimental RBCs including TEGDMA-functionalized (F-nDCPD-RBC) and non-functionalized DCPD nanoparticles (nDCPD-RBC). The null hypotheses were that (I) the inclusion of nDCPD does not lead to a decrease in biofilm formation on the surface of the experimental RBCs in comparison to reference RBCs without nDCPD, and (II) biofilm formation on the surface functionalized nDCPD-RBC was not different in comparison to non functionalized n-DCPD-RBC.

2.4.1 Materials and methods

Nanoparticles synthesis

Triethyleneglycol dimethacrylate (TEGDMA)-functionalized DCPD nanoparticles (F-nDCPD) were synthesized as previously published (Marcela Charantola Rodrigues et al., 2014) by the stoichiometric reaction between ammonium phosphate ((NH4)2HPO4) and calcium nitrate (Ca(NO3)2.4H2O) by a sol-gel process. Two solutions with equal

concentrations (0.078 mol/L) of the previously specified salts were prepared using distilled and deionized water. Using a peristaltic pump (9 mL/min), 400 mL of the calcium nitrate solution were added drop-wise to the same volume of ammonium phosphate solution, which had previously been supplemented with 7 g of TEGDMA (2-methyl 2-propenic acid, Mw = 286 g/mol, ESSTECH, Technology Inc, Essington, PA, USA). Precipitation occurred at room temperature under constant stirring, which was sustained for 30 min after dripping was finished. The pH of the final solution was 5.2. After decantation, the nanoparticles were rinsed with distilled water to remove reminiscent ions and excess TEGDMA. The resulting paste was freeze-dried and a white powder was obtained. For the preparation of non-functionalized DCPD nanoparticles (nDCPD), an analogous synthesis procedure without the addition of TEGDMA to the ammonium phosphate solution was performed.

Specimens preparation

All reagents, including the different resin monomers and the multi-well plates used, were purchased from Sigma-Aldrich (Sigma-Aldrich, St. Louis, MO, USA) unless specified otherwise. An experimental resin matrix blend including equal parts in mols of BisGMA (2,2-bis[4-(2-hydroxy-3-methacryloylpropoxy)]-phenyl propane) and TEGDMA was prepared by adding camphorquinone (0.5% wt.) and N,N-dimethylaminoethyl methacrylate (0.5% wt.). Experimental RBCs were manufactured by supplementing the resin matrix with either:

- 20 vol% TEGDMA-functionalized DCPD nanoparticles (F-nDCPD- RBC),
- 20 vol% non-functionalized DCPD nanoparticles (nDCPD-RBC),
- 20 vol% silanized silica (SiO2- RBC).

The experimental resin matrix blend (control-Resin) and a conventional commercially available nano-hybrid RBC (control-RBC) including a filler fraction of 77 vol% (Grandio, VOCO GmbH, Cuxhaven, Germany) as well as human enamel were used as reference materials.

A total of 36 specimens were manufactured for each of the different materials. For preparation of a single RBC specimen, a standardized amount of uncured RBC was placed into a custom-made steel mold with a diameter of 6.0 mm and a height of 1.5 mm, condensed against a glass plate covered by a cellulose acetate cover (Mylar®) to prevent the formation of an oxygen-inhibited layer, and light-cured employing four overlapping irradiation regimes with a single duration of 40 sec with a LED curing unit (Radii cal, SDI, Bayswater, Australia; curing power: 1200 mW/cm2).

Human permanent teeth extracted for clinical reasons were stored under dry conditions at a temperature of - 20°C until use. Thirty-six round slabs of sound enamel with a diameter of 6.0 mm and a thickness of 1.5 mm were cut from the flat labial surfaces using a water-cooled trephine diamond bur (INDIAM, Carrara, MS, Italy). Enamel specimens were placed into the wells of a polystyrene well plate and sterilized with a chemical peroxide-ion plasma sterilizer (STERRAD, ASP, Irvine, CA, USA) with a maximum temperature of 45°C for preventing heat-related damage of the enamel surfaces. All specimens were subjected to a standardized polishing protocol using 1000/4000-grit grinding paper (Buehler, Lake Bluff, IL, USA) and an automated polishing machine (Motopol 8; Buehler, Düsseldorf, Germany). The resin specimens were stored in well plates under light-proof conditions for 24 h at 37°C to allow complete polymerization of the materials; then, 1000 µL of sterile phosphate-buffered saline (PBS) were added to each well. Plates were stored at room temperature for an additional seven days in order to allow leaching of residual monomers. Each well was rinsed twice a day with 1000 µL of sterile PBS.

Surface analysis

Surface roughness (Ra), Surface free energy (SFE) (Owens approach) and Energy-dispersive X-ray spectroscopy (EDS) were used as already described (cfr.2.1.1.).

Microbiological evaluation

A pure suspension of *S. mutans* ATCC 35668 in Brain Heart Infusion broth (BHI) was obtained as specified before (cf. 2.1.1) and saliva collection was performed as already specified (cf. 2.2.1).
A modified drip-flow reactor (MDFR) was assembled and used to obtain a monospecific *S. mutans* biofilm under continuous flow conditions as previously reported (cf. 2.1.1)
After 48 h of incubation viable biomass was performed using the MTT assay as described previously (cf. 2.1.1).

Statistical analysis

Statistical analyses were performed using JMP 10.0 software (SAS Institute, Cary, NC, USA). Homogeneity of variances was preliminarily checked and verified using Bartlett's test. One-way ANOVA and Student's post hoc t-test were used to highlight significant differences between experimental groups. The level of significance (α) was set to .05.

2.4.2 Results

Surface analysis

Data are shown in **Table 5.** Significantly higher Ra was identified for nDCPD-RBC than for all other materials investigated (P<.005). Intermediate Ra values were identified for F-nDCPD RBC, control-RBC, as well as enamel while significantly lowest Ra was measured for control-Resin and SiO_2-RBC.

nDCPD-RBC showed a significantly higher contribution of the polar component and a significantly lower contribution of the disperse component to total SFE than all other materials (P<.0005 and P<.02, respectively). Enamel yielded a significantly higher total SFE in comparison to the other materials (P<.0005), which was due to a significantly higher polar contribution to total SFE (P<.0001).

Chemical surface analyses indicated higher amounts of calcium and phosphate on the surface of nDCPD-RBC than on F-nDCPD-RBC. Small amounts of fluoride and traces of barium and strontium were identified on the surface of control-RBC.

Table 5: Surface analysis of the tested materials. SR,SFE and EDS data are displayed as means (± 1 standard deviation). Significant differences between groups are marked by different letters ($p<0.05$).

Material	SR (R_a,μm)	SFE (mJ/m^2)			EDS (%)
		Total	Disperse	Polar	C, Ca, P, Si, O
F-nDCPD-RBC	0.185 (0.005)b	44.81 (1.30)b	43.88 (1.23)a	0.93 (0.42)c	73.6, 1.2, 1.4, 0.0, 23.6
nDCPD-RBC	0.256 (0.048)a	40.71 (3.70)c,d	33.79 (3.20)d	6.92 (1.86)b	73.0, 3.7, 2.9, 0.0, 20.3
SiO_2-RBC	0.089 (0.005)c	43.31 (1.50)b,c	41.25 (1.23)a,b	2.21 (0.71)c	65.8, 0.0, 0.0, 7.2, 26.9
control-Resin	0.103 (0.010)c	44.94 (0.75)b	44.01 (0.60)a	0.92 (0.44)c	79.2, 0.0, 0.0, 0.0, 20.7
control-RBC	0.145 (0.008)b	37.95 (0.06)d	37.39 (0.05)c	0.56 (0.02)c	37.9, 0.0, 0.0, 9.9, 46.7 Al:2.2,F:1.6,Ba:0.7,Sr:0.8
Enamel	0.165 (0.031)b	53.68 (2.72)a	39.59 (1.68)b,c	14.06 (2.14)a	23.2, 16.5, 10.0, 0.0, 50.3

Biofilm formation

Results regarding biofilm formation are displayed in **Fig. 30**. Relative absorbance values were significantly lower on the surface of F-nDCPD-RBC than on nDCPD-RBC ($P<.03$), which suggests lower *S. mutans* biofilm formation on the surface of F- nDCPD-RBC. Regardless of functionalization, biofilm formation was similar on the surface of both nDCPD-containing RBCs in comparison to SiO_2-RBC ($P=.21$ and $P=.33$, respectively). Significantly lower relative absorbance values indicating significantly less biofilm formation was identified for control-Resin and enamel in comparison to both experimental RBCs including nDCPD ($P<.05$).

Fig.30: Biofilm formation on the surface of the tested materials after 48h incubation under continuous flow conditions. Values are expressed as means (±1 standard error). Levels not connected by same letter are significantly different ($p<0.05$).

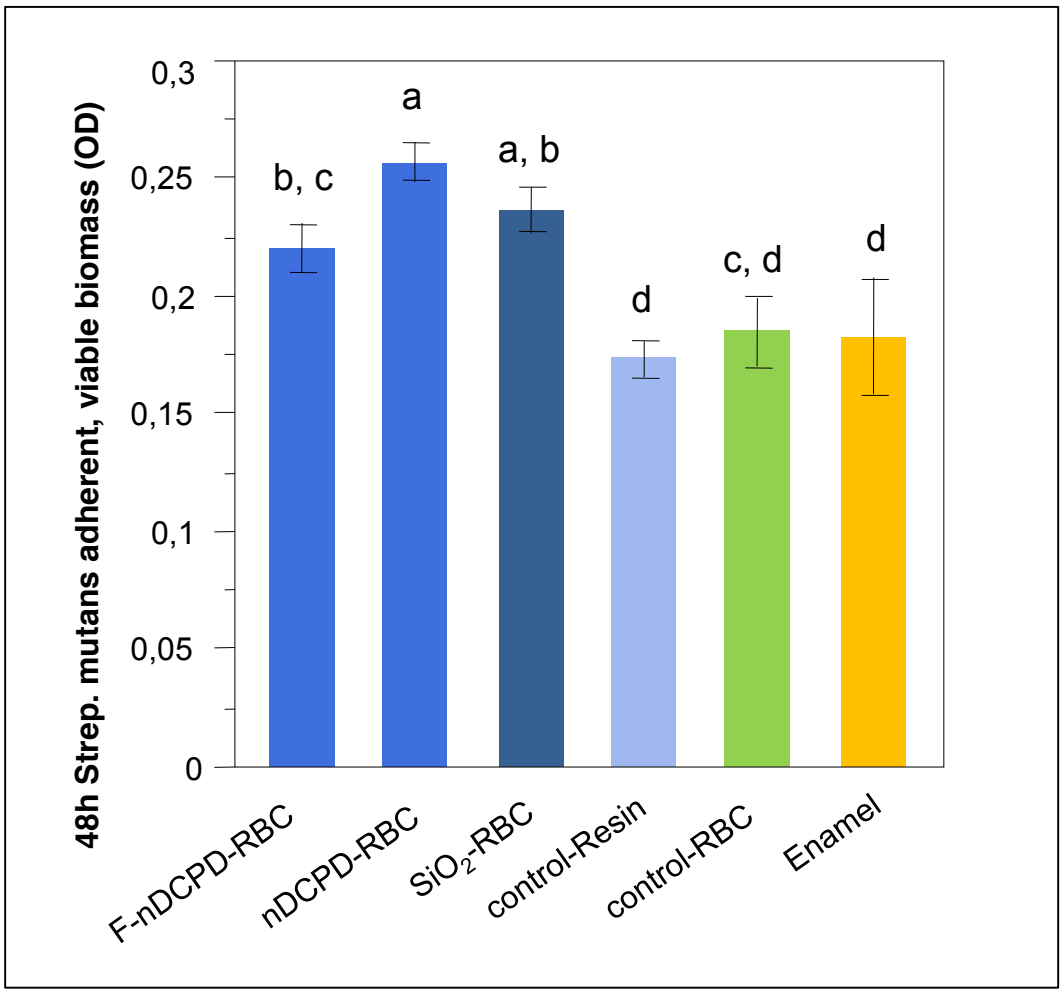

2.4.3 Discussion

The results of the present study suggest acceptance of the first null hypothesis, as it was identified that biofilm formation on RBCs including nDCPD was similar to biofilm formation on the surface of an experimental RBC formulation including SiO_2. The second null hypothesis, suggesting that functionalization of nDCPD does not affect biofilm formation, must be rejected since functionalization of nDCPD with TEGDMA caused a significant decrease in biofilm formation.

It is well-known that surface parameters have an impact on biofilm formation, and the influence of surface roughness on biofilm formation is undoubted. Previous studies have identified a 0.2 µm threshold Ra value, suggesting that lower Ra does not further decrease biofilm formation (Bollen et al., 1997). This phenomenon may explain the differences observed in the present study regarding biofilm formation on the surface of RBCs including F-nDCPD and n-DCPD. TEGDMA functionalization causes a three-fold increase in the surface area of the nanoparticles and reduces their tendency towards agglomeration, although the size of the nanoparticles themselves does not substantially change (Marcela Charantola Rodrigues et al., 2014). In fact, Ra values identified for nDCPD-RBC were higher than the threshold value of 0.2 µm identified by Bollen, which implies that differences in biofilm formation may be attributed to differences in surface roughness. This aspect may elucidate the higher biofilm formation observed on the surface of nDCPD-RBC in comparison to F-nDCPD-RBC and may also explain a similar biofilm formation on control-Resin, control-RBC, and enamel.

However, despite of the high number of studies dealing with biofilm formation on the surface of commercial or experimental RBCs *in vitro* or *in vivo*, they still fails to explain all differences observed in biofilm formation on experimental or commercial RBCs, as also assessed in the previous studies (cf. 2.1,2.2). Current scientific literature provides only limited evidence in how far surface properties such as surface free energy or surface chemistry impact biofilm formation on the surface of complex materials such as dental RBCs (Guggenheim et al., 2001; Andrei Ionescu et al., 2015). RBCs feature an inhomogeneous composition with chemically distinct constituents such as hydrophilic filler particles and hydrophobic resin matrix; thus, in contrast to other polymeric materials such as polytetrafluorethylene or silicone, RBCs never yield homogeneous surfaces (cf. 2.1) (Andrei Ionescu et al., 2015). This circumstance explains the difficulties associated with providing reproducible surface free energy calculations from contact angle measurements on RBCs

and may, at least in part, help to explain why numerous studies have failed to prove a relation between surface free energy and microbial adherence and proliferation on the surface of RBCs, although these have been proven to exist for less complex surfaces. The outcomes of the present study corroborate these previous results, as no significant relation between surface free energy and biofilm formation on the various RBCs could be identified. Furthermore, a recent study has associated the surface free energy of a material with microbial binding forces rather than with microbial adherence and proliferation (Busscher et al., 2010), suggesting that the impact of originally distinct surface free energies gradually disappears as a function of time.

In the present study, biofilm formation was significantly higher on the surface of SiO_2-RBC than on the surface of control-Resin, which supports previously published observations from our groups and may be the result of differences in surface topography on a sub-Ra-level (Hahnel et al., 2014; Andrei Ionescu et al., 2015). Another explanation for the differences in biofilm formation between these RBCs may be the presence of low levels of fluoride and strontium on the surface of control-RBC, which – although the exact mechanism is still to be investigated – feature antimicrobial properties (Dabsie, Gregoire, Sixou, & Sharrock, 2009; Hahnel et al., 2014; Wiegand et al., 2007). However, it is not easy to directly compare the surface characteristics of the control-RBC with the experimental composites, due to the very high differences in filler content (87% wt. vs. 20% wt.) which mean that also more resin matrix is exposed on the surfaces of the experimental RBCs compared to the control one.

To date, very few studies investigated potential antibacterial and antiadhesive properties of calcium-phosphate containing RBCs. Moreau and co-workers (Moreau et al., 2011) demonstrated that an experimental RBC containing nanoparticles of amorphous calcium phosphate (NACP) featured the capacity to neutralize acids and appeared to moderately reduce *S. mutans* growth in an agar disk-diffusion assay, which does not sufficiently respond to the processes involved in biofilm formation. However, the data gathered in the present study corroborate previous studies from other groups, who employed a human *in situ* model and identified no significant differences in biofilm formation between a NACP-including RBC and a conventional RBC (Melo et al., 2013).

Most laboratory studies simulating biofilm formation on RBCs employed monospecies biofilm models, yet due to different experimental settings the results of the studies are hard to compare. It is complex to provide reproducible and valid laboratory conditions for the simulation of biofilm formation that adequately responds to intraoral plaque formation (McBain et al., 2005). Continuous culture systems as employed in the present study operate

under strictly defined experimental conditions (Shu, Wong, Miller, & Sissons, 2000), which ensure reproducible conditions and the development of biofilms with a growth rate, composition, and structure that closely resemble their *in vivo* counterparts (Tang et al., 2003). It is commonly accepted that the presence of a salivary pellicle impacts subsequent adhesion and proliferation of bacteria. Some researchers support the theory that the original substrate surface properties are transferred even through a salivary protein layer and that the surface free energy of a surface influences *S. mutans* adhesion irrespective of saliva coating. In the present study, the formation of *S. mutans* biofilms was simulated after salivary pellicle formation. *S. mutans* is an acidogenic and acidotolerant microbial species (Philip D. Marsh et al., 2011) and an important aetiological agent in the development of dental caries, which are considerations that justify its selection for application in a monospecies biofilm model.

In conclusion, the results of this study did not prove the existence of antibiofilm activity of nDCPD-filled RBCs. However, functionalization of nDCPD reduced surface roughness of RBCs including nDCPD, which helped to minimize biofilm formation on the surface of these materials. It may be possible to suppose that calcium-phosphate nanoparticles can prevent secondary caries by conferring biomimetic, remineralizing capabilities to RBCs rather than by having a direct impact on biofilms.

3 General discussion and conclusions

In this PhD thesis different approaches were evaluated in order to discriminate the parameters influencing the microbiological behaviour of resin-based dental materials and therefore allow the optimization of materials formulation. Hence, the final aim was to promote the development of materials able to modulate oral biofilm formation on their surfaces.

In the last decade, virtually everything we thought to know about the origins and causes of oral disease has been turned upside down. The dental research community learns always more about the unique features of the oral microbiome, the unique natural ecology of the mouth and its role in determining oral and overall health.

Joshua Lederberg first coined the term 'Microbiome' to define the ecological community of commensal, symbiotic, and pathogenic microorganisms that literally share our body space, arguing that microorganisms inhabiting the human body should be included as part of the human genome, as they directly influence the human physiology (Lederberg & McCray, 2001). This new understanding of the essential synergistic and symbiotic relationship between human and microbe has been the focus of the Human Microbiome Project supported by the National Institute of Health. It has also redefined our "humanity" to be that of a microbiome/human *superorganism (Van Duynhoven et al., 2011)*.

For decades the healthcare approach proposed was related to the necessity of completely eradicating oral biofilm from both natural and artificial surfaces.

Innovative research is therefore based on the description of the mouth as an *ecosystem,* that is to say a network or community of microorganisms that live in cooperation with each other and, above all, live in symbiosis with the host.

The oral microbiome is a vital, natural and supportive component to oral health protecting teeth, gums and mouth linings. The problem then, is not that the oral microbiome exists, but rather it can become unbalanced and unhealthy. Disease occurs when the oral microbiome loses homeostasis.

Considering dental caries, this disease results from the complex interactions between the commensal microbiota, host susceptibility, environmental factors and, as it has been demonstrated, restorative materials surfaces. Since dental caries originates from a dysbiotic biofilm, the study of these interactions and the development of materials able to modulate biofilm formation promoting the saprophyte bacteria may be the key to promote oral health.

It is therefore possible to state that the use of resin-based composites with antibacterial properties may represent a simplified approach to prevent secondary caries development since it is just based on the elimination of cariogenic bacteria. On the other hand, the optimization of composites formulation to develop surfaces able to modulate biofilm formation and guide the development of a healthy biofilm without employing antibacterial agents as well as biomimetic materials may represent innovative approaches to modulate the interactions between oral microbiome and the host.

In conclusion, great improvements have been performed to synthesize restorative materials able to successfully prevent the occurrence of secondary caries and Researchers should perform continuous efforts in this direction.

4 References

Adams, H., Winston, M. T., Heersink, J., Buckingham-Meyer, K. A., Costerton, J. W., & Stoodley, P. (2002). Development of a laboratory model to assess the removal of biofilm from interproximal spaces by powered tooth brushing. *American Journal of Dentistry, 15*, 12B-17B.

Al-Ahdal, K., Ilie, N., Silikas, N., & Watts, D. C. (2015). Polymerization kinetics and impact of post polymerization on the Degree of Conversion of bulk-fill resin-composite at clinically relevant depth. *Dental Materials, 31*(10), 1207-1213. doi:10.1016/j.dental.2015.07.004

Albrecht, T. R., Grütter, P., Horne, D., & Rugar, D. (1991). Frequency modulation detection using high-Q cantilevers for enhanced force microscope sensitivity. *Journal of Applied Physics, 69*(2), 668-673.

Allaker, R. P. (2010). The use of nanoparticles to control oral biofilm formation. *Journal of Dental Research, 89*(11), 1175-1186.

Antonson, S. A., Yazici, A. R., Kilinc, E., Antonson, D. E., & Hardigan, P. C. (2011). Comparison of different finishing/polishing systems on surface roughness and gloss of resin composites. *Journal of Dentistry, 39*, e9-e17.

Arcís, R. W., López-Macipe, A., Toledano, M., Osorio, E., Rodríguez-Clemente, R., Murtra, J., . . . Pascual, C. D. (2002). Mechanical properties of visible light-cured resins reinforced with hydroxyapatite for dental restoration. *Dental Materials, 18*(1), 49-57.

Arends, J., Ruben, J., & Dijkman, A. G. (1990). The effect of fluoride release from a fluoride-containing composite resin on secondary caries: an in vitro study. *Quintessence International, 21*(8).

Auschill, T. M., Arweiler, N. B., Brecx, M., Reich, E., Sculean, A., & Netuschil, L. (2002). The effect of dental restorative materials on dental biofilm. *European Journal of Oral Sciences, 110*(1), 48-53.

Avsar, A., Yuzbasioglu, E., & Sarac, D. (2014). The Effect of Finishing and Polishing Techniques on the Surface Roughness and the Color of Nanocomposite Resin Restorative

Materials. *Advances in clinical and experimental medicine: official organ Wroclaw Medical University, 24*(5), 881-890.

Aykent, F., Yondem, I., Ozyesil, A. G., Gunal, S. K., Avunduk, M. C., & Ozkan, S. (2010). Effect of different finishing techniques for restorative materials on surface roughness and bacterial adhesion. *Journal of Prosthetic Dentistry, 103*(4), 221-227. doi:10.1016/S0022-3913(10)60034-0

Baseren, M. (2004). Surface roughness of nanofill and nanohybrid composite resin and ormocer-based tooth-colored restorative materials after several finishing and polishing procedures. *Journal of Biomaterials Applications, 19*(2), 121-134. doi:10.1177/0885328204044011

Bashetty, K., & Joshi, S. (2010). The effect of one-step and multi-step polishing systems on surface texture of two different resin composites. *J Conserv Dent, 13*(1), 34-38. doi:10.4103/0972-0707.62637

Bayne, S. C., Thompson, J. Y., Swift, E. J., Jr., Stamatiades, P., & Wilkerson, M. (1998). A characterization of first-generation flowable composites. *Journal of the American Dental Association, 129*(5), 567-577.

Beyth, N., Bahir, R., Matalon, S., Domb, A. J., & Weiss, E. I. (2008). Streptococcus mutans biofilm changes surface-topography of resin composites. *Dental Materials, 24*(6), 732-736. doi:10.1016/j.dental.2007.08.003

Bollen, C. M., Lambrechts, P., & Quirynen, M. (1997). Comparison of surface roughness of oral hard materials to the threshold surface roughness for bacterial plaque retention: a review of the literature. *Dental Materials, 13*(4), 258-269.

Botta, A. C., Duarte Jr, S., Paulin, F. P. I., Gheno, S. M., & Powers, J. M. (2009). Surface roughness of enamel and four resin composites. *American Journal of Dentistry, 22*(5), 252-254.

Bourbia, M. (2013). Biodegradation of Dental Resin Composites and Adhesives by Streptococcus mutans: An in vitro Study.

Bowen, R. L. (1963). Properties of a silica-reinforced polymer for dental restorations. *Journal of the American Dental Association, 66*, 57-64.

Braga, R. R., Ballester, R. Y., & Ferracane, J. L. (2005). Factors involved in the development of polymerization shrinkage stress in resin-composites: a systematic review. *Dental Materials, 21*(10), 962-970. doi:10.1016/j.dental.2005.04.018

Brambilla, E., Felloni, A., Fadini, B. L., & Strohmenger, C. L. (1998). A simplified micromethod for fluoride analysis. *Archives of Oral Biology, 43*(10), 819-823.

Brambilla, E., Ionescu, A., Fadini, L., Mazzoni, A., Imazato, S., Pashley, D., . . . Gagliani, M. (2013). Influence of MDPB-containing primer on Streptococcus mutans biofilm formation in simulated Class I restorations. *Journal of Adhesive Dentistry, 15*, 431-438.

Brambilla, E., Ionescu, A., Mazzoni, A., Cadenaro, M., Gagliani, M., Ferraroni, M., . . . Breschi, L. (2014). Hydrophilicity of dentin bonding systems influences in vitro Streptococcus mutans biofilm formation. *Dental Materials, 30*(8), 926-935. doi:10.1016/j.dental.2014.05.009

Brentel, A. S., Kantorski, K. Z., Valandro, L. F., Fucio, S. B., Puppin-Rontani, R. M., & Bottino, M. A. (2011). Confocal laser microscopic analysis of biofilm on newer feldspar ceramic. *Operative Dentistry, 36*(1), 43-51. doi:10.2341/10-093-LR

Buchgraber, B., Kqiku, L., Allmer, N., Jakopic, G., & Städtler, P. (2011). Surface roughness of one nanofill and one silorane composite after polishing. *Collegium Antropologicum, 35*(3), 879-883.

Burke, F. M., Ray, N. J., & McConnell, R. J. (2006). Fluoride-containing restorative materials. *International Dental Journal, 56*(1), 33-43.

Busscher, H. J., Rinastiti, M., Siswomihardjo, W., & van der Mei, H. C. (2010). Biofilm formation on dental restorative and implant materials. *Journal of Dental Research, 89*(7), 657-665. doi:10.1177/0022034510368644

Carlen, A., Nikdel, K., Wennerberg, A., Holmberg, K., & Olsson, J. (2001). Surface characteristics and in vitro biofilm formation on glass ionomer and composite resin. *Biomaterials, 22*(5), 481-487.

Cazzaniga, G., Ottobelli, M., Ionescu, A., Garcia-Godoy, F., & Brambilla, E. (2015). Surface properties of resin-based composite materials and biofilm formation: A review of the current literature. *American Journal of Dentistry, 28*(6).

Chae, T., Yang, H., Ko, F., & Troczynski, T. (2014). Bio-inspired dicalcium phosphate anhydrate/poly (lactic acid) nanocomposite fibrous scaffolds for hard tissue regeneration: In situ synthesis and electrospinning. *Journal of Biomedical Materials Research Part A, 102*(2), 514-522.

Chang, W., Mu, X., Zhu, X., Ma, G., Li, C., Xu, F., & Nie, J. (2013). Biomimetic composite scaffolds based mineralization of hydroxyapatite on electrospun calcium-containing poly (vinyl alcohol) nanofibers. *Materials Science and Engineering: C, 33*(7), 4369-4376.

Chen, C., Weir, M. D., Cheng, L., Lin, N. J., Lin-Gibson, S., Chow, L. C., . . . Xu, H. H. K. (2014). Antibacterial activity and ion release of bonding agent containing amorphous calcium phosphate nanoparticles. *Dental Materials, 30*(8), 891-901.

Chen, M. H. (2010). Update on dental nanocomposites. *Journal of Dental Research, 89*(6), 549-560. doi:10.1177/0022034510363765

Cheng, L., Weir, M. D., Xu, H. H. K., Antonucci, J. M., Lin, N. J., Lin-Gibson, S., . . . Zhou, X. (2012). Effect of amorphous calcium phosphate and silver nanocomposites on dental plaque microcosm biofilms. *Journal of Biomedical Materials Research Part B: Applied Biomaterials, 100*(5), 1378-1386.

Choi, K. K., Ferracane, J. L., Hilton, T. J., & Charlton, D. (2000). Properties of packable dental composites. *Journal of Esthetic Dentistry, 12*(4), 216-226.

Cobb, D. S., MacGregor, K. M., Vargas, M. A., & Denehy, G. E. (2000). The physical properties of packable and conventional posterior resin-based composites: a comparison. *Journal of the American Dental Association, 131*(11), 1610-1615.

Costa, J. D., Ferracane, J., Paravina, R. D., Mazur, R. F., & Roeder, L. (2007). The effect of different polishing systems on surface roughness and gloss of various resin composites. *Journal of Esthetic and Restorative Dentistry, 19*(4), 214-224.

Da Costa, J. B., Goncalves, F., & Ferracane, J. L. (2011). Comparison of two-step versus four-step composite finishing/polishing disc systems: evaluation of a new two-step composite polishing disc system. *Operative Dentistry, 36*(2), 205-212.

Dabsie, F., Gregoire, G., Sixou, M., & Sharrock, P. (2009). Does strontium play a role in the cariostatic activity of glass ionomer?: Strontium diffusion and antibacterial activity. *Journal of Dentistry, 37*(7), 554-559.

Dauvillier, B. S., Aarnts, M. P., & Feilzer, A. J. (2000). Developments in shrinkage control of adhesive restoratives. *Journal of Esthetic Dentistry, 12*(6), 291-299.

Deligeorgi, V., Mjor, I. A., & Wilson, N. H. (2001). An overview of reasons for the placement and replacement of restorations. *Primary Dental Care, 8*(1), 5-11.

Demarco, F. F., Correa, M. B., Cenci, M. S., Moraes, R. R., & Opdam, N. J. (2012). Longevity of posterior composite restorations: not only a matter of materials. *Dental Materials, 28*(1), 87-101. doi:10.1016/j.dental.2011.09.003

Dermaut, W., Van den Kerkhof, T., van der Veken, B. J., Mertens, R., & Geise, H. J. (2000). Cold stretching of PPV with water as a plasticizer. *Macromolecules, 33*(15), 5634-5637.

Dezelic, T., Guggenheim, B., & Schmidlin, P. R. (2009). Multi-species biofilm formation on dental materials and an adhesive patch. *Oral Health Prev Dent, 7*(1), 47-53.

Dijkman, G., De Vries, J., Lodding, A., & Arends, J. (1993). Long-term fluoride release of visible light-activated composites in vitro: a correlation with in situ demineralisation data. *Caries Research, 27*(2), 117-123.

Eick, S., Glockmann, E., Brandl, B., & Pfister, W. (2004). Adherence of Streptococcus mutans to various restorative materials in a continuous flow system. *Journal of Oral Rehabilitation, 31*(3), 278-285. doi:10.1046/j.0305-182X.2003.01233.x

Ereifej, N. S., Oweis, Y. G., & Eliades, G. (2012). The effect of polishing technique on 3-D surface roughness and gloss of dental restorative resin composites. *Operative Dentistry, 38*(1), E9-E20.

Ergücü, Z., & Türkün, L. S. (2007). Surface roughness of novel resin composites polished with one-step systems. *Operative Dentistry, 32*(2), 185-192.

Feagin, F., & Thiradilok, S. (1979). Effects of magnesium and fluoride on ion exchange and acid resistance of enamel. *Journal of Oral Pathology and Medicine, 8*(1), 23-27.

Ferracane, J. L. (2005). Developing a more complete understanding of stresses produced in dental composites during polymerization. *Dental Materials, 21*(1), 36-42. doi:10.1016/j.dental.2004.10.004

Ferracane, J. L. (2011). Resin composite--state of the art. *Dental Materials, 27*(1), 29-38. doi:10.1016/j.dental.2010.10.020

Filoche, S., Wong, L., & Sissons, C. H. (2010). Oral biofilms: emerging concepts in microbial ecology. *Journal of Dental Research, 89*(1), 8-18. doi:10.1177/0022034509351812

Fleming, G. J., Hall, D. P., Shortall, A. C., & Burke, F. J. (2005). Cuspal movement and microleakage in premolar teeth restored with posterior filling materials of varying reported volumetric shrinkage values. *Journal of Dentistry, 33*(2), 139-146. doi:10.1016/j.jdent.2004.09.007

Forssten, S. D., Bjorklund, M., & Ouwehand, A. C. (2010). Streptococcus mutans, caries and simulation models. *Nutrients, 2*(3), 290-298. doi:10.3390/nu2030290

Giessibl, F. J. (2000). Atomic resolution on Si (111)-(7× 7) by noncontact atomic force microscopy with a force sensor based on a quartz tuning fork. *Applied Physics Letters, 76*(11), 1470-1472.

Giessibl, F. J., & Trafas, B. M. (1994). Piezoresistive cantilevers utilized for scanning tunneling and scanning force microscope in ultrahigh vacuum. *Review of Scientific Instruments, 65*(6), 1923-1929.

Guggenheim, B., Giertsen, E., Schupbach, P., & Shapiro, S. (2001). Validation of an in vitro biofilm model of supragingival plaque. *Journal of Dental Research, 80*(1), 363-370.

Hahnel, S., Rosentritt, M., Burgers, R., & Handel, G. (2008). Surface properties and in vitro Streptococcus mutans adhesion to dental resin polymers. *Journal of Materials Science: Materials in Medicine, 19*(7), 2619-2627. doi:10.1007/s10856-007-3352-7

Hahnel, S., Wastl, D. S., Schneider-Feyrer, S., Giessibl, F. J., Brambilla, E., Cazzaniga, G., & Ionescu, A. (2014). Streptococcus mutans biofilm formation and release of fluoride from experimental resin-based composites depending on surface treatment and S-PRG filler particle fraction. *Journal of Adhesive Dentistry, 16*(4), 313-321. doi:10.3290/j.jad.a31800

Hannig, C., & Hannig, M. (2009). The oral cavity--a key system to understand substratum-dependent bioadhesion on solid surfaces in man. *Clinical Oral Investigations, 13*(2), 123-139. doi:10.1007/s00784-008-0243-3

Hannig, M., & Joiner, A. (2006). The structure, function and properties of the acquired pellicle. *Monographs in Oral Science, 19*, 29-64. doi:10.1159/000090585

Hannig, M., Kriener, L., Hoth-Hannig, W., Becker-Willinger, C., & Schmidt, H. (2007). Influence of nanocomposite surface coating on biofilm formation in situ. *Journal of nanoscience and nanotechnology, 7*(12), 4642-4648.

He, J., Söderling, E., Österblad, M., Vallittu, P. K., & Lassila, L. V. J. (2011). Synthesis of methacrylate monomers with antibacterial effects against S. mutans. *Molecules, 16*(11), 9755-9763.

Honda, T. (2004). Study on the film layer produced from S-PRG filler. *Japanese Journal of Conservative Dentistry, 47*(3), 391-402.

Ikeda, M., Matin, K., Nikaido, T., Foxton, R. M., & Tagami, J. (2007). Effect of surface characteristics on adherence of S. mutans biofilms to indirect resin composites. *Dental Materials Journal, 26*(6), 915-923.

Ilie, N., Jelen, E., Clementino-Luedemann, T., & Hickel, R. (2007). Low-shrinkage composite for dental application. *Dental Materials Journal, 26*(2), 149-155.

Imazato, S. (2009). Bio-active restorative materials with antibacterial effects: new dimension of innovation in restorative dentistry. *Dental Materials Journal, 28*(1), 11-19.

Imazato, S., Chen, J.-h., Ma, S., Izutani, N., & Li, F. (2012). Antibacterial resin monomers based on quaternary ammonium and their benefits in restorative dentistry. *Japanese Dental Science Review, 48*(2), 115-125.

Imazato, S., & McCabe, J. F. (1994). Influence of incorporation of antibacterial monomer on curing behavior of a dental composite. *Journal of Dental Research, 73*(10), 1641-1645.

Ionescu, A., Brambilla, E., Wastl, D. S., Giessibl, F. J., Cazzaniga, G., Schneider-Feyrer, S., & Hahnel, S. (2015). Influence of matrix and filler fraction on biofilm formation on the surface of experimental resin-based composites. *Journal of Materials Science: Materials in Medicine, 26*(1), 1-7.

Ionescu, A., Wutscher, E., Brambilla, E., Schneider-Feyrer, S., Giessibl, F. J., & Hahnel, S. (2012). Influence of surface properties of resin-based composites on in vitro Streptococcus mutans biofilm development. *European Journal of Oral Sciences, 120*(5), 458-465. doi:10.1111/j.1600-0722.2012.00983.x

Jedrychowski, J. R., Caputo, A. A., & Kerper, S. (1983). Antibacterial and mechanical properties of restorative materials combined with chlorhexidines. *Journal of Oral Rehabilitation, 10*(5), 373-381.

Jenkinson, H. F. (2011). Beyond the oral microbiome. *Environmental Microbiology, 13*(12), 3077-3087. doi:10.1111/j.1462-2920.2011.02573.x

Jenkinson, H. F., & Lamont, R. J. (2005). Oral microbial communities in sickness and in health. *Trends in Microbiology, 13*(12), 589-595. doi:10.1016/j.tim.2005.09.006

Jung, M. (1997). Surface roughness and cutting efficiency of composite finishing instruments. *Operative Dentistry, 22*(3), 98-104.

Kamijo, K., Mukai, Y., Tominaga, T., Iwaya, I., Fujino, F., Hirata, Y., & Teranaka, T. (2009). Fluoride release and recharge characteristics of denture base resins containing surface pre-reacted glass-ionomer filler. *Dental Materials Journal, 28*(2), 227-233.

Khurshid, Z., Zafar, M., Qasim, S., Shahab, S., Naseem, M., & AbuReqaiba, A. (2015). Advances in nanotechnology for restorative dentistry. *Materials, 8*(2), 717-731.

Kindblom, C., Davies, J. R., Herzberg, M. C., Svensater, G., & Wickstrom, C. (2012). Salivary proteins promote proteolytic activity in Streptococcus mitis biovar 2 and Streptococcus mutans. *Molecular Oral Microbiology, 27*(5), 362-372. doi:10.1111/j.2041-1014.2012.00650.x

Klein, M. I., DeBaz, L., Agidi, S., Lee, H., Xie, G., Lin, A. H., . . . Koo, H. (2010). Dynamics of Streptococcus mutans transcriptome in response to starch and sucrose during biofilm development. *PloS One, 5*(10), e13478. doi:10.1371/journal.pone.0013478

Kleinberg, I. (2002). A mixed-bacteria ecological approach to understanding the role of the oral bacteria in dental caries causation: an alternative to Streptococcus mutans and the specific-plaque hypothesis. *Critical Reviews in Oral Biology and Medicine, 13*(2), 108-125.

Lang, B. R., Jaarda, M., & Wang, R. F. (1992). Filler particle size and composite resin classification systems. *Journal of Oral Rehabilitation, 19*(6), 569-584.

Langhorst, S. E., O'Donnell, J. N. R., & Skrtic, D. (2009). In vitro remineralization of enamel by polymeric amorphous calcium phosphate composite: quantitative microradiographic study. *Dental Materials, 25*(7), 884-891.

Ledder, R. G., Madhwani, T., Sreenivasan, P. K., De Vizio, W., & McBain, A. J. (2009). An in vitro evaluation of hydrolytic enzymes as dental plaque control agents. *Journal of Medical Microbiology, 58*(Pt 4), 482-491. doi:10.1099/jmm.0.006601-0

Lederberg, J., & McCray, A. T. (2001). Ome SweetOmics--A Genealogical Treasury of Words. *The Scientist, 15*(7), 8-8.

Lima, E. M., Koo, H., Vacca Smith, A. M., Rosalen, P. L., & Del Bel Cury, A. A. (2008). Adsorption of salivary and serum proteins, and bacterial adherence on titanium and zirconia ceramic surfaces. *Clinical Oral Implants Research, 19*(8), 780-785. doi:10.1111/j.1600-0501.2008.01524.x

Lima, F. G., Romano, A. R., Correa, M. B., & Demarco, F. F. (2009). Influence of microleakage, surface roughness and biofilm control on secondary caries formation around composite resin restorations: an in situ evaluation. *Journal of Applied Oral Science, 17*(1), 61-65.

Limaye, A. (2012). *Drishti-volume exploration and presentation tool*.

Lu, H., Roeder, L. B., & Powers, J. M. (2003). Effect of polishing systems on the surface roughness of microhybrid composites. *J Esthet Restor Dent, 15*(5), 297-303; discussion 304.

Marsh, P. D. (2004). Dental plaque as a microbial biofilm. *Caries Research, 38*(3), 204-211. doi:10.1159/000077756

Marsh, P. D. (2006). Dental plaque as a biofilm and a microbial community - implications for health and disease. *BMC Oral Health, 6 Suppl 1*, S14. doi:10.1186/1472-6831-6-S1-S14

Marsh, P. D. (2012). Contemporary perspective on plaque control. *British Dental Journal, 212*(12), 601-606. doi:10.1038/sj.bdj.2012.524

Marsh, P. D., Moter, A., & Devine, D. A. (2011). Dental plaque biofilms: communities, conflict and control. *Periodontology 2000, 55*(1), 16-35.

McBain, A. J., Sissons, C., Ledder, R. G., Sreenivasan, P. K., De Vizio, W., & Gilbert, P. (2005). Development and characterization of a simple perfused oral microcosm. *Journal of Applied Microbiology, 98*(3), 624-634.

Mei, L., Busscher, H. J., van der Mei, H. C., & Ren, Y. (2011). Influence of surface roughness on streptococcal adhesion forces to composite resins. *Dental Materials, 27*(8), 770-778. doi:10.1016/j.dental.2011.03.017

Mei, L., Ren, Y., Loontjens, T. J., van der Mei, H. C., & Busscher, H. J. (2012). Contact-killing of adhering streptococci by a quaternary ammonium compound incorporated in an acrylic resin. *The International journal of artificial organs, 35*(10), 854-863.

Melo, M. A. S., Cheng, L., Zhang, K., Weir, M. D., Rodrigues, L. K. A., & Xu, H. H. K. (2013). Novel dental adhesives containing nanoparticles of silver and amorphous calcium phosphate. *Dental Materials, 29*(2), 199-210.

Metwalli, K. H., Khan, S. A., Krom, B. P., & Jabra-Rizk, M. A. (2013). Streptococcus mutans, Candida albicans, and the human mouth: a sticky situation. *PLoS Pathogens, 9*(10), e1003616. doi:10.1371/journal.ppat.1003616

Michalek, S. M., Katz, J., Childers, N. K., Martin, M., & Balkovetz, D. F. (2002). Microbial/host interactions: mechanisms involved in host responses to microbial antigens. *Immunologic Research, 26*(1-3), 223-234. doi:10.1385/IR:26:1-3:223

Mitra, S. B., Wu, D., & Holmes, B. N. (2003). An application of nanotechnology in advanced dental materials. *Journal of the American Dental Association, 134*(10), 1382-1390.

Mjor, I. A. (2005). Clinical diagnosis of recurrent caries. *Journal of the American Dental Association, 136*(10), 1426-1433.

Moreau, J. L., Sun, L., Chow, L. C., & Xu, H. H. K. (2011). Mechanical and acid neutralizing properties and bacteria inhibition of amorphous calcium phosphate dental nanocomposite. *Journal of Biomedical Materials Research Part B: Applied Biomaterials, 98*(1), 80-88.

Ono, M., Nikaido, T., Ikeda, M., Imai, S., Hanada, N., Tagami, J., & Matin, K. (2007). Surface properties of resin composite materials relative to biofilm formation. *Dental Materials Journal, 26*(5), 613-622.

Owens, D. K., & Wendt, R. C. (1969). Estimation of the surface free energy of polymers. *Journal of Applied Polymer Science, 13*(8), 1741-1747.

Ozel, E., Korkmaz, Y., Attar, N., & Karabulut, E. (2008). Effect of one-step polishing systems on surface roughness of different flowable restorative materials. *Dental Materials Journal, 27*(6), 755-764.

Palin, W. M., Fleming, G. J., Nathwani, H., Burke, F. J., & Randall, R. C. (2005). In vitro cuspal deflection and microleakage of maxillary premolars restored with novel low-shrink dental composites. *Dental Materials, 21*(4), 324-335. doi:10.1016/j.dental.2004.05.005

Pandit, S., Kim, G. R., Lee, M. H., & Jeon, J. G. (2011). Evaluation of Streptococcus mutans biofilms formed on fluoride releasing and non fluoride releasing resin composites. *Journal of Dentistry, 39*(11), 780-787. doi:10.1016/j.jdent.2011.08.010

Paster, B. J., Boches, S. K., Galvin, J. L., Ericson, R. E., Lau, C. N., Levanos, V. A., . . . Dewhirst, F. E. (2001). Bacterial diversity in human subgingival plaque. *Journal of Bacteriology, 183*(12), 3770-3783. doi:10.1128/JB.183.12.3770-3783.2001

Pereira, C. A., Eskelson, E., Cavalli, V., Liporoni, P. C., Jorge, A. O., & do Rego, M. A. (2011). Streptococcus mutans biofilm adhesion on composite resin surfaces after different finishing and polishing techniques. *Operative Dentistry, 36*(3), 311-317. doi:10.2341/10-285-L

Polydorou, O., Hammad, M., Konig, A., Hellwig, E., & Kummerer, K. (2009). Release of monomers from different core build-up materials. *Dental Materials, 25*(9), 1090-1095. doi:10.1016/j.dental.2009.02.014

Pratt-Terpstra, I. H., Weerkamp, A. H., & Busscher, H. J. (1987). Adhesion of oral streptococci from a flowing suspension to uncoated and albumin-coated surfaces. *Journal of General Microbiology, 133*(11), 3199-3206. doi:10.1099/00221287-133-11-3199

Reis, A. F., Giannini, M., Lovadino, J. R., & Ambrosano, G. M. (2003). Effects of various finishing systems on the surface roughness and staining susceptibility of packable composite resins. *Dental Materials, 19*(1), 12-18.

Rodrigues, M. C., Hewer, T. L. R., de Souza Brito, G. E., Arana-Chavez, V. E., & Braga, R. R. (2014). Calcium phosphate nanoparticles functionalized with a dimethacrylate monomer. *Materials Science and Engineering: C, 45*, 122-126.

Rodrigues, M. C., Natale, L. C., Arana-Chaves, V. E., & Braga, R. R. (2015). Calcium and phosphate release from resin-based materials containing different calcium orthophosphate nanoparticles. *Journal of Biomedical Materials Research Part B: Applied Biomaterials, 103*(8), 1670-1678.

Rosentritt, M., Hahnel, S., Groger, G., Muhlfriedel, B., Burgers, R., & Handel, G. (2008). Adhesion of Streptococcus mutans to various dental materials in a laminar flow chamber system. *Journal of Biomedical Materials Research Part B: Applied Biomaterials, 86*(1), 36-44. doi:10.1002/jbm.b.30985

Rueggeberg, F. (2005). Visible light curing. *J Esthet Restor Dent, 17*(4), 200-201.

Sbordone, L., & Bortolaia, C. (2003). Oral microbial biofilms and plaque-related diseases: microbial communities and their role in the shift from oral health to disease. *Clinical Oral Investigations, 7*(4), 181-188. doi:10.1007/s00784-003-0236-1

Selwitz, R. H., Ismail, A. I., & Pitts, N. B. (2007). Dental caries. *Lancet, 369*(9555), 51-59. doi:10.1016/S0140-6736(07)60031-2

Seppä, L., Torppa-Saarinen, E., & Luoma, H. (1992). Effect of Different Glass Ionomers on the Acid Production and Electrolyte Metabolism of Streptococcus mutans Ingbritt. *Caries Research, 26*(6), 434-438.

Shimazu, K., Ogata, K., & Karibe, H. (2011). Evaluation of the ion-releasing and recharging abilities of a resin-based fissure sealant containing S-PRG filler. *Dental Materials Journal, 30*(6), 923-927.

Shu, M., Wong, L., Miller, J. H., & Sissons, C. H. (2000). Development of multi-species consortia biofilms of oral bacteria as an enamel and root caries model system. *Archives of Oral Biology, 45*(1), 27-40.

Sideridou, I., Tserki, V., & Papanastasiou, G. (2002). Effect of chemical structure on degree of conversion in light-cured dimethacrylate-based dental resins. *Biomaterials, 23*(8), 1819-1829.

Skrtic, D., Antonucci, J. M., Eanes, E. D., Eichmiller, F. C., & Schumacher, G. E. (2000). Physicochemical evaluation of bioactive polymeric composites based on hybrid amorphous calcium phosphates. *Journal of Biomedical Materials Research, 53*(4), 381-391.

Song, F., Koo, H., & Ren, D. (2015). Effects of material properties on bacterial adhesion and biofilm formation. *Journal of Dental Research*, 0022034515587690.

Stansbury, J. W. (2000). Curing dental resins and composites by photopolymerization. *Journal of Esthetic Dentistry, 12*(6), 300-308.

Stewart, P. S., Rayner, J., Roe, F., & Rees, W. M. (2001). Biofilm penetration and disinfection efficacy of alkaline hypochlorite and chlorosulfamates. *Journal of Applied Microbiology, 91*(3), 525-532.

Svanberg, M., Mjör, I. A., & Ørstavik, D. (1990). Mutans streptococci in plaque from margins of amalgam, composite, and glass-ionomer restorations. *Journal of Dental Research, 69*(3), 861-864.

Takahashi, Y., Imazato, S., Russell, R. R., Noiri, Y., & Ebisu, S. (2004). Influence of resin monomers on growth of oral streptococci. *Journal of Dental Research, 83*(4), 302-306.

Tang, G., Yip, H.-K., Cutress, T. W., & Samaranayake, L. P. (2003). Artificial mouth model systems and their contribution to caries research: a review. *Journal of Dentistry, 31*(3), 161-171.

Temin, S. C., & Csuros, Z. (1988). Long-term fluoride release from a composite restorative. *Dental Materials, 4*(4), 184-186.

Tenover, F. C. (2006). Mechanisms of antimicrobial resistance in bacteria. *The American journal of medicine, 119*(6), S3-S10.

Teughels, W., Van Assche, N., Sliepen, I., & Quirynen, M. (2006). Effect of material characteristics and/or surface topography on biofilm development. *Clinical Oral Implants Research, 17 Suppl 2*, 68-81. doi:10.1111/j.1600-0501.2006.01353.x

Tyas, M. J. (2005). Placement and replacement of restorations by selected practitioners. *Australian Dental Journal, 50*(2), 81-89.

Van Duynhoven, J., Vaughan, E. E., Jacobs, D. M., Kemperman, R. A., Van Velzen, E. J. J., Gross, G., . . . Doré, J. (2011). Metabolic fate of polyphenols in the human superorganism. *Proceedings of the national academy of sciences, 108*(Supplement 1), 4531-4538.

Wang, Z., Shen, Y., & Haapasalo, M. (2014). Dental materials with antibiofilm properties. *Dental Materials, 30*(2), e1-e16.

Wastl, D. S., Speck, F., Wutscher, E., Ostler, M., Seyller, T., & Giessibl, F. J. (2013). Observation of 4 nm pitch stripe domains formed by exposing graphene to ambient air. *ACS Nano, 7*(11), 10032-10037. doi:10.1021/nn403988y

Wastl, D. S., Weymouth, A. J., & Giessibl, F. J. (2013). Optimizing atomic resolution of force microscopy in ambient conditions. *Physical Review B, 87*(24), 245415.

Weinmann, W., Thalacker, C., & Guggenberger, R. (2005). Siloranes in dental composites. *Dental Materials, 21*(1), 68-74. doi:10.1016/j.dental.2004.10.007

Weng, Y., Guo, X., Chong, V. J., Howard, L., Gregory, R. L., & Xie, D. (2011). Synthesis and evaluation of a novel antibacterial dental resin composite with quaternary ammonium salts. *Journal of Biomedical Science and Engineering, 4*(03), 147.

Wiegand, A., Buchalla, W., & Attin, T. (2007). Review on fluoride-releasing restorative materials—fluoride release and uptake characteristics, antibacterial activity and influence on caries formation. *Dental Materials, 23*(3), 343-362.

Xu, K. D., McFeters, G. A., & Stewart, P. S. (2000). Biofilm resistance to antimicrobial agents. *Microbiology, 146*(3), 547-549.

Yap, A. U. J., Yap, S. H., Teo, C. K., & Ng, J. J. (2004). Comparison of surface finish of new aesthetic restorative materials. *Operative Dentistry-University of Washington 29*(1), 100-104.

Yoneda, M., Suzuki, N., Masuo, Y., Fujimoto, A., Iha, K., Yamada, K., . . . Hirofuji, T. (2012). Effect of S-PRG eluate on biofilm formation and enzyme activity of oral bacteria. *International journal of dentistry, 2012*.